Control of
Bilateral Teleoperation Systems

İlhan Polat

Control of
Bilateral Teleoperation Systems

Proefschrift

ter verkrijging van de graad van doctor
aan de Technische Universiteit Delft,
op gezag van de Rector Magnificus prof. ir. K.C.A.M. Luyben,
voorzitter van het College voor Promoties,
in het openbaar te verdedigen op donderdag 45 juli 2012 om 23:30 uur
door İlhan Polat,
ingenieur werktuigbouwkunde,
geboren te Gaziantep, TURKIJE.

Dit proefschrift is goedgekeurd door de promotor:
Prof.dr. C.W. Scherer

Samenstelling promotiecommissie:

Rector Magnificus	voorzitter
Prof.dr. C.W. Scherer	Universität Stuttgart, promotor
Prof.ir. Prof. 1	Technische Universiteit Delft
Prof.dr. Prof. 2	Technische Universiteit Delft
Prof.dr. Prof. 3	Technische Universiteit Delft
Prof.dr. Prof. 4	Technische Universiteit Delft
Prof.dr. Prof. 5	Technische Universiteit Delft
Prof.dr. Prof. 6	Technische Universiteit Delft

Printed by some company

Table Of Contents

List of Tables

List of Figures

Introduction

The success of the technological advances often can be associated with an unprecedented convenience that they bring in. At the heart of this convenience lies the ability to relax the limitations of the human body to a certain extent. From this point of view, it is not a surprise that the three most prominent technological wonders of the last century, namely the *Television*, the *Telephone* and the *radio* (which was originally called "radiotelegraphy"), bears the same Greek prefix *tele-* which corresponds to "*at a distance*" in our context. This shows that there is something of extreme importance about our drive to extend our capabilities beyond the constraints that our bodies impose.

It is quite remarkable, in retrospect, that these "gadgets" did not perish but rather kept on evolving since initially they were far from perfect. Quite the contrary, they were hardly operational. Even the commercialized version of the early TVs had a narrow bandwidth and minimum image quality. Similarly radio and telephone was barely transmitting sensible information as far as the signal-to-noise ratio is concerned. Nevertheless, they have provided the ways of communication which were unimaginable before their time. Therefore the added value dominated the shortcomings and even though they were quite imperfect, we kept using them. The important lesson to be learned is that a technology should not be judged by its imperfections but rather should be weighed by its contribution in this context and the convenience that is either immediately brought in by using it or its foreseen potential by the "early adopters".

The success is also related to the fact that these technologies mainly relied on the human brain itself at their early stages. For example, the human brain did most of the noise filtering and data recovery by just guessing the missing pieces and identifying patterns from the signal brought by the respective medium. Today, with our smart mobile phones and 3D LED TVs, we can assume that the computational load on the human brain is drastically reduced. In other words, it's true that we are still identifying patterns and utilizing the relevant parts of our brain to make sense of a TV broadcast[1]. However, we don't need to use a higher level of concentration to reconstruct the words that we hear or to identify the image on the display thanks to the high quality output. We can not exaggerate the importance of the human brain and its immersion power.

---

[1]Pun intended.

Leaving essentially the same footprints, we are on the same track with the technological developments involving our touch sense. Though various science fiction items already used such ideas extensively, the real technology tends to follow from quite a distance. Considering the importance of our touch sense in any given situation, the added value of extending of our perception in this modality needs no motivation. Take the most familiar, the vibrating mobile phone in the silent mode in our pocket. This is a very important example since every individual learns what that vibration might mean, either an SMS or a call, depending on the vibrational pattern. This means that the touch sense can be used to convey messages and more importantly we can process those messages for inference which forms the basis of the so-called "haptics" and haptic technology.

The type of information from the cell-phone example is said to be received via the haptic channel (or the collaborative use of tactile and proprioceptive modalities). At this point we have to emphasize that, we use the term "touch sense" pretty vaguely as a shortcut and we leave it to the experts of the field to define the sophisticated mechanisms (pertaining to the somatosensory system) that we utilize when we manipulate objects, say with our bare hands.

Since our skin and muscles form one of most sophisticated and complex sensory systems, the somatosensory system, the brain can easily interpret the slightest changes and this extra signal processing power gives us a chance to hack into this system by providing artificial inputs via haptic displays. Still, it is rather conspicuous that this is impossible to achieve a total immersion with today's technology. The essential complication is twofold: the high sensitivity of the very same sensory system makes it difficult to fake or mimic a natural phenomenon by artificial means and on the other hand we do not have a well-defined mapping from the to-be-created sensation to the required excitation signals. Moreover, even if we have such mappings available, the related hardware must execute the computed haptic signal profiles perfectly which is generally not the case.

Then, we could simply ask *Why bother?*

1.1   The Objectives

We first give a summary about the current concepts of the involved technology (as we foresee from a narrow "today's" perspective) and later on, define our microscopic focus of this thesis in this vast generality. This would hopefully provide additional insights to what follows in the later sections.

The touch related applications are diverse. The diversity is not only in terms of sensation they are related to (texture, shape etc.) but also how they encode the information and transmit via various modalities (e.g. vibrational patterns in mobile electronics, variable resistance to motion in game consoles and steering wheels

etc.). There is no particular reason to limit ourselves with the daily needs or even luxurious demands regarding our touch sense as mobile phones taught us that a vibration in our pocket means a contact request from someone which is hardly ever related to the touch sense. This should be pretty awkward to experience if someone actually would come and shake our pockets to draw our attention (unless it is socially accepted). Therefore, we have devised a way to translate one particular message into another by simply teaching ourselves and getting used to it. Thus, it does not seem improbable that other types of physical units in terms temperature, light intensity etc. being converted into pressure or tactile patterns in time domain.

Hence, it is our belief that the crux of this technology is establishing a interpretable protocol between our brain and the machine but not exactly reflecting the particular state of some distant or virtual physical medium. This would be the main argument of this thesis when we distinguish our approach with its comparable counterparts. For this reason, we would like to narrow down our focus further by defining different types of touch related concepts.

1.1.1 *A Terminological Classification*

As we mentioned above, the somatosensory system is quite complex and there are different layers of sensory mechanisms that contribute to the overall perception. The main two branches of technology relating to the touch perception are the tactile and kinesthetic feedback. The terminology is yet to reach a steady-state standard however what follows below is plausible considering the variations and nuances found in the literature. Since there is no fixed definition for such perception we would use a rough classification based on the amplitude-frequency of the motion. We have to emphasize that this classification is completely conceptual and only serves to exclude the parts that are not studied in this thesis. Therefore, we refer the reader to the authoritative resources of the involved physiology, e.g., [71]. We start with a somewhat detailed sensory classification to support our choice of amplitude-frequency based grouping.

Typically, the touch perception is classified into two groups. Tactile feedback and kinesthetic (proprioceptive) feedback. For practical purposes, one can use the analogy of a parallel connected high-pass and low-pass filter. For our control-oriented context, let us define a few key concepts with an engineering point of view.

In physiology, the sensors on the skin which take different physical measurements, are called *receptors* and prefixed with their area of specialization such as *thermoreceptors*, *mechanoreceptors*, *nocioreceptors*(pain) etc. The signals that trigger an action on these receptors are denoted as the *stimuli*. In case of a stimulus, these receptors, through some chemical processes, exhibit a series of *action potentials* or

electrical discharge pulses i.e. a *spike train*. In the engineering terminology, this can be modeled as a nonuniform Dirac comb with varying frequency as a function of the stimuli intensity or a digital frequency modulation (FM) signal. The frequency increases with the stimulus intensity. Furthermore, at the input side of this sensor there is a dead-zone nonlinearity hence the stimuli should exceed a particular threshold to trigger a receptor firing.

There is also another process, *neural* or *sensorial adaptation* which quantifies the frequency decay of firing under constant stimulus. We can see the tangible effect of this process frequently e.g., our nose looses the sensitivity to a powerful smell if exposed to it for some time or we stop noticing the touch of the glasses on the face or the ring on the finger. Some sensors have a slow decay rate whereas others decay in a matter of seconds. The slow sensors often called the *slowly adapting(SA)* and others are called *fast adapting (FA)* or *rapidly adapting* type [14].

As shown in Table 1.1, and also surveyed in [79], there are four main types of mechanisms that are utilized for the force and texture sensing with varying operating conditions and spatial authority. Although all contribute to the high frequency stimulus perception with varying levels, slowly adapting receptors are mainly tuned to detect the low frequency information range (up to 30 Hz). The fast adapting Meissner(FAI) and Pacinian(FAII) Corpuscles can be excited in the frequency range of [10,60] Hz and [60, 1000] Hz respectively. Thus, small-area receptors (Type I) are excited with rate of skin deformation whereas relatively large-area receptors (Type II) are with the acceleration of the skin. Moreover, FAI units are located closer to the skin surface, have high unit density with small surface area forming a grid of sensors. On the other hand, FAII units are located in the subcutaneous tissue and work as a single load cell with relatively large surface area. This allows experts to assume that FAI units are mainly responsible for spatial information about the skin deformation and FAII units are responsible for the high frequency information with response delays in the range of [50,500] ms [164]. Another interesting note in [79] is that due to their single unit nature FAII units offers the possibility to provide high frequency information with a single vibration display but for FAI units it is more appropriate to supply an array of haptic displays for lower frequency range.

The SAI disk receptor has a small, localized receptive surface area as opposed to the SAII with a large field with a decaying sensitivity from center to the edges. Individual Ruffini endings are excited by stretch of the skin in specific directions. The majority of hand receptors consists of FAI units ($> 40\%$), then SAI units are almost a quarter which followed by SAII covering 19% and FAII 13%.

Table 1.1: Functional Features of Cutanous Mechanoreceptors (Adapted from [164])

Feature	Meissner Corpuscles (FAI)	Pacinian Corpuscles (FAII)	Merkel's Disks (SAI)	Ruffini Endings (SAII)
Rate of adaptation	Rapid	Rapid	Slow	Slow
Location	Superficial dermis	Dermis and subcutaneous	Basal epidermis	Dermis and subcutaneous
Mean receptive area	$13\,mm^2$	$101\,mm^2$	$11\,mm^2$	$59\,mm^2$
Spatial resolution	Poor	Very poor	Good	Fair
Sensory units	43%	13%	25%	19%
Response frequency range	[10,200] Hz	[70,1000] Hz	[0.4,100] Hz	[0.4,100] Hz
Min. threshold frequency	40 Hz	[200,250] Hz	50 Hz	50 Hz
Sensitive to temperature	No	Yes	Yes	At > 100 Hz
Spatial summation	Yes	No	No	Unknown
Temporal summation	Yes	No	No	Yes
Physical parameter sensed	Skin curvature, velocity, local shape,flutter, slip	Vibration, slip, acceleration	Skin curvature, local shape, pressure	Skin stretch, local force

Weber ratio and Just-Noticeable-Difference(JND)

Weber ratio is defined as the ratio between the minimal stimulus intensity change in any physical quantity that triggers a change perception and the intensity of the stimulus. In case of a constant or static stimulus the ratio is denoted with Just-Noticeable-Difference (JND). For engineering purposes this derived unit can be beneficial to design the frequency behavior of the haptic systems which exhibit a particular sensitivity pattern.

Tactile Feedback

Tactile feedback, in general, is utilized to distinguish fine details such as shape, curvature, vibration, acceleration, and texture perception. Hence, the high-frequency content of the touch information is indispensable to transmit such information. Since the amplitude of the motion at these frequencies are quite small, the palm and finger tissues act as a low-pass filter and avoid such information to penetrate into the skin. Thus, only a limited part of the sensors have access to this information.

A striking example to the mind-boggling quality of feedback is the Braille system used by visually impaired or disabled individuals (Figure 1.1). The average reading speed with Braille system is about 125-150 words per minute ([1]) in contrast with 200-250 words per minute by eyesight.

Most of today's technological devices utilize this modality to send and receive information. Many mobile phone applications and a few gaming consoles such as Nintendo Wii™, Sony Playstation™ etc., utilize short vibrational patterns to alert
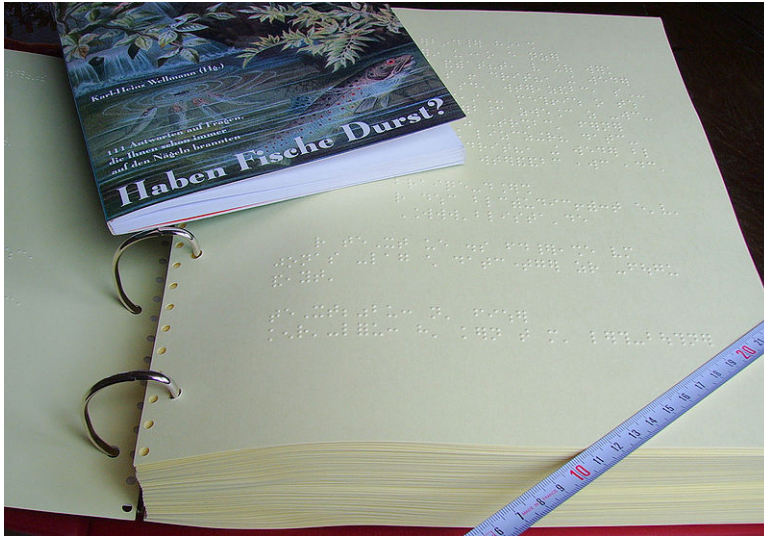
Figure 1.1: The length comparison of the same content in the form of Braille and regular text (Source: Karl-Heinz Wellmann, **[Wikipedia:Brailleschrift]**)

the user that some action has been performed e.g. the user hovers over a hot spot on the screen or some moving object hits an obstacle etc.

The tactile technology is, thus, concerned with the vibrational pattern and high-frequency sweep of stimuli. Communication via small vibrational or textural subtleties allows the tactile technology to focus on the low-stroke, high-bandwidth haptic displays. The required low-stroke action is often generated by a small and agile electrical motor with a load eccentricity with respect to the rotor shaft axis. The angular velocity of the motor then defines the frequency of the vibration. Since the involved mechanisms on the human limbs and hands are rapidly adapting, the bus speed in this modality can be very high compared to the kinesthetic feedback in which the human should track and pick out patterns from relatively slow and large-amplitude motion profiles via measuring muscle stretch amount and various other quantities.

Kinesthetic (Proprioceptive) Feedback

Proprioception[2] (*Proprius+perceptio*: the act of gathering of own) is the ability to sense the body position and motion without using the visual aid. Kinesthetic feedback, together with limited force sensing abilities of muscles and tendons and relatively small interference of tactile feedback system, is "vital" to have control

---

[2]We will not go into the nuances between kinesthetic and proprioceptive feedback

of our own body. It's a futile attempt to describe the importance of this often overlooked perception (or hidden sense) other than referring to the shocking 1998 BBC *Horizon* documentary "*The man who lost his body*" and the paper [96] about Ian Waterman. He is the only person known to date who can cope with the loss of proprioceptive feedback while still being able to stand up, walk, maintain posture etc. without any artificial support. Unfortunately, he is completely dependent on his visual feedback as he tirelessly computes trajectories of his body parts on-the-fly to compensate for the loss of kinesthetic feedback even when gesturing with hands.

Thus, whether we are aware of it or not, proprioception is indispensable for us to survey the environment. The force on our limbs, our body configuration at that instance, and body motion are sensed via sensors in the joints, muscle tendons and muscles themselves. Unlike the tactile feedback characteristics given previously, the compliance, the distribution of pressure and and the shape information is measured in a relatively coarse fashion. Hence, when combined with tactile feedback and the brain's internal comparison database we use an unparalleled sophistication to actually perceive the environment without using any visual feedback even the object is foreign to us. In [10], a convenient summary of the properties is presented. Distilling even further for a general picture about the proprioception, we provide the following quick facts.

The compression or stretch of the receptors covered previously changes the amplitude of the impulse of the action potential which in turn used as the position information. Similarly the frequency of these firings are interpreted as the velocity information. For the limb position and motion, the bandwidth of the kinesthetic sensing is around $[20,30]$ Hz with varying accuracy in terms of JND around $[0.8,2.5]°$. Moreover, the control bandwidth is reported to be task-dependent: $[1,2]$ Hz for unexpected signals; $[2,5]$ Hz for periodic signals, < 5 Hz for generated or learned trajectories and finally about 10 Hz for reflex actions.

Regarding the force sensing, it has been experimentally demostrated that pressure JND decreases as the pressure area increases e.g., overall average JND drops to 3.7% with a contact area of 20.27 cm^2 from 15.6% with a contact area of 1.27 cm^2.

The kinesthetic technology can be used in conjunction with tactile technology to provide a full manipulative immersion. Moreover, in the case of *exoskeletons*, it can be the essential ingredient to protocol between the environment and the human body. Especially, rehabilitation patients can benefit from such technologies via combining the visual and the kinesthetic feedback to amplify the disabled or impaired control action of the problematic limb. Thus, kinesthetic technology is mainly involved as low-frequency based manipulative or explorative motion tasks. Considering the current hardware limitations, many tasks depend primarily and

rather primitively kinesthetic cues for bilateral teleoperation and virtual reality applications.

Teleoperation

Teleoperation is the general name for providing human actions to a different media that is not accessible (or only in a costly way) to direct contact in a precise fashion. Microcomponent assembly, minimal invasive surgery (MIS), space station maintenance and construction, underwater exploration and construction are all typical application examples that the human either can not be present or physically interact with comfortably. The *da Vinci*™ surgery robot from Intuitive Surgical Inc. is a well-known example of *unilateral* human manipulation to achieve high precision tracking with surgical tools inside very tight incision (with other qualities that are not relevant to enumerate here).

However, as often motivated by the *bilateral* teleoperation studies, the human operators, expecially the experienced ones, often lack the ability to employ their precise tactile and kinesthetic abilities to take decisions or to monitor their progress since they rely on vision feedback from the cameras exclusively. In some particular practices, surgeons might resort to inserting their fingers inside the incision to feel the relevant tissue stiffness difference to get a better spatial understanding when the view is contaminated with blood or other bodily fluids. In the case of an obstruction during an insertion of an instrument into the body, they might tend to correct the instrument based on their force feel at hand. Hence, the realism is diminished as opposed to the increased precision by the teleoperation methods.

Bilateral Teleoperation

Bilateral teleoperation is simply teleoperation equipped with force feedback to the human operator with the hope to increase the realism by recreating the force vectors of the distant medium at the local environment. The majority of the bilateral teleoperation research is on the kinesthetic feedback. In particular, the human interacts with the local device by moving a constrained handle to explore the environment or using a stylus-like stick. Hence, the experience is mostly based on the success of imitating a physical tool. Therefore, the tactile cues are of secondary nature. The challenge of course is to increase the performance level to a tactile display level while still maintaining the tool usage capability. The particular MIS tasks that are performed with a scalpel are one of the hot topics of todays research effort and it requires not only kinesthetic feedback, though a major accomplishment by itself, but tactile feedback too, for understanding the nature of the texture or the stiffness of the tissue. Similarly teleoperated peg-in-hole type of tasks are also a major area of investigation e.g., ground-satellite robotic mission directives

or underwater construction tasks would benefit much from such possibilities to reduce the operational cost, duration, and success rate.

There are many interesting challenges when it comes to this recreation process. For example, in a microassembly task, the experienced forces are substantially different than what we feel during daily tasks. Gravity is our main source of reference when interpreting a distant location, however, gravity becomes almost negligible in the micro domain as adhesive forces such as Van der Waals, electrostatic and surface tension forces dominate (the most common example is that the parts that are picked up in microdomain tend to stick to the tweezers).

If we manage to create a believable level force feedback sensation in these otherwise inaccessible domains, there are a few very important quasi-philosophical and also task-dependent questions that need to be answered. A few of these questions are:

- Should the device reflect those forces to the human operator for the sake of realism which are utterly counter-intuitive and even worse appear to be happening at random?

- Is there any correlation between increased realism and increased comfort? In case of a difficult task, what good the realism bring in by replicating the difficult task at a distant location in the local environment?

- Do we need to reflect the human motion to the remote location perfectly since that is a waste of resource? In other words, we neglect the fact that a robot can perform certain tasks much more precisely than a human operator. Is there any downsampling/upsampling protocol to vary the motion precision depending on the receiver?

- If we decide to filter the unnecessary force information that are related to mental/muscular fatigue, how should we know what to filter?

- Do we use the full capacity of our *internal data bus* to transfer touch information, or put differently, is there any space left to encode other quantities on top of the touch sense?

- Can we assume that all users more or less reach to the same understanding given a kinesthetic cue sequence?

These questions are indeed quite interesting and challenging. The reason for enumerating a few of them here is that the scope of this thesis reaches to a point just before we are ready to attack them properly. In other words, we will focus on a framework that would help to set up such teleoperation devices such that experts of these fields can use these devices to answer those items above.

(Computer) Haptics

In general, haptics technology encompasses all the items that are covered up to this point, however, it is also often used as a placeholder for the concept of creating artificial or virtual object perception with a force-feedback capable device. Computer haptics also have additional challenges such as rendering deformations in case of a soft object or realistic graphical presentation of object interaction in terms of collisions etc. In other words, not only the forces are important but the consequences of these force interactions need to be handled in a precise fashion. Conversely, computer haptics is free from the hardware limitations or the noisy measurements as the objects and the physical laws that they should obey are computer generated.

Virtual Reality

This term refers to a set of artificially generated immersion techniques that can rely on either a single or multiple modalities at once. The common applications consist of special googles that cover the human vision. By tracking the head movements and adjusting the scene that is projected to the special headset, the user can immerse into the artificial environment. Combined with headphones and if possible with haptics, the experience can be substantially improved. Especially haptics can increase the immersion level much more compared to only visual+audio supplements since otherwise the realism can be destroyed quickly if the user tries to touch any object or surface while actually waving his hand. The persuasiveness of the scene depicted on the headset needs to be backed up with at least a slight kinesthetic feedback, if not tactile, since the loss of tactile feedback can be swept under various scenario e.g., the user can be placed in a situation with using blunt items, thick gloves, robotic hands etc.

1.1.2 *Structure and Objectives of This Thesis*

Let us turn to our initial question *Why Bother?*. We do because there is no need to obtain the ultimate perfect touch sensation for the human in order to interpret the signals correctly. It is the same principle with LED-TVs. Nowhere on the screen, a color different than Red, Green, and Blue is emitted. However, we tend to approximate the output to the closest color since the emitters are close enough and we achieve the color perception. Therefore, realism is not our primary objective. However, before we even enter this discussion, the teleoperation devices must be stable and should exhibit consistent performance such that experts from neuro-science, psychophysiology, and other related scientific fields can join and assess different ways of protocoling with the human brain in this modality. Otherwise

their conclusions would be contaminated by the device properties (we can even speculate that this is often the case, though no proof will be presented here). Thus it is the point of this thesis at which we consider the stability properties and control problem of bilateral teleoperation and we believe that we have achieved a limited success toward this direction.

To restrict the scope of this thesis further, we exclusively stay in bilateral teleoperation concept as we have defined previously and focus on the control theoretical aspects of the teleoperation for a stable interaction with sufficient performance levels. The reason of such a terminological enumeration above is to precisely draw the boundary of what will follow in the later chapters.

We first give an opinionated version of the literature to point out to the underlying connections between seemingly different methodologies and also provide a simpler explanation to the well-known *wave variables* formalism. By doing so, we classify such methods in the respective mainstream control theory methods and clearly demonstrate that they are indeed outdated if compared to the recent advances. Moreover, we argue that now-standard assumption of *passivity* property on the human and environment is not an experimentally validated one. We also claim that the success of passivity-based methods are due to the conservatism of these tests and not due to the validity of the assumption.

In Chapter 3, we then show also both theoretically and numerically that the frequency methods found in the literature can be combined under one framework via *Integral Quadratic Constraints*. With these results, we demonstrate that the proposed framework of this thesis does not bring in additional complications or conservatism. In fact, via numerical case studies, we show that the results are precisely the same. Therefore, there is no fundamental reason to use a specialized terminology of the networks and microwave systems which in turn alienates mainstream control theory experts. We also remark that uncertainty modeling is a key aspect in obtaining better controllers for bilateral teleoperation. To highlight the reasons why we promote this framework, we also give examples of different combinations of uncertainties for which classical tools that are employed in the teleoperation literature are not suitable but already available in the robust control literature for already 15 years.

After establishing this link with the methods in the literature we turn to the controller synthesis problem in Chapter 4. We formulate the problem as a generalized plant and work out scarce details that are found in the literature to obtain a better model-based control synthesis algorithm using static and dynamic IQCs. We also explicitly identify what the bottlenecks are for the interested reader.

In Chapter 5, we provide some concluding remarks and for the reader's convenience, in Appendix A, we recap the basics of the network theory.

A Brief and Opinionated Literature Survey

The teleoperation systems are structurally interesting and equally challenging systems. This is especially true from a system theoretical point of view. As an example, if we just focus on the local and the remote devices that would be used for manipulation, we see that they are, whether linear or nonlinear, motion-control systems with well-studied properties. Hence, one can view the open-loop teleoperation as a system with a block diagonal structure. However, unlike the typical motion-control systems, these two disjoint systems must be stabilized simultaneously by the same controller, that is performing sufficiently in order to "fool" the user such that the user feels a force feedback as if s/he is actually operating at the remote medium. We need to emphasize that the delayed/undelayed local control loops can be seen as the entries of a structured central controller. Thus, there is no reason to distinguish control methods at this point.

With this structure, the outputs of either of these subsystems become exogenous inputs of the other and these are regulated by the to-be-designed controller. Therefore, it is this controller that makes a teleoperation system perform adequately or, as in many cases, drive to instability.

For example, in the case of the so-called free-air motion (i.e. the remote device is free to roam in the remote site), the human force input to the local device and/or the position of the local device should[1] be tracked by the remote device. In the case of a hard-contact of remote device with the environment, however, these inputs should be counteracted if the force vector points into the obstacle. Hence, the force signal is simultaneously tracked for mimicking the user motion and is defied in case of a resisting force at the remote site. As if this is not challenging enough, when the user suddenly decides to release the local device, this resistance should die out as soon as possible, preventing a kickback. To sample the artificial nature of such behavior, consider a user who leans to a wall located at position $x_0\uparrow$, applying a horizontal force and then retreating after some time. It is not expected that the wall continues to push the user even after the user has the position $x < x_0$. This is not only unrealistic but also misleading as it can be confused

---

[1]or better, that's what we believe today

with a sticky surface as far as the immersion is concerned. There are many other scenarios that would further complicate the requirements but, in short, the user and the environment properties are time-varying and make it difficult to design a straightforward control law such that these and many other details are handled properly, and more importantly, simultaneously.

With this short motivation, we can safely claim that looking at the overall system as a typical motion control system is not sufficient in terms of complexity (though necessary). In general, motion tracking specifications are a subset of the general performance requirements of the bilateral teleoperation systems.

The inception of the bilateral teleoperation technology is often attributed to the work of Raymond Goertz in Argonne National Laboratories, [42] (In [8], it's traced back to Nikola Tesla and, in [142], even some 16th century tools are accepted as precursors of the contemporary teleoperation). The main motivation of Goertz' work (similarly later in Europe by Vertut [154]) was handling and manipulating nuclear material, thus the very first teleoperators were purely mechanical to cope with the hostile environment conditions. Though not much happened in terms of commercial product realizations, the concept of telemanipulation kept its appeal and a large body of research was reported until the 1980s. In that decade, with the help of the ever-increasing computational power and the popularity of Virtual Reality (VR), teleoperation technology received more attention for a possible use in the space-, underwater-, and medical-related tasks. Together with the advances in control theory and network theory (e.g. [37, 103]), a more systematic control methodology is adopted. Especially, stability analysis results that can be related to design guidelines (physical parameter bounds, bandwidth limitations etc.) were utilized and limits of performance were explored. A particular phenomenon, namely the destabilizing effect of the delays in the teleoperation, lead the experts of the field to delve more into the systematic analysis tools and qualitative aspects of teleoperation. Especially, the use of the concepts; passivity, scattering transformations, and wave variables have become the standard methods of analysis and synthesis (see, e.g., [3, 46, 107]). We will start to summarize the advances from this point as this thesis is precisely built on top these systematic analysis and synthesis results gathered in the last two decades. However, the reader is refered to [14, 62], and [142] for a more detailed overview including other practical aspects of teleoperation analysis and the hardware developments with a more historical perspective which we will omit here.

As we keep on narrowing down our focus to the control theoretical parts of this challenging problem, we have to note that many parts of the bilateral teleoperation problem can be scrutinized under different frameworks. Hence, there is no shortage of techniques for which bilateral teleoperation problem is an ideal test case. In this plethora of methods, for example, the variation of human and environment
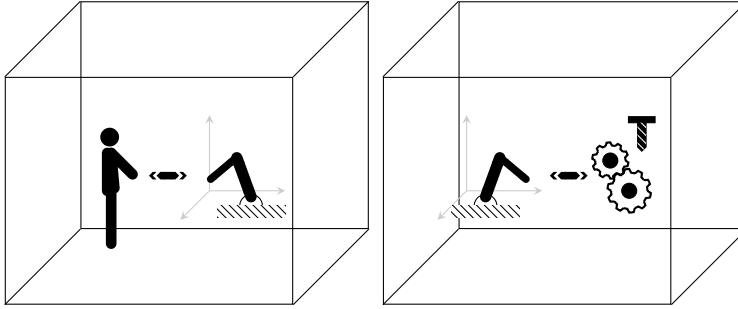
Figure 2.1: General Teleoperation System

properties give naturally rise to a robust or an adaptive control approach, the hard-contact problem can be analyzed under switched control systems, jump control systems or constrained linear systems etc. Thanks to these advances, as we will elaborate later, the main unsolved problem is not a methodolgical one but a motivational one. In other words we are lacking a fundamental understanding of the problem not the solution methods in terms of what the requirements are and what a good device is if compared to another. Before we go into the details of the proposed methods of this thesis, let us sample a few important and successful approaches reported so far together with their shortcomings if any. We emphasize that the literature covered here is far from comprehensive and deliberately shaped with pragmatic intentions. Hence a large body of research is left out. This is certainly not due to their lack of thoroughness or else, but simply due to the irrelevance to the purpose of this chapter.

2.1   Modeling of Bilateral Teleoperation Systems

The dominating modeling paradigm of bilateral teleoperation systems is the two-port network approach. Consider the following quote from 1989:

> The modeling approach is to transform the teleoperation system model into an electrical circuit and simulate it using SPICE, the electronic circuit simulation program developed at UC Berkeley. ([46])

As seen from Hannaford's motivation, the computer-based simulation tools are used extensively since then. Arguably this is one of the main reasons why network based electrical circuit based modeling dominated the teleoperation literature. Reinforced with the circuit simulation tools, experts of the field started to construct analogies that go beyond a mere mechanical-electrical system analogy.

Arguably, the most prominent concept borrowed from these analogies is the two-port network view of the bilateral teleoperation systems. The reader is referred to Appendix A for a short recap of network theory. Today, the quoted convenience also applies to almost all physical systems i.e. one can simulate arbitrary models via many computational packages. Yet, it's a de facto standard to use the circuit modeling while the teleoperation devices are mostly mechanical. Hence, it's not clear whether the benefit of such an artificial step still exists. Once the system is represented by a mathematical model, as it is demonstrated in the later sections, the mechanical/electrical analogy is, roughly, an equivalence based on the resulting model and works in the electrical→mechanical direction too. Therefore, the circuit based modeling is merely a convention rather than a requirement.

2.1.1   *Two-port Modeling of Teleoperation Systems*

In the teleoperation context, if one uses the "load-source" analogy for the manipulated environment and the human, then the system models all the bilateral interaction between the load and the source ports (as in Figure 2.2a). This modeling view is quite powerful since the components are described via their input/output (or external) properties i.e. across variable/through variable relations (e.g. force/velocity, voltage/current etc.). Also, the non/linearity properties of the components are not relevant at the outset if we are only interested in energy exchange which is the basis of the so-called Time-Domain Passivity Methods [47] which we will mention later in this chapter. Thus, the user, the control system, the environment, the remote and local devices and communication delays are seen as 1- and 2-ports exchanging energy in time. Since the external behavior of the ports can be characterized completely by the current and the voltage drop across the terminals, it is indeed very convenient to model these components as interacting "black boxes" (See Figure 2.2a).

Remark 1. *We should emphasize here that in this context, the energy exchange is used as a gauge of a potentially unstable behavior. The motivation relies on the fact that in order to classify a system as an unstable one, the system should exhibit unstable behavior at its port(s) and to exhibit such behavior additional energy is needed. Hence if all the components are incapable of contributing energy in the loop, finite energy excitations will be eventually decay and the system would reach to its steady state after a transient response[2]. As one can directly identify, this is simply the rough sketch of the celebrated passivity theorem. Based on this argument, there is a recurring theme in the literature that a teleoperation system should be passive in order to have a stable interconnection. As we will mention later, this is due to the hypothesis that end terminations are also passive. However, in a few*

---

[2]For the sake of brevity, eigenvalues on the imaginary axis or limit cycles are left out at this point.
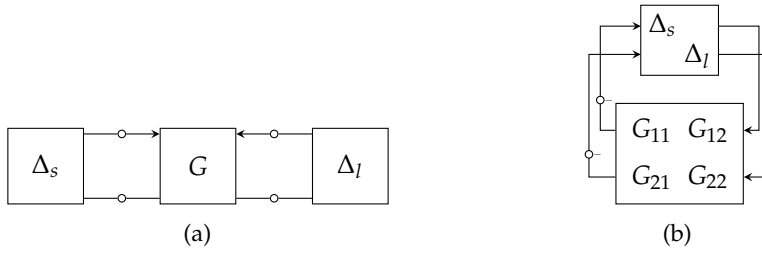
Figure 2.2: Two representations of a 2-port network.

studies, this is mistakenly taken as a sufficient and necessary condition and hence creates quite some confusion for the non-experts of the field. Passivity is not an essential feature of the teleoperation systems but only a convenient shortcut for stability. We should iterate that the stability is the top-priority objective and does not require passivity by any means even if we do guarantee stability by rendering the sub-components passive.

Clearly, thanks to this modeling method, we don't even need to know exactly what Δ_l, Δ_s blocks are, except their class (e.g. linear/nonlinear, time invariant/time varying etc.) to analyze the interconnection via G and its port behavior. Thus, the problem of modeling of the human arm or of the uncertain environment is circumvented. However, with the same reasoning, passivity property does not distinguish particular systems as long as they are passive. That is to say, some of the crucial information is lost about these specific ports, we discard any impedance or admittance relations shared by the port variables.

Energy based modeling is also the natural basis of bond-graphs. Bond-graphs, much like port representations, are graphical tools to model the dynamical systems via energy balancing between subcomponents (See [40] for an introduction). In other words, the bond-graphs are built on top of the notion of bonds representing the instant energy or power exchange between nodes via edges drawn between them. Therefore, bond-graphs already presents a powerful framework for abstraction of the bilateral interaction between the local and the remote site. For a classical use of bond-graphs in impedance control, the reader is referred to the Hogan's trilogy ([59–61]). There are also many studies with application focus, e.g., [82] using hydraulic systems for bilateral teleoperation among many others.

2.1.2 *Assumptions on the Local and Remote "Ports"*

As mentioned above, network theory offers a great opportunity for modeling the teleoperation systems, or better, avoiding the refined modeling. Still, to invoke the stability analysis and synthesis results of the network theory there is a need to

further distinguish Δ_s, Δ_l from the universum of 1-ports. Otherwise there is not much we can conclude from such an interconnection, put differently, they can be any arbitrary models with arbitrary behavior set as long as they respect the port condition. This is obviously a crude approximation of the real physical interaction that teleoperation systems exhibit.

In teleoperation and haptics literature, it is customary to assume the load and the source terminations as "passive" mathematical operators (see Appendix A). Starting with this hypothesis, the stability problem can be converted to a typical energy dissipation problem. Hence the view of the designer is tuned to watch for the energy sources and interaction between two distant media. This approach treats the human and the environment as passive 1-port circuit elements with additional effort sources modeling the intentional force input to the system. The controller(s) act as the energy regulator preventing excess energy generation to avoid a possible instability. Moreover, as summarized in Appendix A and in Chapter 3, one can use the network theory based conditions to assess the stability and performance conditions thanks to this hypothesis.

This brings us to the discussion of the justification of the assumption as it is generally not given in full generality in the literature. If one scans through the literature about the passivity of human operators, it is the Hogan's paper [58] that is almost universally cited. The striking detail is, however, that Hogan never claims that the human hand/arm is a passive system. Instead he clearly shows that under certain conditions, human behavior is indistinguishable from that of a passive system:

> Thus, despite the fact that the limb is actively controlled by neuro-muscular feedback, its apparent stiffness is equivalent to that of a completely passive system. In the light of Colgate's recent proof [3][3] that an apparently passive impedance is the necessary and sufficient condition for a stable actively-controlled system to remain stable on contact with an arbitrary passive environment, this experimental result strongly suggests that neural feedback in the human arm is carefully tuned to preserve stability under the widest possible set of conditions.

Moreover, the task that is given to human operators and analyzed afterwards, can be considered as a biased one because the success of the test is related to the passive behavior of the human. The task is, roughly speaking, holding a handle which is perturbed by random disturbances and trying to keep the handle still at a predefined position on the 2D plane. Hence, the task is simply to mimic a passive system. Had it been the case that the human would exhibit non-symmetric

---

[3]Reference [22] of this thesis.

stiffness matrix, it would simply be a failure of the test subject (regardless of the physical limitations of the human arm in general). Note that this is a plausible situation for the rehabilitation tasks. The other possibility would then be that the test subject was unable to keep up with the changes, or using the control theory jargon, the bandwidth of the subject was lower than the required agility to perform the test adequately. The well-known phenomenon due to such behavior is the "pilot induced oscillations" in which the pilot of an aircraft, while trying to stabilize the aircraft, via overcorrection inputs, destabilizes the system due to many distinct reasons (the phase lag of the pilot, response time of the aircraft etc.). We refer to the interesting report [97] for a more detailed exposition. Also, if for some reason, the task at hand is to prevent the system to reach a steady state at a certain position and the perturbations are applied accordingly i.e., to create a virtual negative potential, the results obtained from the experiments would most probably differ from that of [105]. Thus, it's emphasized here that the passivity of the human is closely linked to the task requirements.

Remark 2. *A particular detail should be clarified about the measurements taken in [58]. It is stated that:*

> *While normal human subjects held the handle of the manipulandum at a stable position in the workspace, small perturbations were applied. Measurements of the human's restoring force were made after the system had returned to steady state following the perturbation but before the onset of voluntary intervention by the subjects.*

Therefore, it is emphasized that only the involuntary response is taken into account during the measurements in order to capture the natural properties human arm before the human correction intervenes.

We believe that it is unaviodable to introduce some concepts from the muscle physiology in order to put Hogan's argument into some mechanical engineering perspective. It is simply impossible for the author to form a detailed analysis, however, mentioning the involved process via some mechanical analogies in order to relate the results of Hogan and Mussa-Ivaldi seems feasible. This would emphasize the reason why we think that the common inference from their experiments in the literature is not inline with the conclusions of these studies. We refer the reader to the physiology literature e.g., [41, 63, 101, 109, 145, 160] and references therein for a full treatment. Hence, we will only give a rough picture about the apparent behavior. Nevertheless the point that we want to emphasize is, fortunately, not related to the inner workings of the human muscles.

The skeletal muscle activation takes place via a process described by the *sliding filaments model*. The muscles consist of muscle fibers and muscle fibers are made
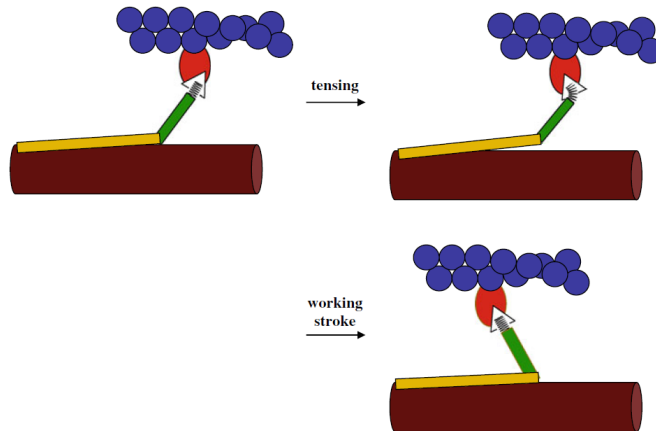
Figure 2.3: Muscle activation mechanism (taken from [109]) Going to be drawn from scratch!!

up of *myofibrils*. The myofibrils involve different types of thin and thick filaments, mainly of the type *actin*, *myosin* and *titin* filaments. The myosin filaments involve extensions that can bind to the thin actin filaments. The relative motion of these filaments are produced due to these extensions via ATP hydrolysis. Moreover, these extensions stay connected or disconnected to actin filament unless more ATP is utilized. Hence, the muscle needs extra energy to relax which is the reason behind "*rigor mortis*" and some types of the muscle spasms when this additional energy source can not be provided or ATP can not bind to the actin filament for some reason.

According to the articles given above, the muscle activation is analogous to a clock escapement mechanism [52]. But in our opinion, one can better use an analogy of a mechanical pencil clutch and sliding filaments with the exception that the spring action is absent in the muscle cell. In other words, when pressed from the eraser head mechanical pencil stays open such that the graphite layer can slide freely until the eraser cap is pulled back. Another important difference is that muscle behavior is not rachet-like but smooth due to the fact that each cycle takes place independently. Thus, at each time instant, different myosin extensions can be found at different phases of the cycle very much like a helical gear pair that are always in contact at one point. Using this analogy, ATP molecules are used to open and to close the pencil clutch made up of myosin extensions and actin filament is pushed forwards. Moreover, titin filaments can be thought as the connecting rod of the pencil from the cap to the clutch which is mostly responsible for the passive elasticity of the muscles.

Note that binding or detachment of these extensions is also regulated by the
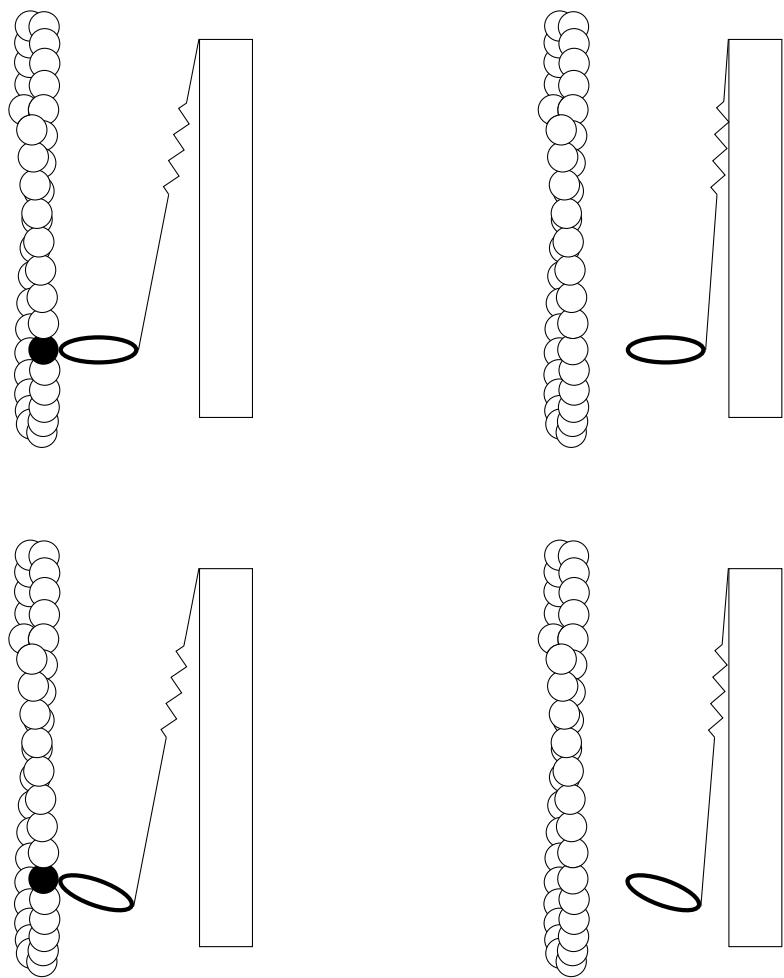
Figure 2.4: asdfasdf

Ca^{++} concentration in the muscle cell and controlled, eventually, by motor neurons using yet another chemical trigger. For the sake of simplicity, we would call a muscle cell activated if the myosin extensions are binded to actin filament.

Coming back to our original discussion, the stiffness of the arm that has been the subject of the experiments mentioned above is, again invoking the analogy, based on the closed clutch response of the arm. In other words, the brain activates a certain number of muscle cells at each limb and when a perturbation is applied what is measured is a cumulative spring-like behavior of the titin filaments, muscle tendons, and the bindings resisting to the applied strain. This is related to the "human's restoring force" given in Remark 2.

Having a spring-like property naturally implies that the arm is passive. But the problem with this argument,as far as the author understands, is that there is no reason to assume that the human arm exhibits a symmetric positive definite matrix at each time instant for an arbitrary trajectory. In fact, as shown clearly in [105], the major eigenvector of the stiffness matrix varies both in terms of direction and magnitude. Therefore, it might be possible to extract energy from the human arm with some particular pathological trajectory. Just in the case of a frozen time analysis of a time-varying operator does not imply stability, the conclusion is only valid for postural analysis at a fixed configuration of the human arm but not for an arm trajectory.

Therefore, it is our belief that the assumption of human arm being a passive operator is not an experimentally validated one.

Since it is customary to include the passivity hypothesis in the literature, we will assume that it is so. The question of how, then, a human can possibly move anything while remaining passive is one that makes the whole story even more complicated. The voluntary input of the human is taken as an exogenous and state independent input to the system. Hence, the human cognitive input is an additional but independent force source acting on the handle together with the passive human arm immitance.

The reader would spot that this is not inline with Hogan's remark since the activation state in the muscle cells should be altered in order to apply force. Once again, invoking our pencil analogy, we have to initiate a super-fast push-pull action on the eraser cap of the pencil. This would certainly alter the postural stiffness matrix but we have neither experience nor expertise to find out how. But, to the best of our knowledge, this is not given in any teleoperation study. In other words, the answer to the question of whether the human's restoring force would exhibit the same properties during the force exertion phase is not known to us. It has been also shown that muscle force is also related to the muscle tension-length properties [64] which we have not considered in our analogy.

Therefore, we have to further separate the human force into two parts, namely,

the active neuromuscular feedback force that keeps the human arm passive and the voluntary and cognitive force input applied to the system. How this is usually performed is not clear in the literature. To the best of our knowledge, this issue is considered (but still briefly) only in [73, Sec. II.B] and references therein.

This ambiguity becomes much more important since the control oriented focus of this thesis necessitates that we concentrate on worst cases rather than the experiments performed within the cognitive range of human operators. In other words, we are interested in the cases where things go wrong due to many other various reasons, sampling disturbances, measurement noises, directionality etc. Therefore it cannot be a satisfactory argument if stability depends on the user's neuromuscular feedback or simply user's stabilization capabilities. In order to use the bilateral teleoperation devices in real-life cases, stability should be addressed regardless of human actions. Hogan's findings are not sufficient for supporting the passivity assumption often found in the literature.

In summary, the passivity of the human and the environment (virtual environment in haptics/virtual reality applications), is only plausible in certain cases which should be verified nevertheless in order to assume that the corresponding mathematical models are passive. Still, analysis and synthesis methods that invoke this assumption lead to many real-world implementations with varying degrees of realism. We argue that the success of these methods is due to the conservatism of the analysis/synthesis tools and does not validate the passivity hypotheses on the respective models.

A compact version of the argument above is given by Yokokohji and Yoshikawa in [162]:

> Passivity of the system can be a sufficient condition of stability only when the system interacts passive environments. In the case of master-slave systems, if we could assume that the operator and the environment are passive systems, then the sufficient condition of stability is that the master-slave system itself must be passive. Strictly speaking, however, the operator is not passive because he/she has muscles as the power source. Colgate et al. [21][4] mentioned that even if the system has an active term, the system stability is guaranteed unless the active term is in some way state dependent. Obviously, the operator is passive when $\tau_{op} = 0$. Therefore, we will give the following assumption about τ_{op}: "*The operators input τ_{op} independent to the state of the master-slave system. In other words, the operator does not generate τ_{op} that will cause the system to be unstable.*" Dudragne et al. [3] gave a similar assumption in order to use the concept of passivity for stability distinction. The above

---

[4]Reference [22] of this thesis

assumption seems tricky in a sense, but it is necessary to ensure the system stability by the passivity.

Finally, a supplementary remark is also given by Buerger and Hogan in [13]:

> When passivity is used as a stability objective, the only assumption made about the environment is that it, too, is passive. This is likely sufficient to guarantee coupled stability with humans (though, to date, it has not been conclusively proven that human limbs are passive; see [29][5] for an argument for treating them as such). However, given the properties of human arms described above, passivity is unnecessarily restrictive. Our experience has shown that some controllers that are known to be nonpassive are adequately stable in clinical rehabilitation tasks [26].

We should mention here that Hogan's paper together with other identification experiments are extremely important for many fields and needs no motivation. The discussion above only points out that the frequently reported inference that follows from his results, is not inline with the results.

The idea of modeling the teleoperation as a two-port network seems to have multiple origins and we have no reference to point out to a common source. However, in general, the popularity of two-ports can be attributed to [3, 46, 107, 123, 162].

2.1.3 *Uncertain Models of Bilateral Teleoperation for Robustness Tests*

Another possibility of modeling the human arm and its cognitive input is to define a reference position signal "filtered" by the human arm impedance[6] e.g., [73, 89]. Various studies pointed out that the identification experiments suggest a mass-spring-damper system pattern is evident in the frequency response data of the human arm recorded under various task performance similar to the one given in [58]. The general method is to instruct the human to perform a specific task and then perturb the hardware with certain predesigned disturbance signals such that the output can be evaluated to obtain a mathematical model. In the literature, the model structure is often set a priori to be a second order transfer function and the parameters are optimized to minimize the mismatch between the experimental and predicted response. It is also well-known that the human can change the inherent impedance of the arm during the task execution (see, e.g., [150]). Therefore, the

---

[5]Reference [58] in this thesis
[6]The term *impedance* is used in a more general sense than its common usage to denote LTI transfer functions such that no distinction is made between linear and nonlinear or time-invariant and time-varying operators.
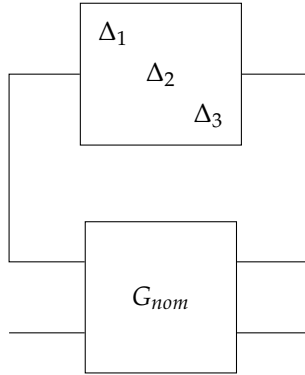
Figure 2.5: Uncertain model representation by taking out the uncertainty blocks

studies are performed in the ranges where it is safe to assume that the human arm characteristics are constant or constant up to negligible changes.

The modeling is straightforward via uncertain mass-spring-damper system differential equation manipulations. Suppose the human arm assumes the second order model:

$$M(\Delta_1)\ddot{x} + B(\Delta_2)\dot{x} + K(\Delta_3)x = F_h - F_m$$

where F_h, F_m denote the human force and the force feedback inputs, respectively. Then choosing a multiplicative or additive uncertainty structure and via basic linear fractional transformations, the signal relations are converted to the interconnection shown in Figure 2.5. The arrows are deliberately left out as it's up to the designer to get different immitance models.

Many studies have appeared in the literature regarding such modeling and the majority of these assume a mechanical model of order from two to five. Note that this is an assumption made a priori and only applies to the specific task performed by the human in the experiment from which the frequency response data is collected. The commonly utilized models can be found in [4, 13, 24, 36, 65, 73, 81, 86, 90, 144, 149]. Obtaining these measurements are time-consuming and difficult to parameterize. For this reason, although the results along this direction are scarce, they are, as in the passivity case, very valuable.

The disadvantage of such parametrization of the human arm is contrasted with the passivity approach methods invoking the argument of time-varying nature of the arm parameters. It is often rightfully argued that the uncertainty ranges in which the stiffness and damping (and partially inertial) coefficients change, are too large to be considered in the structured singular value based robustness tools. Moreover, many auxiliary effects such as the visual feedback, cognitive lag of the brain etc. are not considered in the identification experiments, but in the passivity

approach all of these are lumped into a single port condition. Obviously, the main difficulty is to get a model (out of hypothetical insights, identification experiments etc.) which is not required in the passivity approach.

The papers [89, 121] offer interesting alternatives for human modeling as they attempt to incorporate many of the aforementioned effects but the results are prospective and yet to be utilized.

2.2 Analysis

The stability analysis is one of the major problems in designing stable yet high-performance teleoperation systems. It's often not feasible to manually tune some local controllers and make test subjects use it in order to verify the design specifications. Moreover, relying only on the experiments can miss an important destabilizing scenario if the field experiments do not cover that particular case. Hence, an a priori certificate of stability is much sought after. The stability analysis can also give some guidelines about the parameter selection in the hardware design phase and can lead to minimized design iterations. Therefore, having a realistic stability test is essential in building these systems.

Similar to the modeling section, the analysis in the literature extensively relies on network theory based results. In fact this is where the network theory stands out as a complete tool for analysis and synthesis of bilateral teleoperation systems via the celebrated hypothesis that human and the environment models are passive.

The common terminology for stability is somewhat different than that of the contemporary control theory as *nominal stability* is used for the stability properties of isolated two disjoint media and when the interaction is setup between these two media the closed-loop stability problem is called *coupled stability*. To the best of our knowledge, this terminology is introduced in [22] hence we refer to this paper (or Colgate's thesis [21]) for a more detailed motivation.

It's also worth mentioning that the passivity and stability is used often interchangeably and also usually referred to the classical texts [16, 51, 102] for the precise definitions. Hence, there is a little guesswork required to classify the stability definitions given in the literature. The important distinguishing point is that the marginal stability is often accepted in the definition of stability results since it arises frequently in lossless (hence passive) models where energy conservation is assumed. However, the analysis results often rely on such assumptions do not guarantee asymptotic interconnection stability but only lead to certain passivity properties of the interconnection (see [75, Thm. 6.1] and [87, Sec. V] for the discussion on strict passivity).

As given in Section 2.1, passivity property is crucial to many studies in the literature. The direct physical interpretation of the abstract concepts gives even

Figure 2.6: A transparent two-port network with passive terminations. The actuation of the railcar is taken as state-independent input to the system. (Source: Fred Dean Jr., [Flickr:Fred Dean Jnr])

more appeal to such energy book-keeping methods. Another advantage of passivity methods is that the nonlinear counterparts of the results are also available in the literature and relatively easy to utilize.

Theorem 1. *The negative feedback connection of two passive systems is passive. The negative feedback connection of a passive system with a strictly passive system is asymptotically stable.*

Note that, this result is valid for both nonlinear and linear systems. Invoking the theorem twice on the teleoperation system allows us to conclude that, under the passivity assumption of the human and the environment, if the two-port is passive then the interconnection is passive. Moreover, if any of the involved operators is strictly passive the teleoperation system is asymptotically stable.

The passivity assumptions are not necessary for stability but only sufficient. Because there exist stable interconnections that involves nonpassive subsystems. Hence, the conservatism brought in by passivity theorem is quite high (especially in the nonlinear case). Facetious as it may seem, the test also takes into account the port terminations shown in Figure 2.6 for a table-top joystick. We have to emphasize that the three-carriage railcar with two cabs, is a valid, almost perfectly transparent two-port network. It's that conservative.

The major disadvantage of the passivity methods is that the procedure is focused almost only on the energy exchange. The performance specifications are very difficult to formulate and also difficult to integrate into the analysis and synthesis steps using only the inner product structure. As an example, the signals that are not port variables such as position errors, and nonlinear effects that are

functions of these signals, can't be utilized easily in the performance specifications. Same difficulty arises in the normed space structures though much can be achieved. Unfortunately, much sought after $\mathcal{L}_\infty$ methods are not mature enough to handle any practical system without excessive conservatism.

Another disadvantage is that the power- or the energy-based analysis, due to the inner-product structure, can not distinguish the individual signal properties. Consider the ideal case where the human and the local device is pushing each other and cancelling each other's contribution. In this case the external or observable energy exchange based on the port variables is zero (negligible) which can not be distinguished from the case of not touching at all (a small motion on the device).

When the network,human, and the environment models are assumed to be Linear Time Invariant (LTI), the frequency domain methods allow us the analyze the teleoperation systems for stability and performance. The most common stabiliy analysis tool for such models is the Llewellyn's stability criteria (also often called absolute stability theorem or unconditional stability theorem). For linear networks, the following definitions seem to be used quite widely (modified from [16]):

Definition 1 (Potential Instability at $i\omega_0$)**.** *A two-port network is said to be potentially unstable at $i\omega_0$ on the real frequency, if there exist two passive one-port immitances that, when terminated at the ports, produce a persisting natural frequency at $i\omega_0$.*

Definition 2 (Absolute Stability at $i\omega_0$)**.** *A two-port network is said to be absolutely stable at $i\omega_0$ on the real frequency, if it is not potentially unstable at $i\omega_0$.*

Note that when the models are assumed to be LTI then absolute stability theorem is an exact stability characterization.

2.2.1 *Llewellyn Stability Criteria*

The well known conditions for stability of a two-port network, formulated in [11, 91, 127], are recalled in Appendix A. As shown in [127], the conditions stated in Theorem 23 are invariant under immitance substitution. This result forms the basis for almost all passivity-based frequency domain bilateral teleoperation stability analysis approaches in the literature. We would also derive this theorem from an IQC perspective and show that it is actually the passivity counterpart of the of the D-scalings in the μ-tools. Thanks to the frequency domain formulation, it is possible to rewrite the condition (A.12) as a fraction and see the problematic regions in which the fraction gets close to or crosses to the instability, together with one of the conditions given in (A.11).
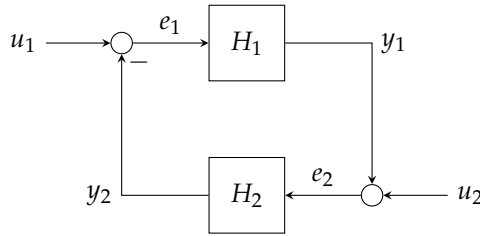
Figure 2.7: Negative feedback interconnection

2.2.2   *μ-analysis*

As given in Section 2.1.3, stability in the face of uncertainties can also be analyzed in the generalized plant framework of robust control. After rewriting the signal relations, the teleoperation system can be written as an uncertain interconnection as shown in Figure 2.8. In this setting, G is the model of the nominal bilateral teleoperation system and Δ is a block diagonal collection of uncertainties, such as the human, the environment, delays, etc. Stability tests are based on structural hypotheses on the diagonal blocks of the operator Δ such as gain bounds or passivity. These properties should allow us to develop numerically verifiable conditions for the system G that guarantee interconnection stability. This is intuitive because we have no access to the actual Δ and we can only describe its components by means of indirect properties.

If the interconnection subsystems are represented in the scattering parameters, the μ test is precisely equivalent to the test of Llewellyn's theorem and often called as Rollett's stability parameter. This is due to the well-known equivalence between the small-gain and passivity theorem [28]. We have to note that the equivalence is stated in terms of the stability characterization. Otherwise, small-gain theorem requires a normed space structure whereas passivity theorem requires an inner product space structure, hence the applicability is relatively limited. This is also related to the fact that we need to work with power variables exclusively in the passivity framework and this is not always convenient if the performance specifications are related to other variables.

In the literature, this analysis method often follows the scattering transformations such that, the passivity assumption avoids the explicit modeling and small-gain theorem allows to handle the delay problem via with bounded operators. A refinement can be found in [120] as the authors utilize a direct μ-analysis to reduce the conservatism, however rather remarkably, it's not picked up by other studies and the analysis is mainly limited to small-gain conditions even in the linear cases.
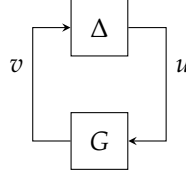
Figure 2.8: Uncertain Interconnection

We can also directly take the uncertain modeling of the human and the environment and utilize μ-analysis for the teleoperation system.

2.2.3 *Modeling the Communication Delay*

Over the past two decades, it has been confirmed in various studies that, if present, the communication delays are a major source of instability (reports date back to 60's, e.g., [141] and the references in [3]). Even when the delay duration t is known and constant, delay operator can be shown to be nonpassive since e^{-st} is not positive real. Hence, when combined with the passivity framework, it violates the assumptions on the uncertain operators.

At end of the 80's and early 90's, two prominent studies ([3, 107]) proposed a direct handle to handle delay robustness problem using the scattering transformations. This notion is best explained, in our humble opinion, by loop transformations since the original articles refer to microwave and transmission line theories which use quite specialized terminology. One can also find a slightly different system theoretical view of these transformations in [23]. If we restrict the discussion to LTI operators[7], the key concept of the scattering transformation or the wave variables methods is mapping the closed right half plane to the closed unit disk via a special case of bijective Möbius (or linear fractional or bilinear) transformations:

$$W : [0, \infty] \times i[-\infty, \infty] \mapsto \{z \in \mathbb{C} \mid |z| \leq 1\} \ , \ W(z) = \frac{z-1}{z+1} \tag{2.1}$$

One can directly verify that $1 \mapsto 0, \infty \mapsto 1$ and $0 \mapsto -1$ under W. Pictorially, the mapping is given in Figure 2.9 using a Smith chart which is located at the origin. Hence, positive real transfer matrices become norm bounded by 1 such that we can analyze the interconnection using the small-gain theorem.

Let us demonstrate a few properties of this transformation. First, this mapping can be shown with a block diagram. Assume a proper positive real LTI SISO system $G(s)$ and let the input/output relation is given by $y = Gu$. Then, with a

---

[7]In the nonlinear case, it's a *completion of square* argument to switch from the inner product structure to a norm structure provided that the signal space is suitable for such operation.
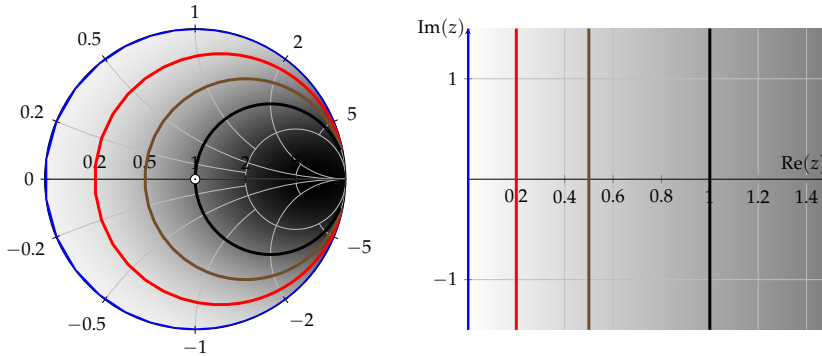
Figure 2.9: Mapping the closed right half plane onto the unit disc.

standard manipulation, we obtain a feedback interconnection that leads to the mapping

$$W(G(s)) = \frac{G(s) - 1}{G(s) + 1} = -1 + \frac{2G(s)}{G(s) + 1} \implies$$

Simply following the signal paths, we also see that the the input/output relation becomes

$$\tilde{y} := \sqrt{2}(-u + y) = W(G(s))\tilde{u} := W(G(s))\sqrt{2}(u + y).$$

Usually these variables are normalized with $\sqrt{2}$ at the outset. The distribution of $\sqrt{2}$ is a matter of convention and provides symmetry in the block diagrams. Also we have,

$$(W \circ W)(G) = \frac{-1}{G},$$
$$(W \circ W \circ W)(G) = \frac{-1}{W(G)},$$
$$(W \circ W \circ W \circ W)(G) = G$$

which is nothing but the $90°$ clock-wise rotations of the Riemann sphere about the axis parallel to the imaginary axis (W is an element of Möbius group with $\circ$ operation). This is closely related to the stability parameter of Edwards and Sinsky ([29]).

Obviously once this transformation is introduced, there is a need for the "inverse" of W on the operator that is seen by the operator G such that the loop equations remain unchanged, that is to say we have to introduce another
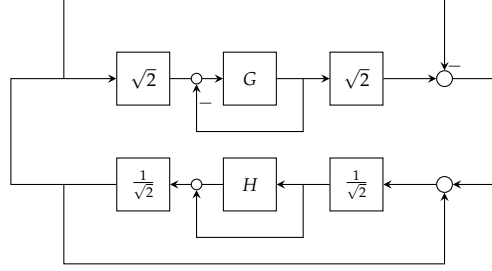
Figure 2.10: Scattering transformation and its inverse.

transformation that undoes W. The simplest way to obtain a mapping $\hat{W}$ is to follow the block diagram backwards as shown in Figure 2.10. A block diagram reduction step(or rotating three more times as shown above) shows that

$$\hat{W}(z) = -\frac{z+1}{z-1} = -\frac{1}{W(z)}$$

The negative sign usually does not show up in the formulations in the literature because the passive interconnections require a sign change in the loop to indicate the "from" and "to" ports. A more detailed derivation is given in [23]. Also note that a positive real transfer matrix, when negated, has its Nyquist curve confined in the close left half plane (anti-positive real) which is equivalent to a $180°$ rotation. Thus, some care is needed for the book-keeping of the negative signs and seemingly the best practice is to absorb the negative sign into H at the outset and work with $-H$ afterwards. This makes the required transformations identical. One can see that there are variants of this mapping, especially in wave variables definition, e.g., $\frac{z-b}{z+b}$ but for simplicity we take $b = 1$ as it doesn't play any role in our presentation of the method.

Under the mapping W, the Nyquist curve of e^{-sT} (unit circle) is mapped onto the imaginary axis, hence unbounded, i.e.

$$\frac{e^{-i\omega T} - 1}{e^{-i\omega T} + 1} = i\tan\frac{\omega T}{2}$$

One can also obtain a similar qualitative result by seeing the unit circle $\mathbb{T}$ as the image of the imaginary axis under W:

$$W(\mathbb{T}) = (W \circ W)(i\widetilde{\omega}T) = \frac{1}{i\widetilde{\omega}T}$$

We don't need to track the points individually as we are only interested in the domain and its image under these transformations.

This once again shows that delay uncertainty does not satisfy the norm constraint $\|W(e^{-i\omega t})\|_\infty \leq 1$ to invoke the small-gain theorem in the transformed coordinates. Had it been the case that the uncertainty was bounded by one, then it would have been possible to conclude stability directly in the passivity theorem anyhow. Thus, these transformations are not directly beneficial for analysis, however, following the cue from the previous mapping results, studies [3] and [107] made it possible to design controllers that takes into account this delay uncertainty. The resulting loop is stable regardless of delay period, hence they belong to the class of methods often distinguished by "delay-independent" methods. According to the literature, these are the most common methods applied in the face of delay uncertainty.

Delay is Small-Gain

Another possibility is to utilize the simple fact that the delay operator is gain-bounded and obtain the generalized plant by pulling out the uncertainty out of the loop. Obviously, this would be a very crude characterization of the unit circle since as unit disk is used as the uncertainty instead. However, as we show later, wave variables/scattering transformations directly use this conservative formulation to model the delay in the stabilization of the loop.

A similar approach is reported in [90] using μ-synthesis. By exploiting the low frequency property of the operator $e^{-sT} - 1$ and covering with a dynamic filter, the conservatism is reduced. But the authors have omitted the uncertainty of the human and the environment. Therefore, their analysis is only valid for nominal teleoperation systems. Though, this can be extended to more general cases, we have to note that, they don't consider the human as "some impedance+state-independent force input" but as an finite-energy force input signal filtered through the human characteristics. Technically, this amounts to the common disturbance input-filtering often used in the H_∞ design problems.

2.3 SYNTHESIS

Complementary to the analysis section, we cover a few popular controller structures among many others except the art of control engineering; manual PID tuning.

2.3.1 *Two-, Three-, and Four-Channel Control Architectures*

In the teleoperation literature, the control laws are categorized in terms of how many measurement signals are sent over to the opposite medium during the teleoperation for control. The actual controller synthesis method is often not

considered in this classification. Hence, the naming "*n*-channel control". The naming scheme can be better visualized as shown in Figure 2.11.

Position-Postion and Position-Force Controllers

The most basic control architecture among all is probably the PERR (position error) control in which the position of both local and the remote site devices are collected by the controller and control input is produced.

Assume that the local and the remote device are at rest at position $x = 0$ in the respective world coordinates. Also assume that the user moves the local device to position $x = 10\,\text{cm}$. What the control algorithm should do is to measure the position difference and force each device accordingly to minimize the error. Hence, the control law is of the form

$$\begin{pmatrix} F_l \\ F_r \end{pmatrix} = \begin{pmatrix} -1 \\ 1 \end{pmatrix} K_p(s)(x_l - x_r).$$

where F_r, F_l denote the control action at the local and the remote sites. $K(s)$ can be a constant or a SISO dynamical system or any other esoteric control law. One can perform the same with velocity signals (to comply with the passivity analysis) if available in noise-free measurements. Otherwise, position drift is unaviodable even with integral action.

Typically, this control architecture would give a sluggish performance since there is no preference or priority in correcting the error signal on each side. Therefore, while the remote site is pulled forward to track the local device, simultaneously, the local device is pushed back with the same force. This results with a feel similar to extending a damper, only in this case, it softens up according to the position error instead of travel velocity.

Another widely used, control architecture is the so-called Position-Force Controller. In this method the first channel in the PERR control structure is replaced with the remote site force input. Hence, local site device tracks the remote site encountered force while the remote site device tracks the position of the local site device.

$$\begin{pmatrix} F_l \\ F_r \end{pmatrix} = \begin{pmatrix} K_f(s)F_{env} \\ K(s)(x_l - x_r) \end{pmatrix}.$$

Clearly, the side-effect of PERR type control is avoided since the position and force errors are tracked independently in two seperate channels. But this brings in another tuning problem: If the position control gain dominates, the force tracking behaves aggresively in the hard contact case due to the overuse of control action to drive the remote device into the obstacle and generally results with kickback or the local device. Conversely, domination of the force gain results with chattering

of the remote device on the obstacle due to the discontinuous nature of the force reference signal if the user touches the handle with just softly enough to sustain an oscillation. Therefore, not only the gains of the individual channels are hard to tune, but also relative magnitudes of the gains makes the tuning more tedious.

Force-Force+PERR

To increase the bandwidth and to reduce the side-effects of aforementioned methods, a feedforward controller is added to the position-force control architecture.

$$\begin{pmatrix} F_l \\ F_r \end{pmatrix} = \begin{pmatrix} K_{f1}(s)F_{env} \\ K(s)(x_l - x_r) + K_{f2}(s)F_{hum} \end{pmatrix}.$$

Hence, the name a three-channel controller. This has been introduced in [50] and also analyzed in CITE!.

Lawrence Control Architecture

In [87], a general control scheme is proposed (later extended by [30, 48]). In this architecture, also the remaining channel of remote position is sent over to the local site, completing the number of channels transmitted to four. The individual controller blocks and the resulting overall block diagram is shown in Figure 2.11.

Instead of such classification, one can directly start with a MIMO control structure while keeping the control problem formulation fixed. For this purpose, consider the control mapping $K : \mathbb{R}^{n_1} \times \mathbb{R}^{n_2} \times \mathbb{R}^3 \times \mathbb{R}^3 \to \mathbb{R}^{m_1} \times \mathbb{R}^{m_2}$ from the measurements to the local and remote control actions via

$$\begin{pmatrix} F_l \\ F_r \end{pmatrix} = K \begin{pmatrix} x_l \\ x_r \\ F_{hum} \\ F_{env} \end{pmatrix} := \begin{bmatrix} -C_m & C_4 & C_5 & -C_2 \\ C_1 & C_s & C_3 & -C_6 \end{bmatrix} \begin{pmatrix} x_l \\ x_r \\ F_{hum} \\ F_{env} \end{pmatrix} \tag{2.2}$$

where n_1, n_2 denote the number position measurements and m_1, m_2 denote the actuation inputs with overactuated robotic manipulators in mind. The grayed entries are the control subcomponents that works with the variables sent over the network. If we recap the architectures above with this notation, they can be represented as

$$K = \begin{bmatrix} -k & k & 0 & 0 \\ k & -k & 0 & 0 \end{bmatrix} \begin{pmatrix} x_l \\ x_r \\ F_{hum} \\ F_{env} \end{pmatrix},$$
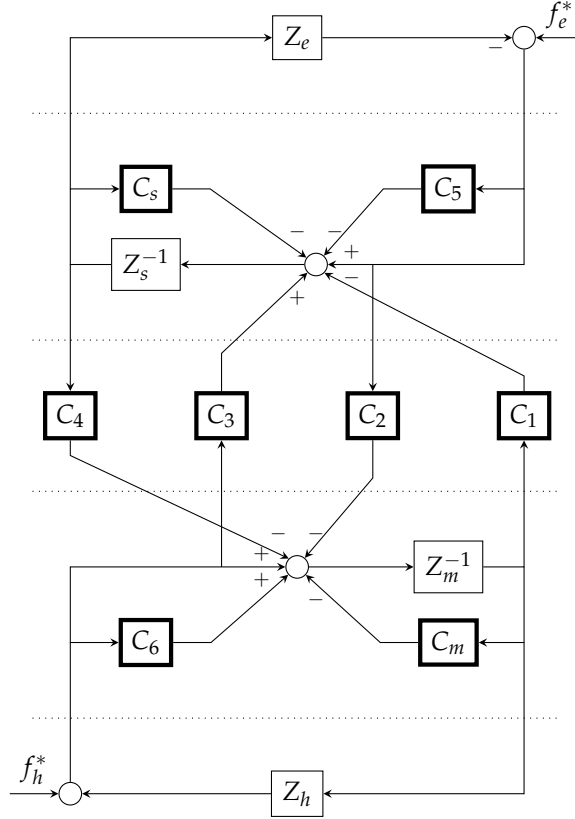
Figure 2.11: Extended Lawrence Architecture, adapted from [50]. Starred signals are the exogenous force inputs by the human/environment

$$K = \begin{bmatrix} 0 & 0 & 0 & k_f \\ k & -k & 0 & 0 \end{bmatrix} \begin{pmatrix} x_l \\ x_r \\ F_{hum} \\ F_{env} \end{pmatrix},$$

$$K = \begin{bmatrix} 0 & 0 & 0 & k_{f1} \\ k & -k & 0 & k_{f2} \end{bmatrix} \begin{pmatrix} x_l \\ x_r \\ F_{hum} \\ F_{env} \end{pmatrix}$$

respectively. Each of the lower case k_i represents some constant or dynamic controller. Obviously, one can generate many more architectures populating different entries and the zero blocks.
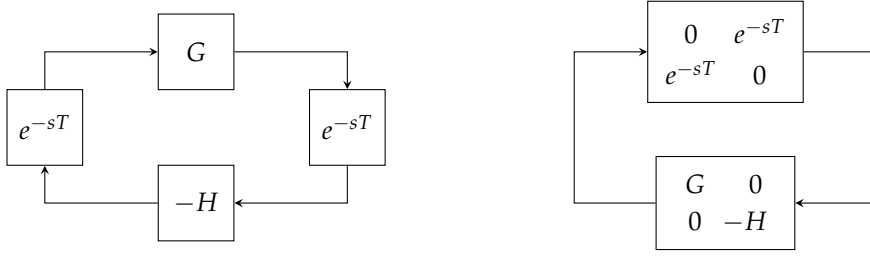
Figure 2.12: A delayed interconnection in the input/output setting and block diagram as a two block interconnection.

2.3.2 *Wave Variable-Scattering Transformation Control for delays*

We have discussed the transformation from a passive interconnection to small-gain interconnection however we have assumed that the interconnection did not involve any communication delays. When the delays are introduced to the loop as depicted in Figure 2.12, the transformations actually shift the stability problem from one domain to another. In other words, the transformations make the delay operators unbounded-gain as we have showed previously. Therefore, interconnection of passive and small-gain operators avoids to be handled by neither small-gain nor passivity theorems. Hence, we are left with the only option to modify the system. This technique has dominated the literature thanks to [3, 107, 108].

Suppose we are given strictly passive LTI systems G, H interconnected as shown in Figure 2.12 on the left with communication delays. We, then, rewrite the interconnection as a two block interconnection as shown on the right for which we will use the shorthand $P - \Delta$ interconnection (delay block being the Δ). Now if the system was small-gain we would directly conclude with stability since $\|\Delta\|_\infty = 1$, i.e.,

$$\begin{bmatrix} 0 & e^{i\omega T} \\ e^{i\omega T} & 0 \end{bmatrix} \begin{bmatrix} 0 & e^{-i\omega T} \\ e^{-i\omega T} & 0 \end{bmatrix} = I \quad \forall \omega, T$$

which also justifies why this methodology works regardless of the delays involved. However, we have P strictly passive, thus not necessarily a unity gain-bounded operator. But we have showed how to transform such operators into norm bounded ones. This is actually the key point of the wave variables. We simply use the mapping $W(P)$ and obtain

$$W(P) = (P - I)(P + 1)^{-1} = \begin{bmatrix} G - I & 0 \\ 0 & -H - I \end{bmatrix} \begin{bmatrix} G + I & 0 \\ 0 & -H + I \end{bmatrix}^{-1} \tag{2.3}$$

$$= \begin{bmatrix} W(G) & \\ & W(-H) \end{bmatrix} \tag{2.4}$$

This constitutes as a simple justification of the common "left" and "right" scattering transformation of the port terminations, leaving the delay operators in the "hybrid" structure untouched in the two port network terminology. Note that, we have only applied the mapping W to P and there is no inverse mapping to "undo" this in the loop. Technically speaking, this is not precisely a loop transformation but actually a change to the system structure via control action. The block diagrams that we have presented earlier is precisely achieved by the use of a feedforward/feedback control law, which can be represented by Equation (2.2), to create this transformation. The explicit derivation of the wave variable controller entries, in terms of a MIMO controller, is given in [20]. One can also verify that the control law given in [3] can be obtained via this formulation.

It is this very reason that the motivation often found in the literature is slightly misleading. Because, we did not and also could not do any modification on the delays. Quite the contrary, we have modified our system such that we can use the small-gain theorem to conclude stability in the face of Δ. Therefore, we refrain from seeing this method as a passification of the communication channel. It is certainly possible to reflect the transformation on Δ and invoke an impedance matching argument but we think that this only complicates the presentation since it's the change in the control action that stabilizes the loop, and not the change in the characteristics of the delay operator or making the communication line a lossless LC line. We have to emphasize that this transformation does not guarantee stability if the original P is not strictly passive. However if any other plant $\hat{P}$ from an arbitrary class of systems X can be brought into a unity norm-bounded form with some other transformation/control law. Then we can infer another set of physical interpretations as we would have X-ified the communication channel. However, the communication line stays untouched in both cases, though the control action on the system would be different. Therefore, it is, in our opinion, better to state the changes done on the system instead in terms of control laws.

Clearly, we have introduced the same conservatism by treating Δ as a gain-bounded operator that μ-analysis approaches also utilize. Moreover, we have directly transformed the strictly passive operator to a small-gain operator. In case of a passivity excess, i.e., the mapped operator is confined only in a subregion of the unit disk, we, yet again, introduce conservatism by using the small-gain theorem, for which one can shift the disk to the origin and use the scaled small-gain theorem to reduce the conservatism. We should note also that, this method works for any norm-bounded linear/nonlinear Δ operator as long as the passivity structure is preserved and certainly not limited to delays (as in the passivity case, it's that conservative).

Furthermore, if one shuffles the loop equations and bring the Δ block to a block diagonal form, it's possible to formulate a μ-synthesis problem. By doing so we

can recover the setup of [90]. Then, a wave variables control law above is in the subset of all stabilizing controllers set (due to the particular zero blocks in the controller structure). Thus, in terms of the conservatism involved, μ-synthesis with constant D-scalings ($D = I$) covers the wave variables controller design.

It has been noted the these control algorithms are prone to position drifts due to the velocity communication and different alternatives have been proposed to tackle this mismatch e.g., [19, 161]. Also there are generalizations of the scattering transformations available in the literature, e.g., [57] to exploit the degree of freedom on the mapping W using different rotation-scaling combinations for the unitary transformation matrix and also [147] for multidimensional systems. Delay problems are also addressed in this context e.g., [18, 104, 106, 152] and references therein.

2.3.3 *Time-Domain Passivity Control*

In [47], the passivity approach is formulated in time domain and the energy exchange is literally monitored and regulated. An initial version of this idea can also be found in [161]. The basic idea is to see whether at any port energy is generated, using a "passivity observer" (PO): for an N-port network the observed total energy is given by

$$E_{obsv}(n) = \sum_{k=0}^{n} \Delta T_k (F(k)^T V(k))$$

where ΔT_k is the sampling period at each step with nonuniform sampling in mind. If $E_{obsv}(n)$ is greater than or equal to zero then the energy is dissipated by the network, conversely if it is negative at some k, than the network has generated energy equal to the amount of $-E_{obsv}(n)$,. Note that this is a cumulative term and it is not implied that the energy is generated in the last step analogous to the integral-action control. Also, it has been shown that observing the energy flow only at the open-ports is sufficient to monitor the total "net" energy flow which is analogous to the observability concept in the linear control theory.

The "Passivity Control" (PC) is implemented on top of this as a virtual dissipative element. It relies on the passivity observer and if the energy generation is detected a dissipative element is introduced. The practical implementation is very similar to a safety relay circuit, e.g., it's only active when some relay switch is triggered. Depending on the causality (following the analogy, current sensing or voltage sensing relay), the PC can be implemented in series or parallel to the port.

This concept is then generalized to two-ports in [129, 130] and also results regarding the delay problem in the Time Domain Passivity Control context can be found in [128]. Since the essential architecture is a PI controller, it also suffers
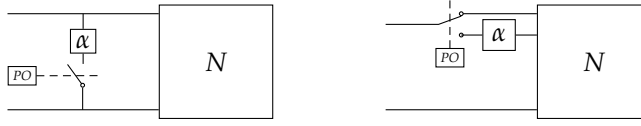
Figure 2.13: Passivity Controller (PC) implemetations.

from the same problems integral-action controllers suffer such as, wind-up and integrator reset etc. Some of these problems are addressed in [77].

2.3.4   *Others*

There are other approaches such as Energy Bounding Algorithm (EBA), [76, 139], sliding mode control, [15, 112], reset control, [155], model predictive control [9, 140] and many more which we will omit here since they are not directly related to the model-based control design methods which we will also propose.

   Once again this is a pragmatic choice and is intentional. We have not performed a rigorous comparison with any algorithm that is skipped in this brief and biased survey. It's our humble opinion, however, that a "one-size-fits-for-all" design toward operator- and task-aware control laws without dedicated modeling and/or classification, seems very unlikely to produce a generally applicable results with high-performance guarantees. Nevertheless, robust control at least addresses the conservatism reduction in a systematic way, if there is no other way to model the teleoperation systems.

   We have shown that most of the proposed methods in the literature use passivity or small-gain theorems and the involved mathematical operators are often indistinguishable from any other physical system. It's our belief that without any further refinements, all above methods can be shown to be, essentially, equivalent stability characterizations as far as the practical implications are concerned.

   As a closing remark, we would like refer to the outstanding survey of [78] which provides a comprehensive outlook to the teleoperation literature.

Analysis

This chapter is based mainly on our publication [118] which is partially presented at [115–117].

In the sequel, instead of 2-port networks, we rather consider system interconnections as depicted in Figure 3.1a. In this setting, G is the model of the nominal bilateral teleoperation system and Δ is a block diagonal collection of uncertainties, such as the human, the environment, delays, etc. Stability tests are based on structural hypotheses on the diagonal blocks of the operator Δ such as gain bounds or passivity. These properties should allow us to develop numerically verifiable conditions for the system G that guarantee interconnection stability. This is intuitive because we have no access to the actual Δ and we can only describe its components by means of indirect properties. Over the past three decades many classical stability results have been unified and generalized in this direction by utilizing quadratic forms (see [98] and [67, 131, 133]).

It is realistic to include a comprehensive treatment of this huge body research, but for the sake of completeness, we present the general methodology by sampling a few important special cases. To begin with, consider the following reformulation
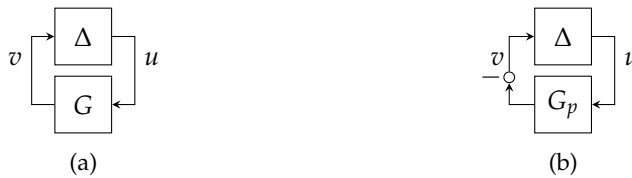
Figure 3.1: The general interconnection (a) and the assumed interconnection for passive systems (b). In general, the power variables require a sign change relative to the "from" and "to" ports in order to indicate the travel direction which translates to a negative sign in the block diagrams.

of the conditions of the small-gain theorem:

$$
\begin{aligned}
\|\Delta\|_\infty \leq 1 \\
\|G\|_\infty < 1
\end{aligned}
\iff
\begin{aligned}
\begin{pmatrix} \Delta(i\omega) \\ 1 \end{pmatrix}^* \begin{pmatrix} -1 & 0 \\ 0 & 1 \end{pmatrix} \begin{pmatrix} \Delta(i\omega) \\ 1 \end{pmatrix} \geq 0 \\
\begin{pmatrix} 1 \\ G(i\omega) \end{pmatrix}^* \begin{pmatrix} -1 & 0 \\ 0 & 1 \end{pmatrix} \begin{pmatrix} 1 \\ G(i\omega) \end{pmatrix} < 0
\end{aligned}
\tag{3.1}
$$

for all $\omega \in \mathbb{R}_e$. The middle 2×2 matrix on the right-hand side is called the "*multiplier*" (typically denoted by Π). It has been observed that the appearance of the same multiplier on both inequalities is far from a mere coincidence. In fact, it led to the following stability test: Assume that $G, \Delta \in \mathcal{RH}_\infty^{\bullet \times \bullet}$. Then, the $G - \Delta$ interconnection in Figure 3.1a is well posed and stable if there exists a Hermitian matrix Π such that

$$
\begin{pmatrix} \Delta(i\omega) \\ I \end{pmatrix}^* \Pi \begin{pmatrix} \Delta(i\omega) \\ I \end{pmatrix} \succeq 0, \quad \begin{pmatrix} I \\ G(i\omega) \end{pmatrix}^* \Pi \begin{pmatrix} I \\ G(i\omega) \end{pmatrix} \prec 0
\tag{3.2}
$$

hold for all $\omega \in \mathbb{R}_e$; one only requires the mild technical hypothesis that the left-upper/right-lower block of Π is negative/positive semi-definite. Thus, the intuition that we touched upon above is mathematically formalized by (3.2). Indeed, one can see that the former condition constrains the family of uncertainties, while the latter provides the related condition imposed on the plant for interconnection stability, both expressed in terms of the multiplier Π. In particular, we recover the passivity theorem in a similar fashion, if using the constant symmetric matrix $\Pi = \begin{pmatrix} 0 & I \\ I & 0 \end{pmatrix}$ as the multiplier under negative feedback. See [131] for a lucid "topological seperation" argument. Various other classical stability tests fall under this particular scenario based on the so-called static (frequency-independent) multipliers which, therefore, presents a significantly unified methodology.

If Δ admits a diagonal structure [as in Figure 2.2a], it is well known that the small-gain theorem and passivity theorem are conservative. A natural generalization toward a tighter analysis test is using a frequency-dependent Π matrix, which can be interpreted as adding dynamics to the multiplier. Two prominent examples of interest are the celebrated upper bound computations for μ or κ_m in robust control theory and, as we will show later, Llewellyn's stability conditions. As a shortcoming, these results are only valid for LTI operators but the real power and flexibility of these multiplier methods come from their generalizations to classes of nonlinear/time-varying operators via the IQC framework that appeared in [98].

An IQC for the input and output signals of Δ is expressed as

$$
\int_{-\infty}^{\infty} \begin{pmatrix} \widehat{\Delta(v)}(i\omega) \\ \hat{v}(i\omega) \end{pmatrix}^* \Pi(i\omega) \begin{pmatrix} \widehat{\Delta(v)}(i\omega) \\ \hat{v}(i\omega) \end{pmatrix} d\omega \succeq 0.
\tag{3.3}
$$

A bounded operator $\Delta : \mathcal{L}_2^m \to \mathcal{L}_2^n$ is said to satisfy the constraint defined by $\Pi(i\omega)$ if (3.3) holds for all $v \in \mathcal{L}_2^m$. The following sufficient stability condition for the interconnection in Figure 3.1a forms the basis for the IQC framework.

Theorem 2 ([98]). *Let $G \in \mathcal{R}\mathcal{H}_\infty^{m \times n}$ be given and let $\Delta : \mathcal{L}_2^m \to \mathcal{L}_2^n$ be a bounded causal operator. Suppose that*

1. *for every $\tau \in [0, 1]$, the interconnection of G and $\tau\Delta$ is well posed;*

2. *for every $\tau \in [0, 1]$, $\tau\Delta$ satisfies the IQC defined by $\Pi(i\omega)$ which is bounded as a function of $\omega \in \mathbb{R}$;*

3. *there exists some $\epsilon > 0$ such that*

$$\begin{pmatrix} I \\ G(i\omega) \end{pmatrix}^* \Pi(i\omega) \begin{pmatrix} I \\ G(i\omega) \end{pmatrix} \preceq -\epsilon I \text{ for all } \omega \in \mathbb{R}. \tag{3.4}$$

Then the $G - \Delta$ interconnection in Figure 3.1a is stable.

We include a few remarks about this result:

Remark 3. *Note that both properties 1 and 2 in Theorem 2 have to hold for $\tau\Delta$ if τ moves from $\tau = 0$ (for which stability is obvious) to the target value $\tau = 1$ (for which stability is desired). But, the reason for using a scalar τ is to scale the uncertainty size, therefore it does not have to be a multiplication operation, e.g., in the delay uncertainty cases, scaling the uncertainty τe^{-sT} is incorrect for the application of IQC theorem. Instead, the result can still be used if one considers $e^{-s\tau T}$ for $\tau \in [0, 1]$, as we will derive a multiplier class later in this chapter. In summary, the homotopy argument can be customized and by no means limited to $\tau\Delta$.*

Let the multiplier $\Pi(i\omega)$ partitioned as

$$\Pi = \begin{pmatrix} \Pi_1 & \Pi_2 \\ \Pi_2^* & \Pi_3 \end{pmatrix} \tag{3.5}$$

In our examples the left-upper $m \times m$ block is negative semi-definite for all $\omega \in \mathbb{R}_e$ which guarantees concavity. In other words, convex combinations of two particular uncertainty element Δ_1, Δ_2 that satisfies the IQC, also satisfy the IQC since

$$\begin{pmatrix} \tau\Delta_1 + (1-\tau)\Delta_2 \\ I \end{pmatrix}^* \begin{pmatrix} - & \cdot \\ \cdot & \cdot \end{pmatrix} \begin{pmatrix} \tau\Delta_1 + (1-\tau)\Delta_2 \\ I \end{pmatrix}$$

is a concave function. Furthermore, we assume that the right-lower $m \times m$ block of $\Pi(i\omega)$ positive semidefinite for all $\omega \in \mathbb{R}_e$. Then

$$\begin{pmatrix} 0 \\ I \end{pmatrix}^* \begin{pmatrix} \cdot & \cdot \\ \cdot & + \end{pmatrix} \begin{pmatrix} 0 \\ I \end{pmatrix} \geq 0$$

i.e. $0 \in \Delta$. *Hence, given a Δ that satisfies the IQC with $\Pi_1 \geq 0, \Pi_3 \leq 0$, select $\Delta_1 = 0, \Delta_2 = \Delta$, for every $\tau \in [0,1]$, $\tau\Delta$ satisfies the IQC. The reason why we are so interested in zero is the fact that when $\Delta = 0$, it corresponds to the (unperturbed) nominal system and, as is for the IQC theorem, many stability results rely on tracking the stability property while traveling on the nominal system→fully uncertain system path, say, via root loci, Nyquist test, root boundary crossing theorem, μ etc.*

It is then easy to see that (3.2) implies property 2 in Theorem 2; hence one only needs to verify (3.2) for the original uncertainty Δ.

Remark 4. *Often $\Pi(i\omega)$ is a continuous function of $\omega \in \mathbb{R}_e$. Then property 3 is equivalent to*

$$\begin{pmatrix} I \\ G(i\omega) \end{pmatrix}^* \Pi(i\omega) \begin{pmatrix} I \\ G(i\omega) \end{pmatrix} \prec 0 \text{ for all } \omega \in \mathbb{R}_e. \tag{3.6}$$

If Δ is LTI then (3.3) holds for all $v \in \mathcal{L}_2^m$ if and only if

$$\begin{pmatrix} \Delta(i\omega) \\ I \end{pmatrix}^* \Pi(i\omega) \begin{pmatrix} \Delta(i\omega) \\ I \end{pmatrix} \succeq 0 \text{ for all } \omega \in \mathbb{R}. \tag{3.7}$$

The IQC reduces to a frequency-domain inequality (FDI). This provides the link to our introductory discussion.

Suppose that Δ is LTI and $\Pi(i\omega)$ is a continuous function of $\omega \in \mathbb{R}_e$ and assume that (3.2) holds for both inequalities for all ω. Then, using the relations, $w = \Delta v, v = Gw$ for all $u, y \in \mathcal{L}_2$, we obtain the following contradiction

$$0 \preceq v^* \begin{pmatrix} \Delta \\ I \end{pmatrix}^* \Pi \begin{pmatrix} \Delta \\ I \end{pmatrix} v \tag{3.8}$$

$$= \begin{pmatrix} w \\ v \end{pmatrix}^* \Pi \begin{pmatrix} w \\ v \end{pmatrix} \tag{3.9}$$

$$= w^* \begin{pmatrix} I \\ G \end{pmatrix}^* \Pi \begin{pmatrix} I \\ G \end{pmatrix} w \tag{3.10}$$

$$\prec 0, \tag{3.11}$$

hence

$$\text{im} \begin{pmatrix} I \\ G \end{pmatrix} \cap \text{im} \begin{pmatrix} \Delta \\ I \end{pmatrix} = \{0\}, \forall \omega \in \mathbb{R}_e.$$

Using this we can conclude that

$$\det \begin{pmatrix} I & \Delta \\ G & I \end{pmatrix} \neq 0 \ \forall \omega \in \mathbb{R}_e$$

and, with an application of Schur complement formula, we have (3.6) *and* (3.7) *implying*

$$\det(I - G(i\omega)\Delta(i\omega)) \neq 0 \ \text{for all} \ \ \omega \in \mathbb{R}_e, \tag{3.12}$$

which is the precise condition that forms the basis of SSV theory [110]. This gives some intuition for the validity of the IQC theorem and relates to μ in SSV theory.

Remark 5. *In combination with the previous remarks, properties 2 and 3 imply* $\det(I - \tau G(\infty)\Delta(\infty)) \neq 0$ *for* $\tau \in [0, 1]$ *which is nothing but property 1. Two conclusions can be drawn: On one hand, under these circumstances property 1 is redundant in Theorem 2. On the other hand, if 1 and 2 have been verified, it suffices to check* (3.6) *only for finite* $\omega \in \mathbb{R}$ *in order to infer stability with the IQC theorem.*

If we have an IQC constraint that is satisfied for all $\Delta \in \mathbf{\Delta}$ with some particular uncertainty set $\mathbf{\Delta}$, checking robust stability boils down to the verification of the corresponding FDI (3.4) or (3.6). Instead of validating these in a frequency-by-frequency fashion, one can make use of the Kalman - Yakubovich - Popov (KYP) Lemma (see [125] and below) in order to convert the FDI into a genuine linear matrix inequality (LMI) by using state space representations. For the finite frequency intervals, one can further use the Generalized KYP Lemma ([66]) to limit the analysis to some physically relevant frequency band.

3.2 BASIC IQC MULTIPLIER CLASSES

In the previous section, we have shown how classical frequency domain techniques can be embedded into the IQC formulation. In this section, we focus on the types of existing multipliers for different uncertainty classes. Although they frequently appear in the robust control literature, we include them for completeness.

3.2.1 *Parametrized Passivity*

Another well-known version of the passivity theorem, which we will denote as theorem of parameterized passivity (see e.g. [28, Thm. VI.5.10]), allows to consider cases in which the "non-passivity" of some block is compensated by an excess of passivity in other blocks without endangering stability. This can even be utilized to determine the lowest tolerable level of passivity of the uncertainties for which a given interconnection remains stable. For output strictly passive uncertainties, stability can be characterized as in the next result, which is a direct consequence of the general IQC theorem.
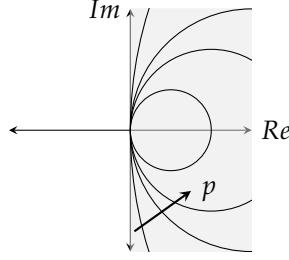
Figure 3.2: As p increases, the admissible region for the Nyquist curves of Δ shrinks to smaller disks in the right half plane.

Corollary 3. *The interconnection of $G_p, \Delta \in \mathcal{RH}_\infty^{\bullet \times \bullet}$ as in Figure 3.1b is stable if there exist a $p \geq 0$ such that*

$$\begin{pmatrix} \Delta(i\omega) \\ I \end{pmatrix}^* \begin{pmatrix} -pI & I \\ I & 0 \end{pmatrix} \begin{pmatrix} \Delta(i\omega) \\ I \end{pmatrix} \succeq 0 \tag{3.13}$$

$$\begin{pmatrix} I \\ -G_p(i\omega) \end{pmatrix}^* \begin{pmatrix} -pI & I \\ I & 0 \end{pmatrix} \begin{pmatrix} I \\ -G_p(i\omega) \end{pmatrix} \prec 0 \tag{3.14}$$

hold for all $\omega \in \mathbb{R}_e$.

Remark 6. *Note that (3.13) and (3.14) are nothing but*

$$\Delta(i\omega) + \Delta^*(i\omega) \succeq p\Delta^*(i\omega)\Delta(i\omega), \tag{3.15}$$

$$G_p(i\omega) + G_p^*(i\omega) \succ -pI. \tag{3.16}$$

The case $p = 0$ recovers the classical passivity theorem. Moreover, the larger the value of $p > 0$, the smaller is the set of uncertainties described by (3.15), as illustrated in Figure 3.2 for different values of p. In fact, this result is used in Colgate's condition thanks to the damping term b and closely related to the impedance bounds of Bounded Impedance Absolute Stability [45] using "impedance circles".

3.2.2 *Dynamic LTI Uncertainties*

Often system identification experiments lead to system representations that match the physical system within some tolerance levels. There can be also other sources of such frequency dependent mismatch and they are usually captured by frequency dependent weights. The usual practice is to define a nominal system that always "pass through middle point of the error bound" at each frequency and the rest is defined either multiplicatively that is in the form of $G_{nom}(I + W\Delta)$ or additively that is $G_{nom} + W\Delta$ which can be converted from one form to another.

For the sake of simplicity, let us assume that Δ, G_{nom} are SISO LTI systems. Since the magnitude of the uncertainty is scaled by the weight W and in turn the weight can be absorbed by the plant, without loss of generality, we can assume that $\|\Delta\|_\infty \leq 1$ i.e.

$$1 \geq \Delta(i\omega)^* \Delta(i\omega) \quad \forall \omega \in \mathbb{R}_e$$

Obviously, this inequality remains true if we multiply both sides with a positive scalar that is

$$\lambda \geq \lambda \Delta(i\omega)^* \Delta(i\omega) \quad \forall \omega \in \mathbb{R}_e, \lambda > 0$$

We can also represent this inequality as follows,

$$\begin{pmatrix} \Delta(i\omega) \\ 1 \end{pmatrix} \begin{pmatrix} -\lambda & 0 \\ 0 & \lambda \end{pmatrix} \begin{pmatrix} \Delta(i\omega) \\ 1 \end{pmatrix} \geq 0, \quad \forall \omega \in \mathbb{R}_e \lambda > 0$$

Note that, validity of this step relies on the commutative property of $\Delta\lambda = \lambda\Delta$. Hence, we have parametrized all the unity norm bounded uncertainty constraints. For some historical reason, this type of norm-bound multipliers is referred to as D scalings. In particular we have obtained the family of constant(static) D scalings. One can see that, we might use a different λ at each freqency and the inequality still holds true.

$$\begin{pmatrix} \Delta(i\omega) \\ 1 \end{pmatrix} \begin{pmatrix} -\lambda(i\omega) & 0 \\ 0 & \lambda(i\omega) \end{pmatrix} \begin{pmatrix} \Delta(i\omega) \\ 1 \end{pmatrix} \geq 0, \lambda(i\omega) > 0 \quad \forall \omega \in \mathbb{R}_e$$

Note again that this result relies on the commutativity property

$$\Delta(i\omega)\lambda(i\omega) = \lambda(i\omega)\Delta(i\omega).$$

This type of multipliers are the celebrated Dynamic D-scalings that are made famous by the μ-syntesis tool DK-iteration. Also, one can get a rough picture of the fast plant size growth in the DK-iteration process in the classical μ-synthesis. Since the approximation quality is increased via higher order terms as we try to reconstruct a function of ω from its finitely many discrete points, the approximate function involving the higher order terms absorbed by the plant at the D-analysis step for another K-synthesis step.

Now assume that $\Delta \in \mathcal{RH}_\infty^{n \times m}$. We can follow the same idea,

$$I \succeq \Delta(i\omega)^* \Delta(i\omega) \quad \forall \omega \in \mathbb{R}_e.$$

However, introducing a positive definite matrix λ necessitates a particular structure since we have lost the commutativity property i.e. $\Delta(i\omega)\lambda(i\omega) \neq \lambda(i\omega)\Delta(i\omega)$ in general[1]. The commutativity can be restored if we assume a diagonal structure,

---

[1]To the best of our knowledge, there is no systematic way to parameterize all matrices that satisfy $AB = BA$ for an arbitrary matrix A.

since $\Delta(i\omega)(\lambda_0(i\omega)I) = (\lambda_0(i\omega)I)\Delta(i\omega)$ where $\lambda_0 : \mathbb{R} \mapsto \mathbb{R}_+$. Thus, along the same lines with the SISO case, the constraints take the form

$$\begin{pmatrix} \Delta(i\omega) \\ I \end{pmatrix} \begin{pmatrix} -\lambda_0(i\omega)I & 0 \\ 0 & \lambda_0(i\omega)I \end{pmatrix} \begin{pmatrix} \Delta(i\omega) \\ I \end{pmatrix} \succeq 0, \lambda_0(i\omega) > 0 \quad \forall \omega \in \mathbb{R}_e$$

Clearly, one can repeat the same machinery for the repeated SISO Δ blocks to obtain "full-block" D-scalings.

As we have mentioned in the previous chapter and also will demonstrate again in this chapter, this particular multiplier type is the difference between small-gain theorem and μ-analysis, and a similar argument holds for passivity theorem and Llewellyn's criteria.

Furthermore, although it's conservative, we have to emphasize that constant scalings are often employed for the analysis of norm-bounded static or time-varying nonlinearities where the Fourier transform of Δ does not make sense.

3.2.3 *Real Parametric Uncertainties*

In many applications, the uncertainties also originate from the lack of the precision on the actual values of the parameters in the system model. This applies in particular to the models used in bilateral teleoperation. Parameters such as the stiffness and the damping of the environment or the human arm are the simplest examples of this kind. After re-scaling and shifting, the real parametric uncertainties are assumed to take values in the interval $[-r, r]$ centered around the nominal value zero.

LTI uncertain parameters

The well-known DG multiplier family ([33, 100]) is used to assess robustness against unknown but constant parameters. In fact, for all bounded functions $D : \mathbb{R} \mapsto (0, \infty)$ and $G : \mathbb{R} \mapsto i\mathbb{R}$ one has

$$\begin{pmatrix} \delta \\ 1 \end{pmatrix}^* \begin{pmatrix} -D(\omega) & G(\omega) \\ G^*(\omega) & r^2 D(\omega) \end{pmatrix} \begin{pmatrix} \delta \\ 1 \end{pmatrix} \geq 0$$

for all $\delta \in [-r, r]$, just because it reads as

$$-D(\omega)|\delta|^2 + r^2 D(\omega) + (G(\omega)^* + G(\omega))\delta \geq 0$$

this holds since $|\delta|^2 \leq r^2$, $D(\omega) > 0$ and $G(\omega) + G(\omega)^* = 0$. Hence, the realness property $\delta = \delta^*$ is exploited via G scalings for all the elements in the uncertainty set which otherwise are only constrained to be norm bounded by r. Similar to the dynamic LTI uncertainties, we enlarge the set of multipliers by adding dynamics.

As a remark on such multipliers, we give a simple example on how to modify the plant/multiplier if the parameter interval is not centered around zero which apply to all real parametric uncertainties given in this subsection. We assume that the parameter lives in the interval $[a, b]$ with/out some physical units with $ab > 0$.

- The first step is always to check whether zero is in the interval. If not, by dummy feedforward/feedback in the loop one can always set the interval such that zero is included. In other words, the parameter interval $[a, b]$ can be rewritten as $\frac{a+b}{2} + [\frac{a-b}{2}, \frac{b-a}{2}]$. Then, including the constant feedthrough term as a feedback loop in the plant we obtain $[-r, r]$ interval with $r = \frac{b-a}{/2}$.

- Alternatively, we can modify the multiplier using

$$\delta \in [a, b] \iff \left| \delta - \frac{b+a}{2} \right|^2 \leq \left(\frac{b-a}{2} \right)^2 \iff -\delta^2 + (b+a)\delta - ab \geq 0$$

and hence,

$$\begin{pmatrix} \delta \\ 1 \end{pmatrix}^* \begin{pmatrix} -D(\omega) & \frac{b+a}{2}D(\omega) + G(\omega) \\ \frac{b+a}{2}D(\omega) + G^*(\omega) & abD(\omega) \end{pmatrix} \begin{pmatrix} \delta \\ 1 \end{pmatrix} \geq 0.$$

Time-varying parameters with arbitrary rate of variation

In this case we employ constant multipliers; the time-varying parameter $\delta : [0, \infty) \mapsto [-r, r]$ satisfies the quadratic constraint

$$\begin{pmatrix} \delta(t) \\ 1 \end{pmatrix}^* \begin{pmatrix} -D & iG \\ -iG & r^2D \end{pmatrix} \begin{pmatrix} \delta(t) \\ 1 \end{pmatrix} \geq 0$$

for all $D > 0$, $G \in \mathbb{R}$ and for all $t \geq 0$. This implies the validity of (3.3) for the multiplication operator which maps $v \in \mathcal{L}_2^n$ into $w \in \mathcal{L}_2^n$ with $w(t) = \delta(t)v(t)$.

Time-varying parameters with bounded rate of variation

If there is a known bound on the rate-of-variation (ROV) of the time-varying parameter, it is conservative to use constant DG scalings. To characterize slowly-varying real parametric uncertainties, we use the so-called "swapping lemma" ([53, 69, 80], cf. [111]) which allows to take the ROV bound explicitly into account. For the sake of completeness, we include a scalar version of this well known result from adaptive control.

Lemma 4 (Swapping Lemma). *Consider the bounded and differentiable function $\delta : [0, \infty) \to \mathbb{R}$ whose derivative is bounded as $|\dot{\delta}(t)| \leq d$ for all $t \geq 0$. Moreover, let*

$T(s) = C(sI - A)^{-1}B + D$ be a transfer function with a stable state-space realization and define

$$T_c(s) := C(sI - A)^{-1}, \quad T_b(s) := (sI - A)^{-1}B.$$

If viewing T, T_c, T_b and δ (by point-wise multiplication) as operators $\mathcal{L}_2 \to \mathcal{L}_2$, one has $\delta T = T\delta + T_c \dot{\delta} T_b$ and thus

$$\underbrace{\begin{pmatrix} T & T_c \\ 0 & I \end{pmatrix}}_{T_{\text{left}}} \underbrace{\begin{pmatrix} \delta \\ \dot{\delta} T_b \end{pmatrix}}_{\Delta_s} = \underbrace{\begin{pmatrix} \delta & 0 \\ 0 & \dot{\delta} I \end{pmatrix}}_{\Delta_x} \underbrace{\begin{pmatrix} T \\ T_b \end{pmatrix}}_{T_{\text{right}}}$$

where x, s stand for "eXtended" and "Stacked" respectively.

We now claim that

$$\Pi(i\omega) = (\star)^* M_s \begin{pmatrix} T_{\text{left}}(i\omega) & 0 \\ 0 & T_{\text{right}}(i\omega) \end{pmatrix}$$

with

$$M_s = \begin{pmatrix} -D_a & 0 & iG_a & 0 \\ 0 & -D_b & 0 & iG_b \\ -iG_a & 0 & r^2 D_a & 0 \\ 0 & -iG_b & 0 & d^2 D_b \end{pmatrix}$$

for $T^* D_a T > 0$, $D_b > 0$ and G_a, $G_b \in \mathbb{R}$ is a valid IQC multiplier for the uncertainty Δ_s. In fact, one easily verifies

$$\begin{pmatrix} \Delta_x(t) \\ I \end{pmatrix}^T M_s \begin{pmatrix} \Delta_x(t) \\ I \end{pmatrix} \succeq 0 \text{ for all } t \geq 0$$

in the time domain. If we choose any $v \in \mathcal{L}_2$ and define $w = \begin{pmatrix} \Delta_x \\ I \end{pmatrix} T_{right} v$, we hence infer $\int_0^\infty w(t)^T M_s w(t)\, dt \geq 0$. On the other hand, due to Lemma 4, we also have

$$w = \begin{pmatrix} T_{\text{left}} \Delta_s \\ T_{\text{right}} \end{pmatrix} v = \begin{pmatrix} T_{\text{left}} & 0 \\ 0 & T_{\text{right}} \end{pmatrix} \begin{pmatrix} \delta \\ \dot{\delta} T_b \\ 1 \end{pmatrix}$$

which proves the claim. Thus, after augmenting the corresponding channel with zero columns so as to make the plant compatible with Δ_s, the robustness test can be performed.
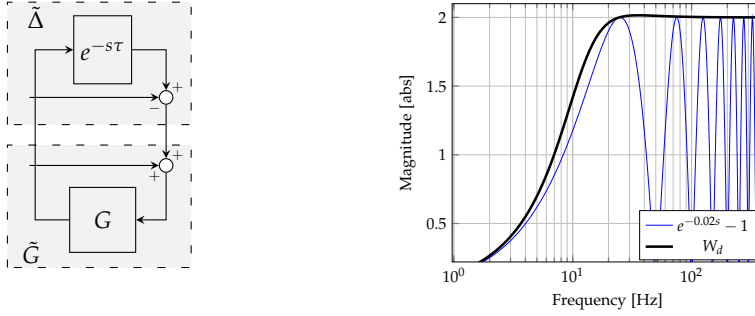
Figure 3.3: (a) Rewriting the interconnection such that $\tau = 0$ implies $\tilde{\Delta} = 0$. (b) Frequency domain covering of the shifted delay operator.

3.2.4 *Delay Uncertainty*

The delay robustness problem has been studied extensively and the dominating approach is the use of scattering transformations/wave variable techniques, among other methods ([3, 5, 6, 31, 62, 88, 90, 94, 107, 108, 112, 161]). We refer to the survey article [62] for a detailed exposition of these methods. A great deal of research has been devoted to delay robustness tests in robust control that are applicable to a wide class of teleoperation systems. We also refer to [126] for a general treatment of the subject (e.g. based on Lyapunov-Krasovskii functionals as utilized by [27]) and to IQC based results as e.g. in [35, 70, 72, 138].

Here, we consider constant but uncertain delays and the maximum delay duration is bounded from above by $\bar{\tau} > 0$ seconds. We emphasize that it requires only a simple modification of the multiplier in order to arrive at robustness tests for different types of delays as reported in the literature.

If using the uncertainty $\Delta(s) = e^{-s\tau}$ in the configuration of Figure 3.1a, the nominal value $\tau = 0$ leads to $\Delta(s) = 1$ and not to zero as desired. This is resolved by utilizing the shifted uncertainty $\tilde{\Delta}(s) = e^{-s\tau} - 1$ and correspondingly modifying the system to $\tilde{G}$ (by unity feedback around G) as in Figure 3.3a and without modifying the interconnection (cf. [90]).

The uncertainty is then characterized by using two properties of $\tilde{\Delta}$: For all ω, τ, the complex number $z = e^{-i\omega\tau} - 1$ is located on the unit circle centered at $(-1, 0)$ in the complex plane. Since condition $|z + 1| = 1$ translates into $z^*z + z^* + z = 0$, we infer for all bounded $\Omega : \mathbb{R} \to \mathbb{R}$ that

$$\begin{pmatrix} \tilde{\Delta}(i\omega) \\ 1 \end{pmatrix}^* \begin{pmatrix} \Omega(\omega) & \Omega(\omega) \\ \Omega(\omega) & 0 \end{pmatrix} \begin{pmatrix} \tilde{\Delta}(i\omega) \\ 1 \end{pmatrix} = 0 \ \ \forall \omega \in \mathbb{R} \qquad (3.17)$$

for any delay time $\tau \in \mathbb{R}$. Furthermore, we need to take the low frequency property

of the magnitude of the frequency response into account. This is typically captured by a frequency dependent weight. If we define,

$$W_d(s) = 2\frac{(s + \frac{4}{\pi\bar{\tau}})(s + \frac{\beta}{\bar{\tau}})}{(s - \frac{\pi}{2\bar{\tau}}e^{i\theta})(s - \frac{\pi}{2\bar{\tau}}e^{-i\theta})}$$

with $\theta = \left(\frac{\pi}{2}\right)^2$ and some small $\beta > 0$, then W_d covers the delay uncertainty in the sense that $|\tilde{\Delta}(i\omega)| \leq |W(i\omega)|$ for all $\omega \in \mathbb{R}$ and for all $\tau \in [0, \bar{\tau}]$. An example of magnitude covering is shown in Figure 3.3b.

This property, in turn, translates into $(\tilde{\Delta})^*\tilde{\Delta} \leq (W_d)^*W_d$ for all $\omega \in \mathbb{R}$. Then we can utilize the classical D-scalings to obtain the following constraint with a dynamic multiplier:

$$(\star)^* \begin{pmatrix} -\mathcal{D}(\omega) & 0 \\ 0 & W_d(i\omega)^*\mathcal{D}(\omega)W_d(i\omega) \end{pmatrix} \begin{pmatrix} \tilde{\Delta}(i\omega) \\ 1 \end{pmatrix} \geq 0 \qquad (3.18)$$

for all bounded $\mathcal{D} : \mathbb{R} \to (0, \infty)$. Then the overall multiplier family results from a conic combination of (3.17) and (3.18):

$$(\star)^* \begin{pmatrix} -\mathcal{D} + \Omega & \Omega \\ \Omega & W_d^*\mathcal{D}W_d \end{pmatrix} \begin{pmatrix} \tilde{\Delta} \\ 1 \end{pmatrix} \geq 0 \quad \forall \omega \in \mathbb{R}_e$$

3.3   EQUIVALENT IQC BASED STABILITY TESTS FOR COMMON STABILITY ANALYSIS APPROACHES

3.3.1   *Llewellyn's Stability Criteria*

As shown in [127], the conditions stated in Theorem 23 are invariant under immittance substitution. Hence, we assume that the network and the terminations are represented with an input/output mapping as depicted in Figure 3.1b.

The stability conditions of Theorem 23 can be reproduced via the IQC theorem as follows. If Δ_l and Δ_s are passive and stable LTI systems, they satisfy

$$\Delta_l + \Delta_l^* \geq 0 \text{ and } \Delta_s + \Delta_s^* \geq 0$$

for all $\omega \in \mathbb{R}_e$. If we choose arbitrary $\lambda_1(\omega) > 0$ and $\lambda_2(\omega) > 0$, it is clear that the inequalities $\lambda_2(\Delta_l + \Delta_l^*) \geq 0$ and $\lambda_1(\Delta_s + \Delta_s^*) \geq 0$ persist to hold, which can, in turn, be combined into

$$\begin{pmatrix} \Delta_s & 0 \\ 0 & \Delta_l \\ 1 & 0 \\ 0 & 1 \end{pmatrix}^* \left(\begin{array}{cc|cc} 0 & 0 & \lambda_1 & 0 \\ 0 & 0 & 0 & \lambda_2 \\ \hline \lambda_1 & 0 & 0 & 0 \\ 0 & \lambda_2 & 0 & 0 \end{array}\right) \begin{pmatrix} \Delta_s & 0 \\ 0 & \Delta_l \\ 1 & 0 \\ 0 & 1 \end{pmatrix} \succeq 0.$$

After division by $\lambda_2(\omega)$ and with $\lambda(\omega) = \frac{\lambda_1(\omega)}{\lambda_2(\omega)}$ we obtain

$$
\begin{pmatrix} \Delta_s & 0 \\ 0 & \Delta_l \\ \hline 1 & 0 \\ 0 & 1 \end{pmatrix}^* \left(\begin{array}{cc|cc} 0 & 0 & \lambda & 0 \\ 0 & 0 & 0 & 1 \\ \hline \lambda & 0 & 0 & 0 \\ 0 & 1 & 0 & 0 \end{array} \right) \begin{pmatrix} \Delta_s & 0 \\ 0 & \Delta_l \\ \hline 1 & 0 \\ 0 & 1 \end{pmatrix} \succeq 0. \tag{3.19}
$$

In this fashion we have constructed a whole family of multipliers, parameterized by $\lambda(\omega) > 0$, such that the quadratic constraint (3.19) holds for all passive $\Delta_l, \Delta_s \in \mathcal{RH}_\infty$. Stability of the $N - \Delta$ interconnection is then guaranteed if one can find a positive $\lambda(\omega)$ for which the frequency domain inequality

$$
\begin{pmatrix} 1 & 0 \\ 0 & 1 \\ \hline -N_{11} & -N_{12} \\ -N_{21} & -N_{22} \end{pmatrix}^* \left(\begin{array}{cc|cc} 0 & 0 & \lambda & 0 \\ 0 & 0 & 0 & 1 \\ \hline \lambda & 0 & 0 & 0 \\ 0 & 1 & 0 & 0 \end{array} \right) \begin{pmatrix} 1 & 0 \\ 0 & 1 \\ \hline -N_{11} & -N_{12} \\ -N_{21} & -N_{22} \end{pmatrix} \prec 0 \tag{3.20}
$$

is also satisfied at each frequency $\omega \in \mathbb{R}_e$ (Negation of N results from the application of the IQC theorem to the negative feedback interconnection Figure 3.1b). The resulting condition is equivalent to checking whether, at each frequency, there exists a $\lambda > 0$ such that

$$
H = \begin{bmatrix} -2\lambda R_{11} & -\lambda N_{12} - N_{21}^* \\ -\lambda N_{12}^* - N_{21} & -2R_{22} \end{bmatrix} \prec 0
$$

holds. This leads us to the relation with the classical results. Indeed, the 2×2 matrix H is negative definite if and only if

$$
R_{11} > 0 \quad \text{or} \quad R_{22} > 0
$$

and

$$
\det H = \left(-R_{12}^2 - X_{12}^2 \right) \lambda^2 - R_{21}^2 - X_{21}^2 + \left(4R_{11}R_{22} - 2R_{12}R_{21} + 2X_{12}X_{21} \right) \lambda > 0.
$$

Since the leading and constant coefficient of the involved polynomial are negative, the apex of the corresponding parabola should stay above the λ-axis. Using the apex coordinates of a concave parabola one can show that this is equivalent to (A.12). Symmetry of the resulting conditions with respect to the indices is shown by simply switching the roles of λ_1 and λ_2 in our derivation.

Remark 7. *In the previous FDI condition (3.20) and if assuming $\lambda = 1$ over all frequencies, we also recover the Raisbeck's conditions [122]. A comparison of Raisbeck's and Llewellyn's criteria indicates that the use of frequency dependent multipliers demonstrates*

the possibility of a substantial decrease of conservatism in stability analysis. In fact, the difference between Llewellyn's conditions and of Raisbeck's is the use of dynamic multipliers instead of static ones.

Remark 8. *One should also note that Llewellyn's original conditions are both sufficient and necessary and, hence, involve no conservatism. Exactness is due to the vast generality of the uncertainties, since one just assumes that the human and the environment are represented by passive LTI operators. The Nyquist curves of the corresponding positive real functions are only constrained to be lying in the closed right half plane. In reality, however, one is rather interested in operators whose Nyquist curves are confined to a sub-region of the closed right-half plane (or even to other bounded sets elsewhere in the complex plane). Covering the relevant region of interest in the complex plane with the full closed right-half plane for describing the involved uncertainty provides a clear account of the conservatism of the stability tests in teleoperation systems. Thus, if one wishes to reduce conservatism, additional structural information about the operators should be included in order to further constrain the uncertainty set (e.g. [17, 45, 49, 157]). It will be illustrated in Section 3.4 how this can be achieved by using conic combinations of different multipliers which express refined properties of the involved operators.*

3.3.2 *Unconditional Stability Analysis of 3-port Networks*

For the analysis of 3-port networks, there exists no obvious unconditional stability result other than terminating one of the ports with a known environment model and then performing an analysis on the resulting 2-port network (see e.g. [74] and references therein). Still, we can obtain the exact conditions for a 3-port case in a straightforward fashion along the above described lines without port termination. However, as expected, the test derived in this section is more conservative than those of port termination based methods since the additional information about the model with which the port is terminated renders the uncertainty set significantly smaller.

If compared to the previous section, the only modification is to take a system representation $N \in \mathcal{RH}_\infty^{3\times3}$ and three passive uncertainty blocks living in $\mathcal{RH}_\infty$ which are collected as

$$\Delta(i\omega) = \mathrm{diag}\left(\Delta_1(i\omega), \Delta_2(i\omega), \Delta_3(i\omega)\right) \tag{3.21}$$

in order to model the three port terminations. With

$$\Lambda(i\omega) = \mathrm{diag}\left(\lambda_1(\omega), \lambda_2(\omega), \lambda_3(\omega)\right) \succ 0 \tag{3.22}$$

we obtain the following quadratic constraint

$$\begin{pmatrix} \Delta \\ I \end{pmatrix}^* \begin{pmatrix} 0 & \Lambda \\ \Lambda & 0 \end{pmatrix} \begin{pmatrix} \Delta \\ I \end{pmatrix} \succeq 0$$

which reflects passivity of the three sub-blocks. The corresponding FDI for guaranteeing stability reads as

$$\begin{pmatrix} I \\ -N \end{pmatrix}^* \begin{pmatrix} 0 & \Lambda \\ \Lambda & 0 \end{pmatrix} \begin{pmatrix} I \\ -N \end{pmatrix} \prec 0. \tag{3.23}$$

Theorem 5 (Llewellyn's 3-port Criteria). *A network, represented by its 3×3 transfer function $N \in \mathcal{RH}_\infty^{3\times3}$ and interconnected to the stable, passive and block diagonal Δ as given in (3.21) is stable if and only if there exists a structured Λ with (3.22) such that (3.23) holds for all $\omega \in \mathbb{R}_e$.*

Exact conditions for unconditional stability could be obtained from (3.23) by symbolic computations. However, getting formulas similar to those in (A.11), (A.12) would lead to quite cumbersome expressions (see e.g. [74, 84, 148]). Moreover, variants of expressing negative definiteness would result in different formulations of the stability conditions in terms of scalar inequalities. In the IQC formulation this is completely avoided while it is still possible to easily verify the resulting conditions numerically.

3.3.3   *Rollett's Stability Condition*

With almost identical arguments as for Llewellyn's test, one derives the following quadratic constraints for positive λ and for stable LTI systems $\tilde{\Delta}_l$ and $\tilde{\Delta}_s$ whose gains are bounded by one:

$$\begin{pmatrix} \tilde{\Delta}_s & 0 \\ 0 & \tilde{\Delta}_l \\ 1 & 0 \\ 0 & 1 \end{pmatrix}^* \left(\begin{array}{cc|cc} -\lambda & 0 & & \\ 0 & -1 & & \\ \hline & & \lambda & 0 \\ & & 0 & 1 \end{array} \right) \begin{pmatrix} \tilde{\Delta}_s & 0 \\ 0 & \tilde{\Delta}_l \\ 1 & 0 \\ 0 & 1 \end{pmatrix} \succeq 0.$$

Interconnection stability is then assured if one can find a positive frequency dependent λ for which the FDI

$$\begin{pmatrix} 1 & 0 \\ 0 & 1 \\ S_{11} & S_{12} \\ S_{21} & S_{22} \end{pmatrix}^* \left(\begin{array}{cc|cc} -\lambda & 0 & & \\ 0 & -1 & & \\ \hline & & \lambda & 0 \\ & & 0 & 1 \end{array} \right) \begin{pmatrix} 1 & 0 \\ 0 & 1 \\ S_{11} & S_{12} \\ S_{21} & S_{22} \end{pmatrix} \prec 0 \tag{3.24}$$

or, equivalently,

$$H = \begin{bmatrix} |S_{21}|^2 + \lambda(|S_{11}|^2 - 1) & S_{22}S_{21}^* + \lambda S_{12}S_{11}^* \\ S_{22}^*S_{21} + \lambda S_{12}^*S_{11} & |S_{22}|^2 - 1 + \lambda |S_{12}|^2 \end{bmatrix} \prec 0$$

hold for all $\omega \in \mathbb{R}_e$. Then, it is elementary to express $H \prec 0$ by $\det(H) > 0$ and by negativity of the diagonal entries of H for all $\omega \in \mathbb{R}_e$. Positivity of the determinant of H means

$$(1 - |S_{22}|^2 - |S_{11}|^2 + |\nabla|^2)\lambda - |S_{12}|^2 \lambda^2 - |S_{21}|^2 > 0.$$

If this is expressed as $f(\lambda) = -a\lambda^2 + b\lambda - c > 0$ with $a, c > 0$, we require the apex coordinates $\left(\frac{b}{2a}, \frac{b^2 - 4ac}{4a}\right)$ both to be positive. Since $a > 0$, we have

$$(1 + |\nabla|^2 - |S_{22}|^2 - |S_{11}|^2)^2 > 4 |S_{12} S_{21}|^2 \tag{3.25}$$

due to $b^2 > 4ac$. Moreover, negativity of the diagonal terms is expressed as

$$\lambda(1 - |S_{11}|^2) > |S_{21}|^2 \quad \text{or} \quad 1 - |S_{22}|^2 > \lambda |S_{12}|^2. \tag{3.26}$$

To make the connection to the classical auxiliary conditions, observe that evaluating $f(\lambda)$ at $\lambda_0 = \sqrt{\frac{c}{a}} = \frac{|S_{21}|}{|S_{12}|}$ would lead to the condition $b > 0$ since $f(\lambda_0) = b\sqrt{\frac{c}{a}} - 2c > 0$. Hence (3.26) becomes

$$1 - |S_{11}|^2 > |S_{12} S_{21}| \quad \text{or} \quad 1 - |S_{22}|^2 > |S_{12} S_{21}|. \tag{3.27}$$

In the literature, the quantity λ_0 is called the "maximum stable power gain". Finally, after explicitly including the condition $b > 0$, one can take the square root of (3.25) and obtain

$$1 + |\nabla|^2 - |S_{22}|^2 - |S_{11}|^2 > 2 |S_{12} S_{21}|,$$

which is precisely Rollett's first condition.

There has been quite some discussion in various studies (e.g. [29, 93, 114, 159]) whether testing both conditions in (3.27) is really required, while it rolls out from our FDI arguments that one of these auxiliary inequalities is sufficient. In fact, (3.24) renders this discussion obsolete since we deal with a single matrix inequality to be tested at each frequency. This test is equivalent to the one based on the Edwards-Sinsky stability parameter μ ([29]) in the sense that only one condition needs to be verified. Alternatively, one can perform a symbolic computation of the largest eigenvalue of H and search for a positive λ that renders that quantity strictly negative. Recently, the μ parameter has been used in the context of teleoperation in [45] and their results can also be recovered by using multipliers similar to the ones given in the next section.

3.3.4   *Colgate's Minimum Damping Condition*

In this section, the analysis problem from [23, 25] is investigated by IQCs. In this example, the master device is modeled as $\frac{1}{ms+b}$ and is combined with a passive
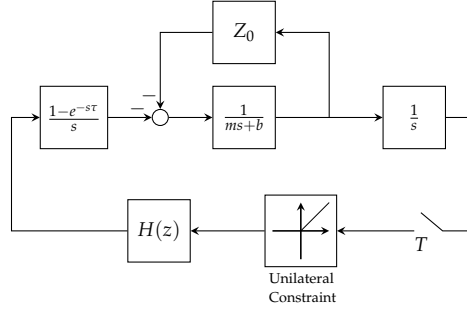
Figure 3.4: The teleoperation setup from [24]

operator impedance $Z_0(s)$ as shown in Figure 3.4. We limit the analysis to the situation without the unilateral constraint. The overall operator and master device transfer function reads as $\Delta(s) = \frac{1}{ms+b+Z_0(s)}$. Since $Z_0(s)$ is passive and b is positive, the Nyquist curve of $\Delta^{-1}(s)$ is confined to the half-plane $\{z \in \mathbb{C} : \mathrm{Re}\,\{z\} \geq b\}$ and $\Delta^{-1}(s)$ is strictly input passive with parameter b. In [25], the problem is converted to the small gain theorem with a geometric reasoning. In our setting, passivity is expressed as

$$\begin{pmatrix} 1 \\ \Delta(i\omega)^{-1} \end{pmatrix}^* \begin{pmatrix} -2b & 1 \\ 1 & 0 \end{pmatrix} \begin{pmatrix} 1 \\ \Delta(i\omega)^{-1} \end{pmatrix} \geq 0$$

which is clearly equivalent to

$$\begin{pmatrix} \Delta(i\omega) \\ 1 \end{pmatrix}^* \begin{pmatrix} -2b & 1 \\ 1 & 0 \end{pmatrix} \begin{pmatrix} \Delta(i\omega) \\ 1 \end{pmatrix} \geq 0$$

for all $\omega \in \mathbb{R}_e$. The FDI guaranteeing stability then reads as

$$\begin{pmatrix} 1 \\ -G_d(i\omega) \end{pmatrix}^* \begin{pmatrix} -2b & 1 \\ 1 & 0 \end{pmatrix} \begin{pmatrix} 1 \\ -G_d(i\omega) \end{pmatrix} < 0$$

for all $\omega \in \mathbb{R}_e$. Using the closed form formula in [25],

$$G_d(i\omega) = \frac{T}{2} \frac{e^{i\omega T} - 1}{1 - \cos(\omega T)} H(e^{i\omega T}),$$

this directly leads to Colgate's original condition:

$$-2b - G_d^*(i\omega) - G_d(i\omega) < 0$$
$$\iff b > \frac{T}{2} \frac{1}{1 - \cos(\omega T)} \mathrm{Re}\left\{ (1 - e^{-i\omega T}) H(e^{i\omega T}) \right\}.$$

The employed multiplier can be transformed into the one for the small-gain theorem along the following lines:

$$
\begin{aligned}
0 \leq 2b &\begin{pmatrix} \Delta(i\omega) \\ 1 \end{pmatrix}^* \begin{pmatrix} -2b & 1 \\ 1 & 0 \end{pmatrix} \begin{pmatrix} \Delta(i\omega) \\ 1 \end{pmatrix} \\
&= \begin{pmatrix} \Delta(i\omega) \\ 1 \end{pmatrix}^* \left[\begin{pmatrix} 2b & -1 \\ 0 & 1 \end{pmatrix}^T \begin{pmatrix} -1 & 0 \\ 0 & 1 \end{pmatrix} \begin{pmatrix} 2b & -1 \\ 0 & 1 \end{pmatrix} \right] \begin{pmatrix} \Delta(i\omega) \\ 1 \end{pmatrix} \\
&= \begin{pmatrix} 2b\Delta(i\omega) - 1 \\ 1 \end{pmatrix}^* \begin{pmatrix} -1 & 0 \\ 0 & 1 \end{pmatrix} \begin{pmatrix} 2b\Delta(i\omega) - 1 \\ 1 \end{pmatrix} \Longleftrightarrow |2b\Delta(i\omega) - 1| \leq 1.
\end{aligned}
$$

This links our arguments to those appearing in [23, 25] and reveals that the direct application of tools from robust control allows to circumvent any transformation to scattering parameters (or, in other words, the application of a loop transformation) for obtaining the stability conditions. In fact, the congruence transformation

$$
\left(\frac{1}{\sqrt{2b}} \begin{pmatrix} 1 & -b \\ 1 & b \end{pmatrix} \right)^T \begin{pmatrix} -1 & 0 \\ 0 & 1 \end{pmatrix} \left(\frac{1}{\sqrt{2b}} \begin{pmatrix} 1 & -b \\ 1 & b \end{pmatrix} \right) = \begin{pmatrix} 0 & 1 \\ 1 & 0 \end{pmatrix}
$$

with the scattering transformation matrix turns the small-gain multiplier into the one for passivity. This observation allows to easily show the equivalence of the small gain and passivity theorems through scattering transformations ([3]) and wave variable methods ([107, 108]).

3.3.5 *Regions in the Complex Plane*

Using a similar mechanism to what is given above, one can also characterize different domains in the complex plane different than the whole right half plane as long as it can be represented (or covered with) with a quadratic constraint. Thus, once a multiplier family is set, it's a matter of evaluating the respective FDI for the system at hand. For example, recently in [68], a vertical strip-like domain for one of the LTI uncertainties is assumed i.e. $-a \leq \Delta_l + \Delta_l^* \leq b$ for all $\omega \in \mathbb{R}_e$ with $a, b > 0$ and stability conditions are derived similar to those of Llewellyn's test along the lines of [29]. In terms of quadratic constraints, a direct verification of the constraints below

$$
\begin{pmatrix} \Delta(i\omega) \\ 1 \end{pmatrix}^* \begin{pmatrix} 0 & 1 \\ 1 & a \end{pmatrix} \begin{pmatrix} \Delta(i\omega) \\ 1 \end{pmatrix} \geq 0 \text{ and } \begin{pmatrix} \Delta(i\omega) \\ 1 \end{pmatrix}^* \begin{pmatrix} 0 & -1 \\ -1 & b \end{pmatrix} \begin{pmatrix} \Delta(i\omega) \\ 1 \end{pmatrix} \geq 0
$$

show that these constraints characterize the domain

$$
\{z \in \mathbb{C} : -a \leq \operatorname{Re}\{z\} \leq b \text{ for } a, b > 0\}.
$$

Hence, after introducing dynamic multipliers and scaling the overall multiplier with the corresponding λ of Δ_s, the stability condition can be posed as for all $\omega \in \mathbb{R}_e$ the existence of $\lambda_1(\omega), \lambda_2(\omega) > 0$ such that

$$
\begin{pmatrix} 1 & 0 \\ 0 & 1 \\ -N_{11} & -N_{12} \\ -N_{21} & -N_{22} \end{pmatrix}^*
\left(\begin{array}{cc|cc} 0 & 0 & 1 & 0 \\ 0 & 0 & 0 & \lambda_1 - \lambda_2 \\ 1 & 0 & 0 & 0 \\ 0 & \lambda_1 - \lambda_2 & 0 & \lambda_1 a + \lambda_2 b \end{array} \right)
\begin{pmatrix} 1 & 0 \\ 0 & 1 \\ -N_{11} & -N_{12} \\ -N_{21} & -N_{22} \end{pmatrix} \prec 0 \quad (3.28)
$$

holds. By carrying out the multiplication, we obtain

$$
\begin{pmatrix} -2R_{11} + (\lambda_1 a + \lambda_2 b) |N_{21}|^2 & -N_{12} - (\lambda_1 - \lambda_2)N_{21}^* + (\lambda_1 a + \lambda_2 b)N_{21}^* N_{22} \\ \star & -2(\lambda_1 - \lambda_2)R_{22} + (\lambda_1 a + \lambda_2 b) |N_{22}|^2 \end{pmatrix} \prec 0.
$$

If we compare this with the derived conditions in [68], we can see that their results don't involve any b terms. Hence, contrary to the claim, those results can be, at best, sufficient since their test only deals with the first part of the constraint, namely $-a \leq \mathrm{Re}(\Delta_l)$. Still we cannot see the actual problematic step as we cannot reproduce their conditions by leaving out the constraint involving b term. Nevertheless, their first remark in [68, Theorem 3] is not correct. The upper bound on the real part of the uncertainty certainly plays a role and can not be omitted in the necessity direction in their proof which is omitted in their paper. In other words two uncertainty operators with $\mathrm{Re}\,\Delta \leq b(\geq b)$ for some frequencies respectively, can not be distinguished and this possibility already contradicts with the necessity of the test since both will be evaluated on the basis of parameter a and regardless of b.

Moreover, as is the case for the previous examples, one can impose these constraints and possibly more on both the human and the environment uncertainties, without invoking the passivity theorem explicitly, in a few steps instead of deriving standalone conditions for each individual case.

3.3.6 *Exactness of Robustness Tests*

As mentioned before, IQC-based stability criteria are typically only sufficient. Still the classical conditions as discussed above turn out to be also necessary. Necessity of these criteria can as well be seen to be a specialization of celebrated exactness results in structured singular-value theory. In fact, IQC tests for structured LTI uncertainties with two or three full diagonal blocks as derived above are known to be always exact. This implies, in particular, that the 3-port counterpart of Llewellyn's conditions is indeed a necessary and sufficient test for stability. It's not feasible for us to provide a full treatment of all possible cases in which IQC-based

robustness tests are known to be exact. Nevertheless, for a detailed discussion related to LTI uncertainties we refer to [33, 110, 134].

We would like to emphasize that these beautiful exactness properties come at the price of some limitations of the classical framework. For instance, Llewellyn's conditions are not sufficient for stability any more if we only assume that the uncertainties are passive but not necessarily LTI. On the other hand, if allowing for arbitrary causal and passive uncertainties, stability is still guaranteed if we can find a frequency-independent $\lambda > 0$ which renders the FDI (3.20) satisfied, and this property can be easily verified numerically.

3.4   Numerical Case Studies

In this section, we show how frequently encountered analysis problems can be solved under the IQC formulation with ease. We utilize the multipliers as given above for robustness tests applied to a simple teleoperation system taken from [156, 157]. Our main emphasis is on showing how one can reproduce the numerical results of such frequency domain techniques and how it is possible to substantially widen the range of allowed uncertainties in the IQC framework for which no classical analytical stability tests exist. This serves as an illustration for the possibility to improve analysis and, more importantly in future work, optimization-based controller synthesis results if better human/environment models become available.

3.4.1   *Algorithmic Verification*

We have discussed some classical stability tests that reduce to explicit scalar inequalities which can be verified in a frequency-by-frequency fashion. In contrast, the equivalent re-formulations in terms of IQCs open the way to verifying these conditions numerically, by applying algorithms from the by now well-established area of semi-definite programming [12]. For example, checking at each frequency the existence of some diagonal $\Lambda \succ 0$ which satisfies (3.23) boils down to an efficiently tractable LMI problem in the three diagonal entries of Λ, which can be readily implemented in software environments such as [92]. We also show how it is even possible to avoid any frequency-gridding and to reduce the tests to finite-dimensional semi-definite programming problems that can be solved in one shot.

This section serves to illustrate this procedure for Rollett's stability condition, which requires to determine a frequency-dependent bounded and strictly positive λ satisfying the FDI (3.24). Without loss of generality, it suffices to search for proper and rational functions λ that have no poles and are positive on the extended

imaginary axis. Due to the well-established spectral factorization theorem (e.g. [34]), we can express any such function as $\psi^*\psi$ with some stable transfer function ψ (without zeros in the closed right half-plane). For some fixed pole $a < 0$ let us choose the basis vectors

$$\Phi_n(s) = \begin{pmatrix} 1 & \frac{1}{s-a} & \frac{1}{(s-a)^2} & \cdots & \frac{1}{(s-a)^{n-1}} \end{pmatrix}^T$$

for $n = \mathbb{N}$. By a well-known fact from approximation theory ([113]), the function ψ can be approximated to an arbitrary degree by $L^T\Phi_n$ for some suitable $L \in \mathbb{R}^n$ uniformly on the imaginary axis, if only n is taken sufficiently large. More precisely, $\inf_{L \in \mathbb{R}^n} \|\psi - L^T\Phi_n\|_\infty$ converges to zero for $n \to \infty$. In summary, any proper rational λ with $\lambda(i\omega) > 0$ for $\omega \in \mathbb{R}_e$ can be approximated arbitrarily closely by $\Phi_n^* LL^T\Phi_n$ or, in turn, by $\Phi_n^* D\Phi_n$ with $D = D^T \in \mathbb{R}^{n \times n}$.

This discussion justifies why one can parameterize the multiplier (middle term) in (3.24) as

$$\Psi_n^* \underbrace{\left(\begin{array}{cc|cc} -D & 0 & & \\ 0 & -1 & & \\ \hline & & D & 0 \\ & & 0 & 1 \end{array} \right)}_{M} \underbrace{\left(\begin{array}{cc|cc} \Phi_n & & & \\ & 1 & & \\ \hline & & \Phi_n & \\ & & & 1 \end{array} \right)}_{\Psi_n}$$

in terms of a frequency-dependent outer factor Ψ_n and a diagonally structured real symmetric matrix M in the middle. Let us denote the set of all these matrices M by $\mathcal{M}$ (dropping the dependence on n). For checking Rollet's condition we then need to verify the existence of $M \in \mathcal{M}$ such that the FDIs

$$\Phi_n^* D\Phi_n > 0 \ \text{ and } \ \begin{pmatrix} I \\ S \end{pmatrix}^* \Psi_n^* M \Psi_n \begin{pmatrix} I \\ S \end{pmatrix} \prec 0$$

are satisfied. We include the classical result ([125]) that allows us to convert these frequency domain inequalities into LMIs:

Theorem 6. *[KYP Lemma] Let $G = \left[\begin{array}{c|c} A & B \\ \hline C & D \end{array} \right]$ and suppose that A has no eigenvalues on the imaginary axis. For a real matrix $P = P^T$, the following two statements are equivalent:*

1. *The following FDI holds:*

$$G(i\omega)^* PG(i\omega) \succ 0 \ \ \forall \omega \in \mathbb{R}_e. \tag{3.29}$$

2. *There exists a symmetric matrix X with*

$$\begin{pmatrix} I & 0 \\ A & B \\ C & D \end{pmatrix}^T \left(\begin{array}{cc|c} 0 & X & 0 \\ X & 0 & 0 \\ \hline 0 & 0 & P \end{array} \right) \begin{pmatrix} I & 0 \\ A & B \\ C & D \end{pmatrix} \succ 0. \tag{3.30}$$

Now choose the minimal state space realizations

$$\Phi_n = \left[\begin{array}{c|c} A_\Phi & B_\Phi \\ \hline C_\Phi & D_\Phi \end{array}\right] \quad \text{and} \quad \Psi_n \begin{pmatrix} I \\ S \end{pmatrix} = \left[\begin{array}{c|c} \mathcal{A} & \mathcal{B} \\ \hline \mathcal{C} & \mathcal{D} \end{array}\right].$$

This allows to apply the KYP Lemma in order to equivalently convert $\lambda > 0$ and (3.24) into the feasibility of the LMIs

$$\begin{pmatrix} I & 0 \\ A_\Phi & B_\Phi \\ C_\Phi & D_\Phi \end{pmatrix}^T \begin{pmatrix} 0 & Z & 0 \\ Z & 0 & 0 \\ 0 & 0 & D \end{pmatrix} \begin{pmatrix} I & 0 \\ A_\Phi & B_\Phi \\ C_\Phi & D_\Phi \end{pmatrix} \succ 0 \tag{3.31}$$

and

$$\begin{pmatrix} I & 0 \\ \mathcal{A} & \mathcal{B} \\ \mathcal{C} & \mathcal{D} \end{pmatrix}^T \begin{pmatrix} 0 & \mathcal{X} & 0 \\ \mathcal{X} & 0 & 0 \\ 0 & 0 & M \end{pmatrix} \begin{pmatrix} I & 0 \\ \mathcal{A} & \mathcal{B} \\ \mathcal{C} & \mathcal{D} \end{pmatrix} \prec 0. \tag{3.32}$$

More precisely, if one can computationally verify the existence of $X, Z, M \in \mathcal{M}$ and $D = D^T$ which satisfy (3.31) and (3.32), we have verified Rollet's condition. Conversely, if Rollet's condition holds, then these LMIs are guaranteed to have solutions if n is chosen sufficiently large.

Let us emphasize again that the very same procedure applies to considerable more complex interconnections and structured uncertainties Δ. In fact, for many interesting classes of uncertainties one can systematically construct multiplier families (see e.g. [98]) which are known to admit a description of the form $\Pi = \Psi^* M \Psi$, $M \in \mathcal{M}$ with a stable outer factor transfer matrix Ψ and with some set of structured symmetric matrices $\mathcal{M}$ that can itself be described as the feasible set of an LMI. Checking stability of the $G - \Delta$ interconnection in Figure 3.1a then requires to verify the validity of the FDI

$$\begin{pmatrix} I \\ G \end{pmatrix}^* \Psi^* M \Psi \begin{pmatrix} I \\ G \end{pmatrix} \prec 0.$$

Literally along the same lines as described above this is translated into a semi-definite program with Theorem 6.

Remark 9. *In our numerical examples the basis length n is chosen large enough that the performance level does not significantly change by further increasing n. As shown below, the required length n for adequate accuracy in the multipler approximation is (regardless of the conservatism of the test) often quite small in practice.*

In what follows, we will continue to utilize the shorthand notation of state-space realizations in a similar manner, i.e., $\mathcal{A}, \mathcal{B}, \mathcal{C}, \mathcal{D}$ for the combined outer factors by replacing S with the respective plant, and $A_\Phi, B_\Phi, C_\Phi, D_\Phi$ for the basis vector.

3.4.2 *System Model*

In [156], a simple teleoperation system described with the following equations is considered:

$$F_h + \tau_m = M_m \ddot{x}_m + B_m \dot{x}_m$$
$$\tau_s - F_e = M_s \ddot{x}_s + B_s \dot{x}_s.$$

Here M_m, M_s are the masses, B_m, B_s are the damping coefficients, τ_m, τ_s are the device motor torques, and x_m, x_s are the position coordinates of the local and the remote devices respectively. F_h, F_e denote the human and the environment forces. The human and the environment are assumed to be LTI passive operators and are denoted by Δ_h, Δ_e which substitute Δ_s, Δ_l as employed in the more general network-related context in the earlier sections.

Additionally, a particular PD type of a position-force controller scheme, denoted by **P-F** , is used:

$$\tau_s = K_p(\mu x_m - x_s) - K_v \dot{x}_s, \quad \tau_m = -K_f F_e.$$

The overall teleoperation system is then described, with $Y_m(s) = (M_m s + B_m)^{-1}$ and $Y_s(s) = \frac{\mu K_p}{M_s s^2 + (B_s + K_v)s + K_p}$, in terms of the following admittance matrix:

$$Y = \begin{pmatrix} Y_m & -K_f Y_m \\ -Y_m Y_s & \frac{M_m s^2 + B_m s + \mu K_f K_p}{(M_s s^2 + (B_s + K_v)s + K_p)} Y_m \end{pmatrix}. \tag{3.33}$$

As shown in [156], the system's performance is related to the transparency of the teleoperator, which is characterized by the maximal attainable product μK_f while maintaining stability (see also [26]). We will evaluate our results with respect to this performance measure. For all computations, we have used [32, 92, 151] with MATLAB 7.12.0 on a computer with a 2.4 GHz processor and with 4 GB RAM memory running Win 7-64 Bit OS. The system parameters are $M_m = 0.64, M_s = 0.61, B_m = 0.64, B_s = 11, K_v = 87.8, K_p = 4000$.

3.4.3 *Case 1 : Unconditional Stability Analysis via IQCs*

We start with applying Llewellyn's test based on (3.20) to the system given above. In a first computation, we choose a frequency grid of 2000 logarithmically spaced points in $[0,10\,000]$ rad/s and solve, at each grid point, a feasibility problem in $\lambda > 0$. This is incorporated into a bisection algorithm that searches for the maximum value of μK_f for which feasibility at each grid-point can be guaranteed. Due to gridding, this method typically gives an upper bound rather than the exact value

(a) Unconditional Stability

(b) Uncertain stiff environment
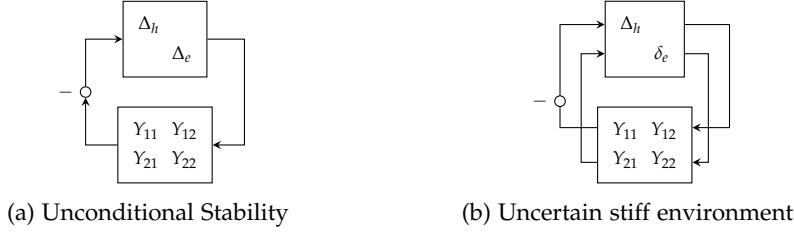
Figure 3.5: System interconnections for Section 3.4.3 and Section 3.4.4.

on the guaranteed performance level, just because there is a chance to miss critical frequencies. Nevertheless, we obtained the exact value ≈ 0.137 as in [156]. The inner search for λ requires 8.52 s, while the overall computation takes about 117 s; note that the latter heavily depends on the initial bisection interval and on the desired accuracy.

In a second computation, we follow the path as described in Section 3.4.1. The resulting FDI is

$$\left(\Psi \begin{pmatrix} I \\ -Y \end{pmatrix} \right)^* M \left(\Psi \begin{pmatrix} I \\ -Y \end{pmatrix} \right) \prec 0 \tag{3.34}$$

where

$$\Psi = \begin{pmatrix} \Phi & 0 & 0 & 0 \\ 0 & 1 & 0 & 0 \\ \hline 0 & 0 & \Phi & 0 \\ 0 & 0 & 0 & 1 \end{pmatrix}, \quad M = \begin{pmatrix} 0 & 0 & M_1 & 0 \\ 0 & 0 & 0 & 1 \\ \hline M_1 & 0 & 0 & 0 \\ 0 & 1 & 0 & 0 \end{pmatrix} \tag{3.35}$$

with some unstructured real symmetric matrix M_1.

Corollary 7. *The $Y - \Delta$ interconnection depicted in Figure 3.5a is stable for all passive blocks Δ_h and Δ_e if there exist symmetric matrices $\mathcal{X}, Z, M_1$ such that*

$$\begin{pmatrix} I & 0 \\ \mathcal{A} & \mathcal{B} \\ \mathcal{C} & \mathcal{D} \end{pmatrix}^T \begin{pmatrix} 0 & \mathcal{X} & 0 \\ \mathcal{X} & 0 & 0 \\ 0 & 0 & M \end{pmatrix} \begin{pmatrix} I & 0 \\ \mathcal{A} & \mathcal{B} \\ \mathcal{C} & \mathcal{D} \end{pmatrix} \prec 0$$

$$\begin{pmatrix} I & 0 \\ A_\Phi & B_\Phi \\ C_\Phi & D_\Phi \end{pmatrix}^T \begin{pmatrix} 0 & Z & 0 \\ Z & 0 & 0 \\ 0 & 0 & M_1 \end{pmatrix} \begin{pmatrix} I & 0 \\ A_\Phi & B_\Phi \\ C_\Phi & D_\Phi \end{pmatrix} \succ 0.$$

We applied Corollary 7 with a basis of length $n = 8$ and with the pole $a = -7$. In this way we computed again the maximal value $\mu K_f \approx 0.137$ for which stability can be guaranteed in about 36 s.

Remark 10. *Since Y is strictly proper, (3.34) cannot be satisfied at $\omega = \infty$ because its left-hand side vanishes. However, the interconnection is certainly well-posed such that the FDI only needs to be verified for all finite frequencies (Remark 5). Therefore, the gridding approach can be applied directly. In the alternative path without gridding, we can circumvent this trouble by replacing Y with $Y + \epsilon I$, with $\epsilon = 10^{-5}$ in our case. Let us stress that this perturbation (also in the cases presented below) is only required in those channels that are related to passive uncertainties.*

3.4.4 *Case 2: Stability with Uncertain Stiff Environments*

We characterize the admissible environments as pure springs modeled by $Z_e = \frac{k}{s}$ with an uncertain constant stiffness coefficient $k \in [0, \bar{k}] \, \mathrm{N/m}$. After merging $-\frac{k}{s}$ with the system (and slightly perturbing the pole of the integrator to render the nominal system stable) we are left with the uncertainty structure $\Delta = \mathrm{diag}(\Delta_h, \delta_e)$ where the human uncertainty is assumed to be passive LTI and δ_e is an uncertain real scalar parameter in the interval $[0, 1]$. Using a modified DG-scaling for the shifted parameter range, we can easily adapt the multiplier and obtain, next to $\lambda > 0$ and $d > 0$, the following FDI for interconnection stability:

$$\begin{pmatrix} 1 & 0 \\ 0 & 1 \\ -Y_{11} & -Y_{12} \\ Y_{21} & Y_{22} \end{pmatrix}^* \left(\begin{array}{cc|cc} 0 & 0 & \lambda & 0 \\ 0 & -d & 0 & \frac{d}{2} + ig \\ \hline \lambda & 0 & 0 & 0 \\ 0 & \frac{d}{2} - ig & 0 & 0 \end{array} \right) \begin{pmatrix} 1 & 0 \\ 0 & 1 \\ -Y_{11} & -Y_{12} \\ Y_{21} & Y_{22} \end{pmatrix} \prec 0. \tag{3.36}$$

With the frequency grid as in the previous case we obtained too optimistic results (after comparing the values with those computed below), which suggests the need to refine the grid. With additional 1500 points in the interval $[10^{-6}, 100] \frac{\mathrm{rad}}{\mathrm{s}}$, we obtained the exact value of $(\mu K_f)_{\max} \approx 0.215$ for $\bar{k} = 1000 \frac{\mathrm{N}}{\mathrm{m}}$ in 127.7 s. We infer that the grid resolution, whether logarithmic or linear, plays a crucial role for the computations.

This reveals that, especially for systems that have high bandwidth and complex dynamics, it is instrumental to choose a sufficiently fine frequency grid in stability analysis. This is the very reason for the alternative path of computations (via multiplier parametrization and LMIs in state-space) as proposed above. In this particular example, the resulting condition boils down to two simple LMIs to be verified numerically. After normalizing the environment uncertainty by scaling, we just need to verify feasibility of the LMIs in the next result.

Corollary 8. *The $Y - \Delta$ interconnection in Figure 3.5b is stable for all passive LTI Δ_h and LTI real parametric uncertainty $\delta_e \in [0, 1]$ if there exist symmetric matrices $\mathcal{X}, Z_2, D_2$*
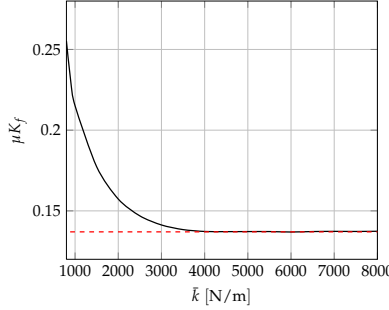
Figure 3.6: Performance loss for increasing environment stiffness uncertainty. The dashed line shows the value for unconditional stability from Section 3.4.3.

and a skew symmetric matrix G_2 such that

$$\begin{pmatrix} I & 0 \\ \mathcal{A} & \mathcal{B} \\ \mathcal{C} & \mathcal{D} \end{pmatrix}^T \begin{pmatrix} 0 & \mathcal{X} & 0 \\ \mathcal{X} & 0 & 0 \\ 0 & 0 & M \end{pmatrix} \begin{pmatrix} I & 0 \\ \mathcal{A} & \mathcal{B} \\ \mathcal{C} & \mathcal{D} \end{pmatrix} \prec 0,$$

$$\begin{pmatrix} I & 0 \\ A_\Phi & B_\Phi \\ C_\Phi & D_\Phi \end{pmatrix}^T \begin{pmatrix} 0 & Z_2 & 0 \\ Z_2 & 0 & 0 \\ 0 & 0 & D_2 \end{pmatrix} \begin{pmatrix} I & 0 \\ A_\Phi & B_\Phi \\ C_\Phi & D_\Phi \end{pmatrix} \succ 0$$

hold, where

$$M = \left(\begin{array}{cc|cc} 0 & 0 & 1 & 0 \\ 0 & -D_2 & 0 & \frac{1}{2}D_2 + G_2 \\ \hline 1 & 0 & 0 & 0 \\ 0 & \frac{1}{2}D_2 - G_2 & 0 & 0 \end{array} \right), \Psi = \left(\begin{array}{cc|cc} 1 & 0 & 0 & 0 \\ 0 & \Phi_2 & 0 & 0 \\ \hline 0 & 0 & 1 & 0 \\ 0 & 0 & 0 & \Phi_2 \end{array} \right).$$

For this example we have used the basis Φ_2 with length 12 and selected the pole $a = -16$. Bisection over μK_f took 29.3 s and the resulting maximum admissible value is found to be 0.215 for a sample value of $\bar{k} = 1000$. Values higher than 0.215 would render the nominal system unstable, which means that we obtain the best possible result. The performance curve for different values of $\bar{k}$ is given in Figure 3.6.

3.4.5   *Case 3: Robustness against Delays*

We reconsider the plant given in (3.33) and modify it in order to relate the results to the undelayed cases given above. We assume that there exist communication delays present in the forward and backward path and, without loss of generality,

we choose both maximally allowed delay durations to be equal for simplicity. We thus consider

$$Y = \begin{pmatrix} Y_m & -K_f Y_m e^{-s\tau} \\ -Y_m Y_s \mu K_p e^{-s\tau} & \frac{M_m s^2 + B_m s + \mu K_f K_p e^{-2s\tau}}{(M_s s^2 + (B_s + K_v)s + K_p)(M_m s + B_m)} \end{pmatrix}$$

where $\tau \in [0, \bar{\tau}]$. By pulling out the delay uncertainties from Y, the nominal plant Y_d is given by

$$Y_d = \begin{pmatrix} Y_m & 0 & -Y_m & 0 \\ 0 & sY_s & 0 & -K_p Y_s \\ 0 & K_f & 0 & 0 \\ \mu Y_m & 0 & -\mu Y_m & 0 \end{pmatrix}$$

and is interconnected to the structured uncertainty block

$$\Delta = \mathrm{diag}\left(\Delta_h, \Delta_e, e^{-s\tau}, e^{-s\tau}\right).$$

In accordance with Section 3.2.4, a unity feedback is applied and two delay weights are included in the plant.

Corollary 9. *The $Y_d - \Delta$ interconnection is stable for all passive LTI Δ_h, Δ_e and LTI delay uncertainties if there exist symmetric matrices $\mathcal{X}, M_1, M_2, D_3, D_4, R_3, R_4$ and Z_i for $i = 1, \ldots, 4$ such that*

$$\begin{pmatrix} I & 0 \\ \mathcal{A} & \mathcal{B} \\ \mathcal{C} & \mathcal{D} \end{pmatrix}^T \begin{pmatrix} 0 & \mathcal{X} & 0 \\ \mathcal{X} & 0 & 0 \\ 0 & 0 & P \end{pmatrix} \begin{pmatrix} I & 0 \\ \mathcal{A} & \mathcal{B} \\ \mathcal{C} & \mathcal{D} \end{pmatrix} \prec 0$$

and

$$\begin{pmatrix} I & 0 \\ A_\Phi^i & B_\Phi^i \\ C_\Phi^i & D_\Phi^i \end{pmatrix}^T \begin{pmatrix} 0 & Z_i & 0 \\ Z_i & 0 & 0 \\ 0 & 0 & Y_i \end{pmatrix} \begin{pmatrix} I & 0 \\ A_\Phi^i & B_\Phi^i \\ C_\Phi^i & D_\Phi^i \end{pmatrix} \succ 0$$

hold where $Y_1 = M_1$, $Y_2 = M_2$, $Y_3 = D_3$, $Y_4 = D_4$,

$$P = \begin{pmatrix} P_{11} & P_{12} \\ P_{12}^T & P_{22} \end{pmatrix}, \begin{cases} P_{11} = \mathrm{diag}\left(0, 0, -D_3, R_3, -D_4, R_4\right), \\ P_{12} = \mathrm{diag}\left(M_1, M_2, 0, R_3, 0, R_4\right), \\ P_{22} = \mathrm{diag}\left(0, 0, D_3, 0, D_4, 0\right) \end{cases}$$

and

$$\Psi = \begin{pmatrix} \Phi_1 & & & & & & \\ & \Phi_2 & & & & & \\ & & \Phi_3 & & & & \\ & & \Phi_5 & & & & \\ & & & \Phi_4 & & & \\ & & & \Phi_6 & & & \\ \hline & & & & \Phi_1 & & \\ & & & & \Phi_2 & & \\ & & & & \Phi_3 W_d & & \\ & & & & \Phi_5 & & \\ & & & & & \Phi_4 W_d & \\ & & & & & \Phi_6 & \end{pmatrix}.$$

This test has been applied for various maximum delay durations $\bar{\tau} \in [0.01, 0.1]$s with 0.005s increments and the results are shown in Figure 3.7. At each $\bar{\tau}$ point, the bisection algorithm took on average 577.4s (varying in $[435, 1040]$s). The basis lengths and the pole locations are selected as $n_i = 3, 3, 3, 3, 5, 5$ and $a_i = -16, -17, -19, -8, -13, -14$ respectively. The pole locations are selected away from the system's poles but arbitrary otherwise.

3.4.6 *Additional Remarks*

In concluding this section, we would like to address the issue of conservatism in our numerical examples. The first two cases involve none at all for sufficiently long basis functions as confirmed numerically.

If considering only passive LTI uncertainties in standard problems, there is no room for further algorithmic improvements since the resulting tests are guaranteed to be exact. On the other hand, there is a huge potential in searching for refined uncertainty characterizations in order to reduce conservatism. We have illustrated that there is no need to confine the analysis to passive uncertainties as long as they can be associated with some integral quadratic constraint, possibly through some physical experiments (see e.g. [13] for a parametric uncertainty case which can be improved directly using the multipliers given above). Thus, once IQCs are known for individual uncertainty blocks, it has been also demonstrated how to computationally verify robust stability against their combined influence on the interconnection with ease.

On the other hand, this might not be the case for the test in Corollary 9. To quantify the potential conservatism, we use extreme values for the stiff environment and the delay uncertainty and determine the maximum achievable values of μK_f for which the transfer function seen by the human is still strictly passive. Environments that are modeled as pure stiffnesses are considered to be "worst cases" since their Nyquist curves are located at the boundary of the closed right

half plane and since their low frequency contribution, unlike pure mass models, is significant. As shown in Figure 3.8, the performance decreases for increasing levels of $\bar{\tau}$ and $\bar{k}$, but the trade-off curve does not change significantly beyond the value $\bar{k} = 100\,000\,\text{N/m}$. We have also overlayed the results of Figure 3.7. If it is indeed true that a pure stiffness environment is the worst case, then the difference between the two lowest curves in Figure 3.8 can be attributed to the conservatism of the test in Corollary 9. Thus, we can conclude that the conservatism is not very large; this is of particular significance for delay-independent robust stability tests which would result in values in the range of $\mu K_f \approx 10^{-5}$.

Let us briefly compare with results obtained for time-varying environments. This makes a particularly interesting case since, in practice, a remote device might explore environments with varying characteristics. We have analyzed the non-delayed system where the environment is a pure spring with a stiffness coefficient $k(t) \in [0, 1000]\text{N/m}$ and different bounds on the rate-of-variation as shown in Figure 3.9. Classical absolute stability tests can only handle arbitrary fast variations which leads to small values of performance of $\approx 2 \cdot 10^{-5}$. The inclusion of information about the ROV (as possible through the class of multipliers discussed above) substantially reduces the conservatism as is visible in the plot.

In the literature, one often encounters PID-based controller architectures which makes it possible to analyze the effect of variations in the controller gains onto the performance of the teleoperation system. In our set-up, we can attribute the increase of performance to the increase of μK_f due to the simplicity of the system structure. If moving towards more complicated controller architectures, such clear relations are not expected to be valid any more. This precludes obtaining graphical or analytical stability and performance tests with robustness guarantees. As we show in chapter 4, IQC framework allows the incorporation of a performance channel and to develop robust performance analysis tests, very much along the same lines as discussed for stability in this chapter. Such formulations of the performance problems make it convenient to compare different PID controllers.

In conjunction with robust performance analysis, we can further utilize robust controller synthesis methods with dynamic IQCs, as recently developed in [135, 153]. In [135], a general class of robust synthesis problems has been identified which can be handled by convex optimization techniques. The well-known μ-synthesis algorithm, based on the so-called D/K-iteration, has been extended to general dynamic IQCs in [153] for problems that do not admit a convex formulation. In addition to robustness analysis for existing PID controller, this opens the way for model based controller synthesis in future work.
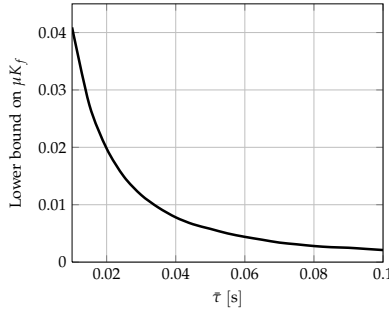
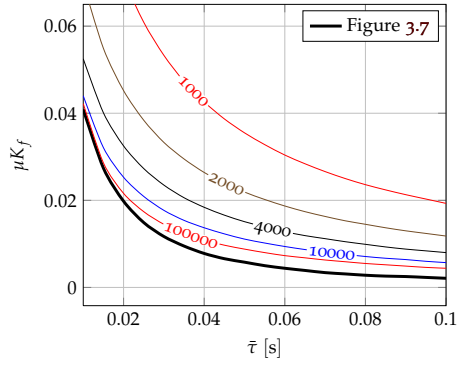Figure 3.7: Performance loss for increasing maximal delay duration.

Figure 3.8: Robust performance for different stiff environment cases in the face of increasing delay uncertainty duration.
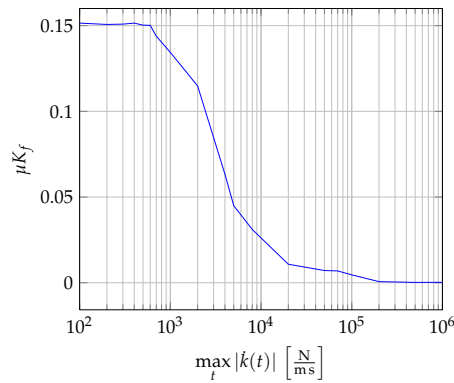

Figure 3.9: The performance loss with respect to the increase in ROV bound of the time-varying uncertain parameter $k(t) \in [0, 1000]$N/m.

3.5 Discussion

In this chapter, we have investigated the analysis problem from a Integral Quadratic Constraints (IQCs) perspective. The content is mainly based on [118]. At this point, we have to openly state a few points about the motivation of such use of these recent tools provided by the control theory. These points have often come up during the author's discussions held with experts, colleagues and practitioners.

First and foremost argument is on the comparison with other passivity-based techniques. As we sampled a few cases in this chapter, IQC tests are far more general than passivity-based analysis results since passivity is a system property and therefore, only specific to a class of systems. IQCs are system property qualifiers by which the designer obtains a robustness test. Thus, if the designer decides to perform a robustness test against passive uncertainties then a particular IQC is selected and the stability test follows from that constraint. Furthermore, via IQCs it is possible to combine different properties of the same class of systems. Suppose we have a class of uncertainties that are both passive and small-gain, then it's not clear how to combine small-gain theorem and passivity theorem exclusively to remove the resulting conservatism had we had used only one of these stability results since each neglects the other system property.

The equivalence we have presented is a consequence of the so-called Main Loop Theorem which is originally formulated for μ-analysis but tailored for our context (see [165, Thm. 11.7]):

Theorem 10. *Let N be an LTI network interconnected to a human model Δ_1 from the class of passive LTI operators and to the environment Δ_2 from some class of models. For our convenience, let us also use M to denote the 1-port immitance operator seen by Δ_1 (or perceived by the human). Then the following two statements are equivalent:*

   i) The interconnection of N with both arbitrary uncertainties Δ_1 and Δ_2 from their respective classes is stable.

   ii) The $M - \Delta_1$ interconnection is stable for all Δ_1 and Δ_2, if M is strictly passive for all Δ_2 in the respective class.

In other words, passivity-based techniques focus on verifying condition ii) by implicitly fixing to one class of uncertainties (here passivity) and then test whether the system seen by that uncertainty is also strictly in that class, while our IQC approach is based on checking i).

This formulation also allows us to exemplify the point that we strongly underline in this chapter: Assertion ii) resists to be utilized in a convenient way if we are aware of an extra property that also characterizes Δ_1 such as the small-gain and passive LTI operator example we have given above. The main difficulty is that in

many cases it is unknown how to translate this information into a test for M that needs to be verified for all admissible Δ_2. However, the IQC formulation based on (i) does not exhibit this complication, which is one of its powerful features as demonstrated with the delay robustness example.

Synthesis

As we have shown in the previous chapters, the bilateral teleoperation problem can be carried over to a more general framework of IQCs. By doing so not only the existing results are preserved, but also substantial generalization options are obtained. Moreover, the shortcomings of the classical results and the underlying relations are clearly seen.

Hence, we can proceed with the controller design problem and obtain controllers using the results for IQC synthesis literature. Since the results here can be considered as established, we adopt "a running example" type of style instead of repeating already available results in the literature with theorems and proofs enumerated after one another.

4.1 Robust Controller Design using IQCs

LMI-based control synthesis methods are in general nonconvex and even the existence of a possible convexification step is not known. The μ-synthesis and Lyapunov-based synthesis methods are the two main classical ways of designing a robust controller.

Clearly, this problem is not much different for IQC synthesis which is closely related to μ tools. As we have shown in chapter 3, the dynamic multipliers are of the most importance when it comes to reducing the conservatism involved in the frequency-domain stability analysis techniques. However including dynamics to the multipliers makes the problem harder for the robust control synthesis problem. Since there is no known convex robust control design method known, we resort back to a nonconvex multiplier/controller iteration as is the case with the classical μ-tools with the so-called *DK*-iteration. However, it has been recently shown that, a large class of robust control design problems are convex depending on the uncertainty contribution on certain entries of the plant data, [135].

4.1.1 *Notation and Definitions*

We start with state-space descriptions of systems in the following form

$$
\begin{pmatrix} \dot{x} \\ z \\ y \end{pmatrix} = \underbrace{\begin{pmatrix} A & B_w & B_u \\ C_z & D_{wz} & D_{uz} \\ C_y & D_{wy} & D_{uy} \end{pmatrix}}_{G} \begin{pmatrix} x \\ w \\ u \end{pmatrix} \tag{4.1}
$$

Here, w denotes the generalized disturbance signals (perturbations, reference signals etc.), z denotes the controlled output signals that is selected as the objectives of the control design (minimization of error norms, control actions etc.) y signals are the measurements and u are the controller inputs. Typically, the second row is called the *performance channel* and the last row is, similarly, the *control channel*. The integers n, n_u, n_w, m_z, m_y denote the number of states, control inputs, disturbance inputs, control outputs, and measurements respectively. For the performance characterization, we also use a quadratic form

$$
\int_0^\infty \begin{pmatrix} w(t) \\ z(t) \end{pmatrix}^T P_p \begin{pmatrix} w(t) \\ z(t) \end{pmatrix} dt \leq -\epsilon \, \|w\|^2. \tag{4.2}
$$

As a typical example, the robust $\mathcal{L}_2$ gain from w to z can be rewritten as such by using

$$
P_p = \begin{pmatrix} -\gamma^2 I_{n_w} & 0 \\ 0 & I_{m_z} \end{pmatrix}
$$

We will also be referring to the state-space representation of a controller K via

$$
\begin{pmatrix} \dot{x}_K \\ u \end{pmatrix} = \begin{pmatrix} A_K & B_K \\ C_K & D_K \end{pmatrix} \begin{pmatrix} x_K \\ y \end{pmatrix} \tag{4.3}
$$

with n_K being the number of states of the controller. The common assumption of $D_{uy} = 0$ is also adopted here. This causes no loss of generality as long as the interconnection of *G-K* interconnection is well-posed i.e. $(I - D_{uy}D_K)$ is nonsingular. Then, the closed loop plant $(G \star K)(s)$ state-space matrices are obtained as

$$
\left[\begin{array}{c|c} \mathcal{A} & \mathcal{B} \\ \hline \mathcal{C} & \mathcal{D} \end{array} \right] = \left[\begin{array}{cc|c} A + B_u D_K C_y & B_u C_K & B_w + B_u D_K D_{wy} \\ B_K C_y & A_K & B_K D_{wy} \\ \hline C_z + D_{uz} D_K C_y & D_{uz} C_K & D_{wz} + D_{uz} D_K D_{wy} \end{array} \right] \tag{4.4}
$$

$$
= \left[\begin{array}{cc|c} A & 0 & B_w \\ 0 & 0 & 0 \\ \hline C_z & 0 & D_{wz} \end{array} \right] + \left[\begin{array}{cc} 0 & B_u \\ I & 0 \\ \hline 0 & D_{uz} \end{array} \right] \left[\begin{array}{cc} A_K & B_K \\ C_K & D_K \end{array} \right] \left[\begin{array}{cc|c} 0 & I & 0 \\ C_y & 0 & D_{wy} \end{array} \right]. \tag{4.5}
$$

Here two-letter subscripts, $\cdot_{ab}$ denote the term that represents the contribution from input a to output b which hopefully gives some relief to the reader since the manipulations quickly get ugly.

Definition 3 (Generalized Plant)**.** *The plant G is said to be a generalized plant if there exists at least one controller K such that the interconnection of G and K is stable. Equivalently, G is a generalized plant if (A, B_u) is stabilizable and (A, C_y) is detectable.*

4.1.2 *Solving Analysis LMIs for Controller Matrices*

Once we have the generalized plant description we can design a controller that achieves closed loop stability and a performance level characterized by P_p. Before we state the nominal controller synthesis conditions, we provide a "trick", the so-called Linearization Lemma which can be found in [137]. It is also important to follow the rationale behind the arguments given in [136] for general quadratic performance synthesis.

Lemma 11. *Assume we are given with a quadratic form in which A, S are constant matrices and $B(v), Q(v)$ and $R(v) \succeq 0$ are matrix functions of some decision variables denoted by v such that*

$$\begin{pmatrix} A \\ B(v) \end{pmatrix}^T \begin{pmatrix} Q(v) & S \\ S^T & R(v) \end{pmatrix} \begin{pmatrix} A \\ B(v) \end{pmatrix} \prec 0 \tag{4.6}$$

should be verified. Also assume that there exists a decomposition such that $R(v) = T(U(v))^{-1}T^T$ where $U(v) \succ$ is affine in v then (4.6) can be converted to the LMI problem

$$\begin{pmatrix} A^T Q(v) A + A^T S B(v) + B^T(v) S^T A & B^T(v) T \\ T^T B(v) & -U(v) \end{pmatrix} \prec 0 \tag{4.7}$$

Proof. Applying Schur Complement formula with respect to the lower right block of the LMI and simply carrying out the block multiplication in the quadratic inequality shows the equivalence. $\square$

Note that, even if $R(v) = R$ i.e. some constant matrix, this step is needed for resolving the quadratic dependence of $B(v)$.

Following our analysis results from the previous chapter, we have seen that for a stable closed loop system $G \star K$ to have a performance level of P_p the condition

$$\begin{pmatrix} I & 0 \\ \mathcal{A} & \mathcal{B} \\ \hline 0 & I \\ \mathcal{C} & \mathcal{D} \end{pmatrix}^T \left(\begin{array}{cc|c} 0 & \mathcal{X} & 0 \\ \mathcal{X} & 0 & 0 \\ \hline 0 & 0 & P_p \end{array} \right) \begin{pmatrix} I & 0 \\ \mathcal{A} & \mathcal{B} \\ \hline 0 & I \\ \mathcal{C} & \mathcal{D} \end{pmatrix} \prec 0$$

should hold for some symmetric matrix $\mathcal{X}$. However, in the absence of the knowledge of a stabilizing controller we encounter an immediate problem. If we assume the controller matrices in calligraphic closed loop matrices as unknowns then they multiply the unknown matrix $\mathcal{X}$ variables and hence destroying the affine dependence on the unknowns, rendering the constraint as a Bilinear Matrix Inequality (BMI). Also in the analysis case the stability was assumed at the outset however here the positivity constraint, $\mathcal{X} \succ 0$ should be included to guarantee closed loop stability. Thus, the synthesis problem is more involved. The resolution of this problem appeared mainly in [95, 136] (also in a strict $\mathcal{H}_\infty$ context, [38, 39] with an two-step procedure of elimination of the controller parameters and obtaining some of the LMI variables and then resolving the LMIs for controller parameters).

The essential trick is to manifacture a new set of derived variables from the original variables such that the problem is not altered but conditions become LMIs again. For this purpose, suppose we partition the matrices

$$\mathcal{X} = \begin{pmatrix} X & U \\ U^T & \bullet \end{pmatrix}, \mathcal{X}^{-1} = \begin{pmatrix} Y & V \\ V^T & \bullet \end{pmatrix},$$

where $\bullet$ denotes the entries that we are not interested in. Also using the relations $\mathcal{X}\mathcal{X}^{-1} = I$, we have

$$\mathcal{Y} = \begin{pmatrix} Y & I \\ V^T & 0 \end{pmatrix}, \mathcal{Z} = \begin{pmatrix} I & 0 \\ X & U \end{pmatrix}$$

and $\mathcal{Y}^T\mathcal{X} = \mathcal{Z}$. Then by a congruence transformation the analysis LMI

$$\begin{pmatrix} Y & 0 \\ 0 & I \end{pmatrix}^T \begin{pmatrix} I & 0 \\ \mathcal{A} & \mathcal{B} \\ 0 & I \\ \mathcal{C} & \mathcal{D} \end{pmatrix}^T \left(\begin{array}{cc|c} 0 & \mathcal{X} & 0 \\ \mathcal{X} & 0 & 0 \\ \hline 0 & 0 & P_p \end{array}\right) \begin{pmatrix} I & 0 \\ \mathcal{A} & \mathcal{B} \\ 0 & I \\ \mathcal{C} & \mathcal{D} \end{pmatrix} \begin{pmatrix} Y & 0 \\ 0 & I \end{pmatrix} \prec 0$$

becomes

$$\begin{pmatrix} I & 0 \\ \mathbf{A} & \mathbf{B} \\ 0 & I \\ \mathbf{C} & \mathbf{D} \end{pmatrix}^T \left(\begin{array}{cc|c} 0 & I & 0 \\ I & 0 & 0 \\ \hline 0 & 0 & P_p \end{array}\right) \begin{pmatrix} I & 0 \\ \mathbf{A} & \mathbf{B} \\ 0 & I \\ \mathbf{C} & \mathbf{D} \end{pmatrix} \prec 0 \tag{4.8}$$

where boldface variables are defined as

$$\left(\begin{array}{c|c} \mathbf{A} & \mathbf{B} \\ \hline \mathbf{C} & \mathbf{D} \end{array}\right) := \left(\begin{array}{cc|c} AY + B_uM & A + B_uNC_y & B_w + B_uND_{wy} \\ K & AX + LC_y & XB_w + LD_{wy} \\ \hline C_zY + D_{uz}M & C_z + D_{uz}NC_y & D_{zw} + D_{uz}ND_{wy} \end{array}\right)$$

together with

$$\begin{pmatrix} K & L \\ M & N \end{pmatrix} := \begin{pmatrix} U & XB_u \\ 0 & I \end{pmatrix} \begin{pmatrix} A_K & B_K \\ C_K & D_K \end{pmatrix} \begin{pmatrix} V^T & 0 \\ C_y Y & I \end{pmatrix} + \begin{pmatrix} XAY & 0 \\ 0 & 0 \end{pmatrix} \tag{4.9}$$

It's indeed not that easy to follow the inner workings of this transformation however after a tedious multiplication exercise it can be seen that the aforementioned bijective transformation does the job. Thus, boldface variables are now functions of X, Y, K, L, M, N matrices and moreover the constraint is once again an LMI (after the application of Lemma 11). For stability characterization we also need $\mathcal{X} \succ 0$ and using the same transformation $\mathcal{Y}^T \mathcal{X} \mathcal{Y} \succ 0$, we obtain

$$\mathbf{X} := \begin{pmatrix} X & I \\ I & Y \end{pmatrix} \succ 0.$$

Therefore, instead of BMIs we have obtained LMI conditions all involving boldface variables entering affinely. This set of variables are typically denoted by $v = \{X, Y, K, L, M, N\}$. Unfortunately, $K(s)$ and K creates a naming clash however we will not resolve this to comply with the literature, instead we'll rely on the reader for the distinction and try to state whichever is meant in case of an ambiguity.

With all this preparation, we arrive at the nominal synthesis problem :

Theorem 12. *The nominal synthesis problem is solvable if there exists a feasible set of variables v such that*

$$\mathbf{X} \succ 0, \quad \begin{pmatrix} I & 0 \\ \mathbf{A} & \mathbf{B} \\ 0 & I \\ \mathbf{C} & \mathbf{D} \end{pmatrix}^T \left(\begin{array}{cc|c} 0 & I & 0 \\ I & 0 & 0 \\ \hline 0 & 0 & P_p \end{array} \right) \begin{pmatrix} I & 0 \\ \mathbf{A} & \mathbf{B} \\ 0 & I \\ \mathbf{C} & \mathbf{D} \end{pmatrix} \prec 0 \tag{4.10}$$

hold. Once a feasible solution is found by the aid of Lemma 11, the controller can be obtained by first by finding arbitrary U and V matrices by solving $I - XY = UV^T$ and then back substituting the variables into (4.9)

In summary, we have obtained a nominally stabilizing and P_p-performance level guaranteeing controller. Next, we include uncertainty channels to our plant G and add a robustness constraint in our design. Unfortunately, this breaks down our "LMIzation" step and there is no known method to obtain LMI solutions from the BMI constraints given below.

4.1.3 *Adding Uncertainty Channels*

We renew our plant representation by the following relations

$$
\begin{pmatrix} \dot{x} \\ q \\ z \\ y \end{pmatrix} = \underbrace{\begin{pmatrix} A & B_p & B_w & B_u \\ C_q & D_{pq} & D_{wq} & D_{uq} \\ C_z & D_{pz} & D_{wz} & D_{uz} \\ C_y & D_{py} & D_{wy} & 0 \end{pmatrix}}_{G} \begin{pmatrix} x \\ p \\ w \\ u \end{pmatrix}
\tag{4.11}
$$

and $p = \Delta q$. The positive integers n_p, m_q are the uncertainty operator row/column numbers respectively. Also this extra channel is often called the "uncertainty channel". Once again we start off with the robustness/performance analysis LMI. For that we also need to connect our stabilizing controller. The new closed loop matrices are obtained as

$$
\left[\begin{array}{c|cc} \mathcal{A} & \mathcal{B}_p & \mathcal{B}_w \\ \hline \mathcal{C}_q & \mathcal{D}_{pq} & \mathcal{D}_{wq} \\ \mathcal{C}_q & \mathcal{D}_{pz} & \mathcal{D}_{wz} \end{array} \right] = \left[\begin{array}{cc|cc} A & 0 & B_p & B_w \\ 0 & 0 & 0 & 0 \\ \hline C_q & 0 & D_{pq} & D_{wq} \\ C_z & 0 & D_{pz} & D_{wz} \end{array} \right] +
$$

$$
\left[\begin{array}{cc} 0 & B_u \\ I & 0 \\ \hline 0 & D_{uq} \\ 0 & D_{uz} \end{array} \right] \left[\begin{array}{cc} A_K & B_K \\ C_K & D_K \end{array} \right] \left[\begin{array}{cc|cc} 0 & I & 0 & 0 \\ C_y & 0 & D_{py} & D_{wy} \end{array} \right].
\tag{4.12}
$$

Suppose a block diagonal collection of uncertainty operators, **Δ** characterized by a family of constant multipliers **P**. Moreover, assume that the $\Delta \star (G \star K)$ is well-posed for all $\Delta \in \Delta$. For notational convenience we also introduce the partitions

$$
P = \begin{pmatrix} Q & S \\ S^T & R \end{pmatrix}, \quad P_p = \begin{pmatrix} Q_p & S_p \\ S_p^T & R_p \end{pmatrix}
$$

Again, as given in Chapter 3, the closed loop system is robustly stable for all $\Delta \in \Delta$ and achieves performance characterized by the multiplier P_p if there exist a $P \in \mathbf{P}$ and a symmetric matrix $\mathcal{X}$ such that

$$
\begin{pmatrix} I & 0 & 0 \\ \mathcal{A} & \mathcal{B}_p & \mathcal{B}_w \\ 0 & I & 0 \\ \mathcal{C}_q & \mathcal{D}_{pq} & \mathcal{D}_{wq} \\ 0 & 0 & I \\ \mathcal{C}_z & \mathcal{D}_{pz} & \mathcal{D}_{wz} \end{pmatrix}^T \left(\begin{array}{cc|cc|cc} 0 & \mathcal{X} & & & & \\ \mathcal{X} & 0 & & & & \\ \hline & & Q & S & & \\ & & S^T & R & & \\ \hline & & & & Q_p & S_p \\ & & & & S_p^T & R_p \end{array} \right) \begin{pmatrix} I & 0 & 0 \\ \mathcal{A} & \mathcal{B}_p & \mathcal{B}_w \\ 0 & I & 0 \\ \mathcal{C}_q & \mathcal{D}_{pq} & \mathcal{D}_{wq} \\ 0 & 0 & I \\ \mathcal{C}_z & \mathcal{D}_{pz} & \mathcal{D}_{wz} \end{pmatrix} \prec 0
\tag{4.13}
$$

For the controller synthesis case, unfortunately previous transformation does not resolve the additional bilinear terms and in fact it is not even known if such a transformation is possible or not. We can either try to solve BMIs directly with nonconvex optimization techniques or we can use another nonconvex solution which is known as the multiplier-controller iteration.

Notice that if we have the stabilizing controller then the outer factors are constant matrices and we have an LMI problem. Conversely, if we have a feasible multiplier such that the inequality is satisfied then it's a matter of applying the aforementioned transformation and linearizing lemma to obtain a controller. Hence, we can perform an iteration by either fixing the multiplier or the controller.

4.1.4 *The Multiplier-Controller Iteration with Frequency-Independent Multipliers*

If we start with a uncertain generalized plant representation, we have neither the controller nor the robustness multipliers. Moreover, we don't have a method to search for both simultaneously. Thus, we first consider the nominal control design problem and obtain a nominally stabilizing controller as given above. It can also be shown that, the closed loop, with the well-posedness assumption and a simple continuity argument, has some, possibly very limited, robustness properties against the uncertainty set we would like to consider. In other words, there is no reason for the controller to be robustly stabilizing against the full uncertainty region that we originally modeled since we did not enforce it by any constraint.

Remark 11. *This is briefly the rationale behind the common assumption of star-shaped uncertainty region, i.e., $[0,1]\Delta \in \Delta$. However, it is important to note that, the scaling needs not to be a simple scalar $r \in [0,1]$ such that the uncertainty is scaled with $r\Delta$. This point is often implicitly assumed and rarely mentioned. However the notation $r\Delta$ should be taken conceptually. As an example, the delay uncertainty cannot be scaled with $re^{-s\tau}$ for any $r \in [0,1]$ since it would scale the unit-circle. In fact what we want to scale is the τ variable as $e^{-sr\tau}$ such that when $r = 0$ we have $e^0 = 1$ i.e. a non-delayed line and for $r = 1$ we have $e^{-s\tau}$ i.e. full duration of the maximum allowed delay. Similarly, for the saturation and dead-zone nonlinearities are examples of such nontrivial scaling cases. Hence, the star-shapedness in this context becomes a parametrization of the size of the uncertainty from the nominal case to the full-sized uncertainty. Nevertheless most uncertainty types are amenable to scaling with r-multiplication hence there is no need to invent yet another notation for an already complicated procedure. Therefore, every uncertainty needs to be scaled in a customized way but for notational convenience we will still use $r\Delta$ to denote the scaled uncertainty size.*

Summarizing our current situation, we have obtained a nominally stabilizing controller and we have parameterized a custom scaling method for each of our
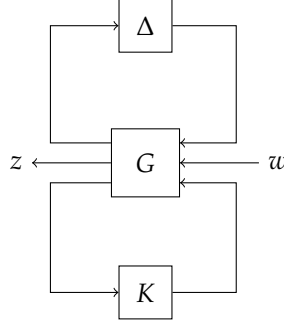
Figure 4.1: The uncertain interconnection

uncertainty subblocks. Now we would like to search for the maximum achievable r via analysis. Hence, we can search over the maximum r such that the scaled closed loop is robustly stable for all $\Delta \in r\mathbf{\Delta}$.

Formally we have the following two theorems that constitutes the initialization and also the two steps of the iteration: We assume that the uncertain LTI plant

$$G : \mathcal{L}_{2e}^{n_p+n_w+n_u} \to \mathcal{L}_{2e}^{m_q+m_z+m_y},$$

is a generalized plant i.e. there exists an LTI controller

$$K : \mathcal{L}_{2e}^{m_y} \to \mathcal{L}_{2e}^{n_u},$$

such that the nominal closed loop plant $G_{nom} \star K \in \mathcal{RH}_{\infty}^{m_z \times n_w}$ where

$$G_{nom}(s) = \begin{pmatrix} 0_{(m_z+m_y) \times m_q} & I_{m_z+m_y} \end{pmatrix} G(s) \begin{pmatrix} 0_{n_p \times (n_w+n_u)} \\ I_{n_w+n_u} \end{pmatrix}.$$

Additionally $\mathbf{P}$ denotes the suitable multiplier that all $\Delta \in \mathbf{\Delta}$ satisfies the quadratic constraint.

Theorem 13 (Analysis Step). *The interconnection of an LTI uncertain plant $G(s)$ given by (4.12) with a nominally stabilizing controller K given by (4.3), depicted in Figure 4.1 and admits the realization given in (4.12) is robustly stable in the face of all $\Delta \in r\mathbf{\Delta}$ and achieves the performance level characterized by P_p if there exist a symmetric matrix $\mathcal{X}$ and $P \in \mathbf{P}$ such that (4.13) hold.*

One can simply perform a line search for the largest possible $r \in [0, 1]$ such that the conditions are numerically verified and P_p is optimized. Then the resulting multiplier P is fixed and we switch to the controller design step.

Theorem 14 (Synthesis Step). *Assume an uncertain LTI plant $G(s)$ given by (4.12) is given. There exist an LTI controller K such that the closed loop is stable for all $\Delta \in r\Delta$ and achieves the performance level characterized by P_p if there exist a set of variables $v = \{X, Y, K, L, M, N\}$ such that the linearized version of the constraint (omitted for brevity)*

$$
\begin{pmatrix} I & 0 & 0 \\ \mathbf{A} & \mathbf{B}_p & \mathbf{B}_w \\ \hline 0 & I & 0 \\ \mathbf{C}_q & \mathbf{D}_{pq} & \mathbf{D}_{wq} \\ \hline 0 & 0 & I \\ \mathbf{C}_z & \mathbf{D}_{pz} & \mathbf{D}_{wz} \end{pmatrix}^T
\left(\begin{array}{cc|cc|cc} 0 & I & & & & \\ I & 0 & & & & \\ \hline & & Q & S & & \\ & & S^T & R & & \\ \hline & & & & Q_p & S_p \\ & & & & S_p^T & R_p \end{array} \right)
\begin{pmatrix} I & 0 & 0 \\ \mathbf{A} & \mathbf{B}_p & \mathbf{B}_w \\ \hline 0 & I & 0 \\ \mathbf{C}_q & \mathbf{D}_{pq} & \mathbf{D}_{wq} \\ \hline 0 & 0 & I \\ \mathbf{C}_z & \mathbf{D}_{pz} & \mathbf{D}_{wz} \end{pmatrix} \prec 0
$$

$$(4.14)$$

and $\mathbf{X} \succ 0$ hold.

Proofs of both theorems are given in [137] in detail.

Again, in this step we optimize over P_p while performing a line search over r. Theoretically, since the analysis result is feasible for some r_a, the controller step should at least give a feasible result for $r = r_a$ and possibly larger values should also return feasible results. However, numerically it's not the case. One might step down a little to actually obtain feasible results. In our cases, we allowed the maximum retreat value to be the $0.99r$ of the previous step. We have also observed that this might actually improve the conditioning of the LMI solution though by no means guaranteed.

Remark 12. *Note that same theorem can be formulated for all $\Delta \in \Delta$ and a closed loop plant $(G(r) \star K)(s)$, in other words we can also modify the plant information to scale the uncertainty by subsuming the r parameter suitably into the plant. To demonstrate the numerical problem, we assume that the uncertainties are of unstructured LTI type and for simplicity assume constant multipliers. For parametric uncertainties, it suffices to scale down the respective uncertainty channels for the scaling as shown in Figure 4.2.*

$$
\begin{pmatrix} r\Delta \\ I \end{pmatrix}^T \begin{pmatrix} Q & S \\ S^T & R \end{pmatrix} \begin{pmatrix} r\Delta \\ I \end{pmatrix} = \begin{pmatrix} \Delta \\ I \end{pmatrix}^T \begin{pmatrix} r^2 Q & rS \\ rS^T & R \end{pmatrix} \begin{pmatrix} \Delta \\ I \end{pmatrix} \succeq 0.
$$

Out of our test experience, we have found out that reflecting the scaling to the plant is better for numerical stability. Seemingly the reason for this is the numerical noise introduced when r is small in the early iteration steps. Notice how the square of r drives the Q block to zero if $0 < r \ll 1$. In case of a feasible multiplier is found, this multiplier should be stripped off from r since it will be again used in the controller step, but due to the numerical inaccuracies wild changes are possible and usually the resulting multiplier information
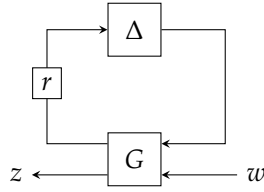
Figure 4.2: Reflecting the uncertainty scaling to the plant

is contaminated. We have found out[1] that we have more freedom in the scaled plant case since one can decrease the bad effect of small numbers via balanced realizations, cleaning up the state-space matrices etc. Moreover as we show later, in the frequency dependent multiplier case, r variable becomes garbled in the factorizations, minimal realizations etc. Hence, in this work, it is recommended to scale the plant instead of the multipliers.

Hence, we have a theoretically increasing sequence of analysis and synthesis uncertainty sizes

$$r_{si} = 0 < r_{a1} \leq r_{s1} \leq \ldots \leq r_{an} \simeq r_{sn}$$

Similarly, the performance objective gets worse or at least stays constant at after each succesful iteration revealing an increasing sequence of real scalar such as the robust $\mathcal{L}_2$ gain or a similar functional.

The iteration terminates when the last approximate equality is satisfied with desired accuracy or both limits are close enough to 1 together with agreeing performance level P_p. Notice that we don't allow the iteration to terminate even if the r values agree, the performance levels should also agree for numerical consistency. The aforementioned numerical difficulty might exhibit a phenomenon such that both r_a and r_s come very close to 1 but don't quite reach to 1. We have coded an extra condition that if r values come close to 1 within the prescribed accuracy, the code simply assumes $r = 1$, such that the oscillations are removed and the $r = 1$ is tested at each step.

Another numerical difficulty is the factorization of $I - XY = UV^T$. Since the controller construction involves the inverses of U and V, it is imperative that the factorization is well-conditioned with respect to inversion.

4.1.5 *The Multiplier-Controller Iteration with Dynamic Multipliers*

From our analysis results it can be seen that dynamic multipliers provide substantial conservatism reduction. However, the iterative control design procedure given

---

[1]Initially suggested by César Lopéz during the experiments.

above can not handle the dynamic multipliers in a straightforward fashion. Although, the mechanism is essentially the same, the only missing step is subsuming the frequency-dependent part of the multipliers into the outer factors. Let us give a conceptual example to demonstrate the obstacle. For notational convenience we partition the closed loop plant into the uncertainty and performance channels

$$H := (G \star K) = \begin{pmatrix} H_q \\ H_z \end{pmatrix}$$

Suppose we are given with a feasible robustness/performance analysis LMI in frequency domain i.e.

$$\begin{pmatrix} I & 0 \\ H_q \\ 0 & I \\ H_z \end{pmatrix}^* \left(\begin{array}{cc|cc} Q(i\omega) & S(i\omega) & & \\ S^*(i\omega) & R(i\omega) & & \\ \hline & & Q_p & S_p \\ & & S_p^T & R_p \end{array} \right) \begin{pmatrix} I & 0 \\ H_q \\ 0 & I \\ H_z \end{pmatrix} \prec 0$$

holds for some $P(i\omega), P_p$ for all $\omega \in \mathbb{R}_e$ and suppose that the frequency-dependent multiplier is parametrized with outer factors, similar to what we have shown in our analysis examples before, as the following;

$$(\star)^* \left(\star \right)^* \left(\begin{array}{cc|cc} M_1 & M_2 & & \\ M_2^T & M_3 & & \\ \hline & & Q_p & S_p \\ & & S_p^T & R_p \end{array} \right) \left(\begin{array}{cc|cc} \Psi_1 & \Psi_2 & & \\ \Psi_3 & \Psi_4 & & \\ \hline & & I & 0 \\ & & 0 & I \end{array} \right) \begin{pmatrix} I & 0 \\ H_q \\ 0 & I \\ H_z \end{pmatrix} \prec 0$$

Now, if we collect the frequency dependent parts together and leave the constant multiplier, we have

$$\left(\star \right)^* \left(\begin{array}{cc|cc} M_1 & M_2 & & \\ M_2^T & M_3 & & \\ \hline & & Q_p & S_p \\ & & S_p^T & R_p \end{array} \right) \begin{pmatrix} \Psi_1 + \Psi_2 H_q \\ \Psi_3 + \Psi_4 H_q \\ 0 \qquad I \\ H_z \end{pmatrix} \prec 0$$

Had it been the case that we have $\begin{pmatrix} I & 0 \end{pmatrix}$ in the top row of the outer factor, we could simply use our previous synthesis technique and we would be done. However, we don't have any technique to cope with such a complication. In other words, the obstacle is due to how we proceed with the synthesis step. Had we had another synthesis method this might not be an obstacle but currently we need to find a way to obtain the structure on that block such that we obtain an augmented plant from which we can extract the controller and hence obtain an augmented open loop plant.

Notice that if we had $\Psi_2(i\omega)$ identically zero and Ψ_1 invertable with a stable inverse, we can multiply the inequality with $\begin{pmatrix} \Psi_1^{-1} & \\ & I \end{pmatrix}$ and obtain the desired structure

$$
\left(\star \right)^* \left(\begin{array}{cc|cc} M_1 & M_2 & & \\ M_2^T & M_3 & & \\ \hline & & Q_p & S_p \\ & & S_p^T & R_p \end{array} \right) \left(\begin{array}{cc|cc} I & & 0 \\ (\Psi_3 + \Psi_4 H_{q1})\Psi_1^{-1} & \Psi_4 H_{q2} \\ \hline 0 & & I \\ H_{z1}\Psi_1^{-1} & & H_{z2} \end{array} \right) \prec 0.
$$

Then, one can show that the resulting open-loop system becomes

$$
G_{aug} = \begin{pmatrix} (\Psi_3 + \Psi_4 G_{pq})\Psi_1^{-1} & \Psi_4 G_{wq} & \Psi_4 G_{uq} \\ G_{pz}\Psi_1^{-1} & G_{wz} & G_{uz} \\ G_{py}\Psi_1^{-1} & G_{wy} & 0 \end{pmatrix} \tag{4.15}
$$

thus, the obstacle that needs to be avoided is to find a way to obtain an equivalent multiplier of the form

$$
P(i\omega) = \begin{pmatrix} \Psi_1(i\omega) & \Psi_2(i\omega) \\ \Psi_3(i\omega) & \Psi_4(i\omega) \end{pmatrix}^* \begin{pmatrix} M_1 & M_2 \\ M_2^T & M_3 \end{pmatrix} \begin{pmatrix} \Psi_1(i\omega) & \Psi_2(i\omega) \\ \Psi_3(i\omega) & \Psi_4(i\omega) \end{pmatrix} \tag{4.16}
$$

$$
= \begin{pmatrix} \hat{\Psi}_1(i\omega) & 0 \\ \hat{\Psi}_3(i\omega) & \hat{\Psi}_4(i\omega) \end{pmatrix}^* \hat{M} \begin{pmatrix} \hat{\Psi}_1(i\omega) & 0 \\ \hat{\Psi}_3(i\omega) & \hat{\Psi}_4(i\omega) \end{pmatrix} \tag{4.17}
$$

$$
=: \hat{P}(i\omega) \tag{4.18}
$$

where $\hat{\Psi}_1$ needs to biproper and bistable. This has been proposed in [43, 44] (see also [153] for state-space derivation). Here the essential difficulty is that Ψ_i are often tall basis transfer matrices and are not invertible. Hence we look for square factorizations that are inherently linked to J-spectral factorizations of quadratic forms. We will first take a detour on the structural properties of the multipliers in general before we state the actual multiplier replacement. The style is based on [55].

Definition 4 (Inertia). *The triple obtained by the enumeration of the number of the positive, zero and negative eigenvalues is said to be the inertia of a hermitian matrix A and denoted by in $A = \{n_+, n_0, n_-\}$ e.g.*

$$
\text{in } I_{2\times 2} = \{2,0,0\} \ , \text{in } 0_{n\times n} = \{0, n, 0\} \ , \text{in } \begin{pmatrix} 1 & & \\ & -1 & \\ & & -1 \end{pmatrix} = \{1,0,2\}
$$

Specifically, $\nu(A) = n_-, \pi(A) = n_+, \zeta(A) = n_0$.

Recall that we have the following two main inequalities that are of interest by the IQC theorem;

$$\int_{-\infty}^{\infty} \begin{pmatrix} \widehat{\Delta(v)}(i\omega) \\ \hat{v}(i\omega) \end{pmatrix}^* \Pi(i\omega) \begin{pmatrix} \widehat{\Delta(v)}(i\omega) \\ \hat{v}(i\omega) \end{pmatrix} d\omega \succeq 0 \tag{4.19}$$

$$\begin{pmatrix} I \\ G(i\omega) \end{pmatrix}^* \Pi(i\omega) \begin{pmatrix} I \\ G(i\omega) \end{pmatrix} \preceq -\epsilon I \tag{4.20}$$

These inequalities impose constraints on the inertia of the frequency-dependent multiplier. Consider the following simple fact: let a multiplier Π partitioned as

$$\Pi = \begin{pmatrix} \Pi_1 & \Pi_2 \\ \Pi_2^* & \Pi_3 \end{pmatrix} \tag{4.21}$$

Lemma 15. *The number of negative eigenvalues of Π is greater then or equal to Π_1*

Proof. Since

$$\begin{pmatrix} I & 0 \\ -\Pi_2^* \Pi_1^{-1} & I \end{pmatrix} \begin{pmatrix} \Pi_1 & \Pi_2 \\ \Pi_2^* & \Pi_3 \end{pmatrix} \begin{pmatrix} I & -\Pi_1^{-1}\Pi_2 \\ 0 & I \end{pmatrix} = \begin{pmatrix} \Pi_1 & 0 \\ 0 & \Pi_3 - \Pi_2^* \Pi_1^{-1}\Pi_2 \end{pmatrix}$$

and since the number can only increase.

Here, we assumed that Π_1^{-1} exists. If not, then, we can make it nonsingular without changing the number of negative eigenvalues by adding a sufficiently small matrix, ϵI. Since we are not interested in the number of zero eigenvalues, this operation causes no problem. $\square$

Next, we show that the inertia is further constrained by the outer factor rank.

Lemma 16. *For a hermitian matrix Π, there exists an $X \in \mathbb{R}^{m \times n}$ such that*

$$\begin{pmatrix} I \\ X \end{pmatrix}^T \Pi \begin{pmatrix} I \\ X \end{pmatrix} \prec 0 \tag{4.22}$$

if and only if Π has at least n negative eigenvalues.

Proof. ($\Rightarrow$) Complete the outer factors to a square matrix as

$$P = \begin{pmatrix} I & 0 \\ X & I \end{pmatrix}^T \Pi \begin{pmatrix} I & 0 \\ X & I \end{pmatrix}$$

and inertia is preserved i.e. in $\Pi = $ in P. Note that $(1,1)$ block of P is (4.22). Hence, from Lemma 15, we have, $n = \nu(P_{11}) \leq \nu(P) = \nu(\Pi)$.

($\Leftarrow$) Assume $n + m \geq \nu(\Pi) \geq n$. Let $U = \begin{pmatrix} U_1 \\ U_2 \end{pmatrix} \in \mathbb{R}^{\nu(\Pi) \times n}$ be a matrix spanning the negative eigenspace where U_1 is square. If U_1 is invertible, then, $X = U_2 U_1^{-1}$ is a solution. Or we perturb with ϵI, and use $X = U_2(U_1 + \epsilon I)^{-1}$. $\square$

Thus a quadratic form has to have at least as many negative eigenvalues as the outer factor rank to be negative definite. Using this information makes it easier to state some conclusions about the inertia of a frequency-dependent multiplier. Obviously we need to make sure that the inertia stays the same on the imaginary axis. Hence we can make use of a result regarding the frequency-dependent case by the following (see [99] and references therein):

Theorem 17. *Let $\phi(i\omega)$ be a hermitian bounded measurable matrix-valued function. The following statements are equivalent:*

1. *the functional*

$$\sigma(f) = \int_{-\infty}^{\infty} \hat{f}^*(i\omega)\phi(i\omega)\hat{f}(i\omega)d\omega$$

   is nonnegative for all $f \in \mathcal{L}_2^k(0, \infty)$.

2. *$\phi(i\omega) \succeq 0$ almost everywhere for $\omega \in (0, \infty)$.*

Proof.
  $(2) \implies (1)$ is a direct consequence.
  $(1) \implies (2)$ The quadratic form $\sigma(f)$ is time-invariant on $\mathcal{L}_2(-\infty, \infty)$. If $\sigma \geq 0$ on $\mathcal{L}_2(0, \infty)$ then $\sigma \geq 0$ on $\mathcal{L}_2(t_0, \infty)$ for any $t_0 > -\infty$. Moreover,

$$\bigcup_{t>-\infty} \mathcal{L}_2(t, \infty)$$

is dense in $\mathcal{L}_2(-\infty, \infty)$ and σ is continuous on $\mathcal{L}_2(-\infty, \infty)$. Therefore $\sigma \geq 0$ on $\mathcal{L}_2(-\infty, \infty)$ and hence item 2 holds.   □

The next result from [44] reveals the IQC multiplier structure for robustness tests.

Theorem 18. *If a hermitian, bounded, matrix-valued, and invertible (on $i\mathbb{R}_e$) multiplier H satisfies the IQC and the corresponding FDI (4.19) and (4.20) then there exists a matrix-valued, bounded and invertible (on $i\mathbb{R}_e$) S such that*

$$H(i\omega) = S^*(i\omega) \begin{pmatrix} -I_{n_p} & 0 \\ 0 & I_{m_q} \end{pmatrix} S(i\omega) \quad \forall \omega \in \mathbb{R}_e$$

Proof. From (4.20) and Theorem 17 we can conclude that for all $\omega \in \mathbb{R}_e$, $H(i\omega)$ has at least n_p negative eigenvalues. Conversely, from (4.19) and the nominal case we also see that H_{22} is positive semi-definite. Finally, from the invertibility of H on the extended imaginary axis, such a diagonalizing congruence transformation with some S always exists.   □

With a slight abuse of the general signature matrix definition, which is a diagonal matrix with all entries on the diagonal are either 1 or -1, we use the following:

Definition 5. *Let M be an invertible, hermitian matrix with $\pi(M) = p, \nu(M) = n$. A diagonal matrix of $J = \mathrm{diag}\{-I_n, I_p\}$ is said to be the signature matrix of M.*

When $\nu(M) \neq 0$ the type of factorizations given in Theorem 18 is known as "*J-spectral factorization*" and exact solvability conditions are derived which relate the solvability of a certain Riccati equation to the existence of such factorizations (see, e.g.,[124]). However, to the best of our knowledge, there is no simple implementable result that guarantees the solvability of such indefinite Riccati equations. Since we aim for an automated iteration algorithm, we can not utilize these nice algebraic results. Additionally, there are also numerous generalizations, nuances about the assumptions whether (A, B) is just stabilizable or also controllable, whether Q is indefinite in general etc (see [83]) in the previous theorem. However, these are not relevant here. Due to this missing technical step, we make use of particular sign assumptions on the subblocks of the multiplier to perform partial factorizations and then obtain an overall factorization in the suitable form with steps that have solutions guaranteed to exist. For these steps, it suffices to use the standard spectral factorization results well-knwon from LQ-type problems. The following is also from [44]:

Theorem 19. *Let*

$$H(s) := \begin{pmatrix} H_{11}(s) & H_{12}(s) \\ H_{12}^*(s) & H_{22}(s) \end{pmatrix} \in \mathcal{RL}_\infty$$

be a hermitian, bounded and invertible transfer matrix on the imaginary axis with $H_{22}(s) \succ 0$ on $i\mathbb{R}_e$. Then there exists a factorization of the form

$$H(i\omega) = S^*(i\omega) J_H S(i\omega) \quad \forall \omega \in \mathbb{R}_e$$

where

$$S(s) := \begin{pmatrix} R(s) & 0 \\ Q(s) & P(s) \end{pmatrix}$$

with $P(s), R(s) \in \mathcal{RH}_\infty$ with stable inverses.

Proof. For the sake of brevity, we omit the frequency dependence from the notation of transfer matrices. First, from the assumption $H_{22} \succ 0$ and Lemma 15 we have

$$H_{11} - H_{12} H_{22}^{-1} H_{12}^* \prec 0 \tag{4.23}$$

for all $\omega \in \mathbb{R}_e$. We write

$$H = \begin{pmatrix} H_{11} - H_{12} H_{22}^{-1} H_{12}^* & 0 \\ 0 & 0 \end{pmatrix} + \begin{pmatrix} H_{12} \\ I \end{pmatrix} H_{22}^{-1} \begin{pmatrix} H_{12}^* & I \end{pmatrix}$$

Hence both H_{22} and (4.23) can be replaced with biproper, bistable spectral factors which will be defined next. Let $\hat{P}$ denote the spectral factor of $H_{22} = \hat{P}^* \hat{P}$ and R denote similarly that of (4.23). Then we have

$$\begin{aligned} H &= \begin{pmatrix} -R^* R & 0 \\ 0 & 0 \end{pmatrix} + \begin{pmatrix} H_{12} \hat{P}^{-1} \\ \hat{P}^* \end{pmatrix} \begin{pmatrix} \hat{P}^{-*} H_{12} & \hat{P} \end{pmatrix} \\ &=: \begin{pmatrix} -R^* R & 0 \\ 0 & 0 \end{pmatrix} + \begin{pmatrix} Q^* \\ P^* \end{pmatrix} \begin{pmatrix} Q^* \\ P^* \end{pmatrix}^* \\ &= \begin{pmatrix} R(s) & 0 \\ Q(s) & P(s) \end{pmatrix}^* \begin{pmatrix} -I & \\ & I \end{pmatrix} \begin{pmatrix} R(s) & 0 \\ Q(s) & P(s) \end{pmatrix} \end{aligned}$$

$\square$

Notice that the claim is only valid on the imaginary axis. For factorizations with respect to other contours, see [7]. The assumption of $H_{22} \succ 0$ is a mild one since many of the practically relevant multipliers have this property. However, passivity multipliers and some other shifted parameter intervals might have positive semi-definite block. In this case either a different factorization is employed (e.g. [43]) or the uncertainty channel is shifted until the desired property is achieved.

Now we are at a point where we know the inertia properties of the multiplier and also we know that the inertia stays the same on the imaginary axis. Moreover, with certain inertia of the lower left block, we can turn back to our problem of finding a suitable replacement of the multiplier with a new one involving invertible, biproper, and bistable factors. First let us state a classical and powerful result regarding the transfer matrix factorization (see [165, Thm. 13.19],[34, Thm. 7.3], and [163, Thm. 2]).

Theorem 20. *Let A, B, Q, S, R be matrices of compatible dimensions such that $Q = Q^T$ and $R = R^T \succ 0$, with (A, B) stabilizable. Suppose either one of the following assumptions is satisfied*

(A1) A has no eigenvalues on the imaginary axis.

(A2) Q is positive or negative semidefinite and (A, Q) has no unobservable modes on the imaginary axis.

Then,

(I) The following are equivalent;

(a) The hermitian matrix

$$\Phi(s) = \begin{pmatrix} (sI - A)^{-1}B \\ I \end{pmatrix}^* \begin{pmatrix} Q & S \\ S^T & R \end{pmatrix} \begin{pmatrix} (sI - A)^{-1}B \\ I \end{pmatrix}$$

satisfies $\Phi(i\omega) \succ 0$ for all $\omega \in \mathbb{R}_e$.

(b) There exists a unique symmetric X such that the matrix Riccati equation

$$XA + A^T X - (XB + S)R^{-1}(XB + S)^T + Q = 0$$

and $A - BR^{-1}(XB + S)^T$ is Hurwitz.

(c) The Hamiltonian matrix

$$\begin{pmatrix} A - BR^{-1}S^T & -BR^{-1}B^T \\ -(Q - SR^{-1}S^T) & -(A - BR^{-1}S^T)^T \end{pmatrix}$$

has no eigenvalues on the imaginary axis.

(II) The following statements are also equivalent:

(d) $\Phi(i\omega) \succeq 0$ for all $\omega \in \mathbb{R}_e$.

(e) There exists a unique symmetric X such that

$$XA + A^T X - (XB + S)R^{-1}(XB + S)^T + Q = 0$$

and $A - BR^{-1}(XB + S)^T$ has all its eigenvalues in the closed left-half plane.

Every such Φ has a spectral factorization $\Phi = \Phi_s^* \Phi_s$ where $\Phi_s, \Phi_s^{-1} \in \mathcal{RH}_\infty$. A Φ_s is denoted as the spectral factor of Φ.

In particular we are interested in the following corollary;

Corollary 21. *Consider a square hermitian transfer matrix $G \in \mathcal{RL}_\infty^{\bullet \times \bullet}$ with its inverse $G^{-1} \in \mathcal{RL}_\infty^{\bullet \times \bullet}$ and $G(\infty) \succ 0$. Then, G has a spectral factorization G_s such that*

$$G = G_s^* G_s$$

where $G_s, G_s^{-1} \in \mathcal{RH}_\infty^{\bullet \times \bullet}$.

Note that the system *G* need not be obtained from a quadratic form as we will continue considering. However, via separating the stable and the unstable modes with a state transformation and from the hermitian property of *G*, we can obtain a

particular structure without loss of generality. The structure is actually simpler to demonstrate; since the LTI system interconnection $y = G_1 G_2 u$ can be realized as

$$\begin{pmatrix} \dot{x} \\ y \end{pmatrix} = \begin{pmatrix} A_1 & B_1 C_2 & B_1 D_2 \\ 0 & A_2 & B_2 \\ C_1 & D_1 C_2 & D_1 D_2 \end{pmatrix} \begin{pmatrix} \dot{x} \\ u \end{pmatrix},$$

(4.24)

then any factorization $G = G_s^* G_s$ admits a realization of the form

$$G = G_s^* G_s = \left[\begin{array}{cc|c} -A_s^T & 0 & 0 \\ 0 & A_s & B_s \\ \hline -B_s^T & 0 & 0 \end{array} \right] + \left[\begin{array}{c} C_s^T \\ 0 \\ \hline D_s^T \end{array} \right] \left[\begin{array}{cc|c} 0 & C_s & D_s \end{array} \right]$$

(4.25)

partitioned accordingly. Also we have $G(\infty) = D_s^T D_s$. For the computation of the spectral factors consider the following multiplier with tall outer factors that satisfies

$$\Phi(i\omega)^* M \Phi(i\omega) \succ 0$$

for all $\omega \in \mathbb{R}_e$ as we had a few examples in Chapter 3. Using the minimal realization for $\Phi(s)$ we also have

$$\begin{pmatrix} B_\Phi^T (sI - A_\Phi)^{-*} \\ I \end{pmatrix} \begin{pmatrix} C_\Phi^T M C_\Phi & D_\Phi^T M C_\Phi \\ C_\Phi^T M D_\Phi & D_\Phi^T M D_\Phi \end{pmatrix} \begin{pmatrix} (sI - A_\Phi)^{-1} B_\Phi \\ I \end{pmatrix}$$

(4.26)

which is the desired form given in Theorem 20. Though we have omitted the proof, the relation with the Riccati equation can be sketched using the LMI version of this constraint. Via KYP Lemma, this is equivalent to the existence of a symmetric matrix X such that

$$\begin{pmatrix} I & 0 \\ A_\Phi & B_\Phi \\ C_\Phi & D_\Phi \end{pmatrix}^T \begin{pmatrix} 0 & X & 0 \\ X & 0 & 0 \\ 0 & 0 & M \end{pmatrix} \begin{pmatrix} I & 0 \\ A_\Phi & B_\Phi \\ C_\Phi & D_\Phi \end{pmatrix} \succ 0$$

(4.27)

holds. This means the Algebraic Riccati Inequality, which is nothing but straightforward multiplication and a Schur complement thanks to $\Phi(\infty) = D_\Phi^T M D_\Phi \succ 0$, also holds:

$$XA_\Phi + A_\Phi^T X - \underbrace{(XB_\Phi + C_\Phi^T M D_\Phi)}_{S} \underbrace{(D_\Phi^T M D_\Phi)^{-1}}_{R^{-1}} (XB_\Phi + C_\Phi^T M D_\Phi)^T + \underbrace{C_\Phi^T M C_\Phi}_{Q} \succ 0$$

(4.28)

Thus the corresponding Riccati Equation

$$XA_\Phi + A_\Phi^T X - (XB_\Phi + C_\Phi^T M D_\Phi)(D_\Phi^T M D_\Phi)^{-1}(XB_\Phi + C_\Phi^T M D_\Phi)^T + C_\Phi^T M C_\Phi = 0$$

(4.29)

has a unique stabilizing solution X and

$$A_\Phi - B_\Phi (D_\Phi^T M D_\Phi)^{-1} (X B_\Phi + C_\Phi^T M D_\Phi)^T$$

is Hurwitz. Since $(D_\Phi^T M D_\Phi) \succ 0$ we can replace this matrix with an arbitrary square factorization (square root, Cholesky etc.) $\hat{D}_\Phi^T \hat{D}_\Phi \succ 0$. Therefore, one possiblity of realization of the spectral factor $\Phi_s(s)$ is given by

$$\Phi_s(s) = \left[\begin{array}{c|c} A_\Phi & B_\Phi \\ \hline \hat{D}_\Phi^{-T}(X B_\Phi + C_\Phi^T M D_\Phi)^T & \hat{D}_\Phi \end{array} \right]$$

such that $\Phi(s), \Phi^{-1}(s) \in \mathcal{RH}_\infty$.

Remark 13. *We have to emphasize that it's the structure that matters and not the method with which we arrive to the desired structure. For a particular custom multiplier, one can utilize other properties of the factorization. However, since many multipliers share the property of having $H_{22} \succ 0$ we use it as an assumption. Therefore, there is nothing holistic about the methodolgy. As an example passivity multipliers that we have utilized before can not be factorized using this argument. Hence, one can use the the results of [43].*

Now that we have given the basic idea behind the dynamic multiplier factorization, we have enough material to describe the steps of the controller-multiplier iteration.

The Pseudo-Code for Controller-Multiplier Iteration

The actual technical problems are all addressed above and can be found in the literature also cited above. However, for the practitioners who are not interested in the proofs and other derivation related issues we provide a standalone rundown of the controller-iteration steps.

PRELIMINARY STEP. Before starting the controller design, it is important to check a few often overlooked issues before starting the design iteration.

- The plant G is a generalized plant and, if any, the D_{uy} block of the state-space representation is zeroed. After the control design, the original controller can be recovered under the assumption that $(I - D_K D_{uy})^{-1}$ is nonsingular.

- The performance weights are not too demanding i.e. high-performance nominal control design might have very little robustness properties hence it's better to redesign the performance weights after looking at the robust controller obtained later. By doing so one can see the effect of the weights by plotting the performance channel entries.

- The control channels are weighted, even slightly, to avoid the controller gains blow up when unconstrained by the LMI solvers. This might not be relevant for the synthesis case however due to the non-convex nature of the iteration it's more likely to get a infeasible analysis certificate even though the synthesis step returns a feasible controller.

- After the interconnection of the weights it is crucial that the state-space data is minimal and balanced. It also helps to cleanup the numerical noise from the state-space matrices i.e. zeroing out the entries that are less than, say, 10^{-6}.

Then we are ready to obtain the first nominal controller that will allow us to start the iteration.

INITIAL STEP.   The initial step is designing *any* controller that stabilizes the system and satisfies some performance specifications that can be described as a quadratic form. For the common transparency case, we can use the $\mathcal{H}_\infty$ norm of the force error and position error for the remote and local site. Then required conditions to be checked while minimizing γ is given by Theorem 12 for

$$P_p = \begin{pmatrix} -\gamma^2 I & \\ & I \end{pmatrix}$$

where γ^2 is inserted into another variable to make the condition affine. Then, using the factorization $I - XY = UV^T$ we obtain U and V. Then using these matrices we backsubstitute the X, Y, K, L, M, N varibles to obtain the controller matrices. Alternatively one can also utilize the results of [39] with a two step approach to solve the LMIs, first eliminating the controller matrices from the LMI and obtain valid Lyapunov matrices then using these, solving the original LMI for the controller matrices. We reemphasize that the method from which we obtain the controller is irrelevant. One can also use the reduced order controller construction algorithm of [54]. It has been demonstrated that the resulting controller is numerically more well-conditioned. Moreover, it has been shown that the unconstrained parts of the problem can be identified which is a major issue in a MIMO setting.

ANALYSIS STEP.   Once we have obtained a nominally stabilizing controller, the nominal part of the uncertain closed loop plant, $(G \star K)$, is obtained. Since this interconnection is for the full uncertainty size, we then parametrize the uncertainty size and reflect it to the system as depicted in Figure 4.3. This allows us to use the same multipliers without scaling with r, hence avoiding multipliying the decision variables with small numbers. Therefore, with the initial balanced and minimal

realization of the plant such parameterization is relatively healthier than scaling the unknowns a priori. Another problem is to strip down the *r* value after a feasible multiplier is found (with spectral factorization in mind). Factorizing a small scalar from a matrix should be avoided.

In summary, we use the parametrization of the dynamic multipliers

$$\Pi(i\omega) = \Psi^*(iw)M\Psi(i\omega)$$

Then, either in frequency domain or via minimal state-space representations, we form the system

$$H_{aug} := \begin{pmatrix} \Psi(i\omega) & \\ & I \end{pmatrix} \begin{pmatrix} I & 0 \\ & H_q \\ \hline 0 & I \\ & H_z \end{pmatrix}.$$

Hence, we have the familiar FDI

$$H_{aug}^* \begin{pmatrix} M & \\ & P_p \end{pmatrix} H_{aug} \prec 0$$

together with individual multiplier class inequalities e.g. positivity of *D*-scalings etc. Hence, along the lines of the examples in Chapter 3 and the conditions given above, the FDIs are converted to LMIs and solved for the performance optimization.

Remark 14. *Once again, it's important to remind that the positivity of the involved Lyapunov certificates in the LMI set are not required in the analysis, since all the systems are stable i.e. the closed loop is stabilized by K(s) and the outer basis matrices live in $\mathcal{RH}_\infty$, there is no need to enforce positivity constraints. Doing so would constrain the set of valid symmetric matrices significantly.*

After the squaring the multipliers, we obtain the new augmented open loop plant by reshaping the augmented closed loop equations given by (4.15). Starting from an arbitrary $r \in [0,1]$ depending on the success/failure of the feasibility result, *r* is increased/decreased, say via a bisection algorithm, until a particular r_a^* is achieved.

SYNTHESIS STEP. The multiplier-augmented new plant is subjected to the variable transformation "controller $\rightarrow v$" is performed and then via Theorem 14 the LMIs are solved. The initial *r* can be taken as r_a^* and the bisection is reduced to the interval $r \in [0.99r_a^*, 1]$ such that if for some numerical reason r_a^* is not feasible, a little play is introduced to relax the numerical conditioning. 0.99 is based on our numerical experience. However, we have also seen improvement if this play value is a function of the iteration number. In other words, in the early iterations the
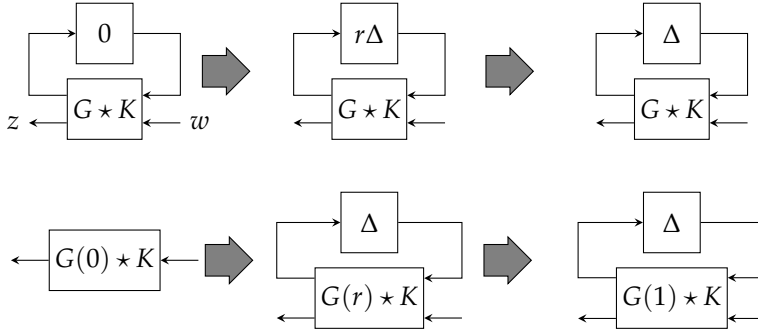
Figure 4.3: Parametrization of the plant with uncertainty size

play value can be relaxed down to 0.95 and then getting stricter as the iteration progresses.

Another important issue after the synthesis is that we have to treat carefully is the innocent looking $I - XY = UV^T$. The numerical noise contaminating U, V entries plays a big role in obtaining healthy controller matrix data due to the inverses of U and V. The essential difficulty is the eigenvalues of XY approaching to unity hence rendering the matrix $I - XY$ badly conditioned with respect to inversion. Some optimization-based remedies regarding the LMI problem setup are given in [137] such that the resulting matrix eigenvalues are forced away from unity. However, even this is established, it's not guaranteed that the resulting matrices U, V would be free of problems. There are many possibilities and in our opinion, a comprehensive code should check as many possibilities as possible. Although, this should be left to numerical analysts, seemingly the easiest method is basing the matrices on $(I - XY)^{-1} = V^{-T}U^{-1}$ instead of factorization and then inversion. We have implemented a simple two-stage validation scheme. First, we try the regular factorize-invert method and clean up the matrices free from dangling tiny entries. Then closed loop is formed and stability is checked. If the closed loop eigenvalues are sufficiently away from zero and the controller matrix entries are less than some large number thenthe result is marked as a valid one. Otherwise, the inverse is factorized and same process is repeated with condition number checks etc. After this step the last known previous attempt is also recorded and if the next analysis step can not improve the current controller is discarded and the last known attempt is utilized. Obviously, many other checks should be implemented however it goes beyond the scope of this manuscript.

Remark 15. *It should be noted that balancing the plant data between the analysis and the synthesis steps lead to worse numerical margins as one particular feasible result in one step tends to be infeasible in another step. We can speculate that this type of modifications don't*

work (though theoretically should help) since the LMI solvers indeed push the decision variables to such an extreme that slight changes in the constant part of the LMIs render the solutions infeasible. Combined with the various factorizations etc. we have decided to not to modify the plant among the iteration steps. However the remark for the initial balancing step is not affected and should be performed regardless of this. It's unfortunately up to the designer to watch for very high-frequency behavior of the plant-controller interaction as this can affect the feasibility of the iteration.

Remark 16. *In the norm minimization cases for performance specification, e.g., $\mathcal{H}_\infty$ norm γ, it's very important to keep the norm constrained from above in a rather stringent fashion. One can see that a single number to drive the whole optimization procedure, often involving hundreds of decision variables, is simply asking for trouble. In practice, it's a good rule of thumb to set the upper bound norm for performance 5-10 times the nominal case performance. Otherwise, unrealistic, nonsensical γ values in the order of $[10^3, 10^4]$ or higher can be obtained resulting with seemingly valid controller matrices. Even if the result is numerically correct, those iterations should be discarded and a smaller γ and/or smaller r values should be assumed. Otherwise, either the next iteration or the discretized implementation are likely to suffer from unpredictable side-effects. If the robust performance γ is much larger than the nominal case then it might be a sign of a drastic qualitative change in the system properties and thus it might help to shift the nominal case such that $\tilde{\Delta} = 0$ corresponds to an uncertain plant already closer to the problematic region in order to start with better robustness properties.*

TERMINATION STEP. After the synthesis and analysis steps, the r value typically gets saturated at some particular r^* or it starts to fluctuate around it. In case of such fluctuations, the algorithm should see whether the performance objective obtained at each step is close to each other. Otherwise it's a sign of a numerically invalid solution. One can either decrease the uncertainty size r or constraint the performance objective further to force each solution come closer. We have chosen another simple rule for the implementation:

- After the synthesis step, check whether it's the first run of the iteration. If so, no convergence checks is necessary.

- Collect r and γ (both of analysis and synthesis steps) of the current iteration and compare it with the previous iteration. (Check if $r \approx 1$. If true, then compare only the performance.) Check if there is any significant (larger than some predefined value).

- Check also whether analysis and synthesis r and γ values are close to each other.

- If all true terminate, otherwise continue.

4.1.6 *Closing Remarks*

We need to emphasize that these numerical issues *are* relevant for control theory and can not be belittled as "mere implemetation details" as often treated in the literature with an unjustified elitism. In fact it's quite the other way around however there is no need to digress here.

Many problems similar to the ones mentioned above would be implicitly solved if better and customized control-oriented solvers that take the numerical accuracy into account as much as the optimization objective, emerge in the future. Especially, commercial software suites should be abandoned and more open-source free-software based solutions should be developed as a community. The tools that contemporary control theorists are utilizing are mediocre and even worse this simple fact goes unnoticed. Based on this observation we regret to assert that many results that appear in the literature are not tested properly under reasonable *stress* and in fact most can not survive under numerical scrutiny. Proving stability is not conclusive but a supportive part of the control engineering however much to our surprise this is completely rejected in academic circles. Therefore it is of utmost importance that the code/simulation/data that lead to the conclusions of the literature should be published without any exception. This would also help to ease the reviewing procedure as the reviewers would get the chance to test out different plants etc. Iteratively, this would force the experts to pay attention to the real control problems instead of intellectual but rather obscure skirmish of generalizations.

Conclusions

Current status: 0%

0   100
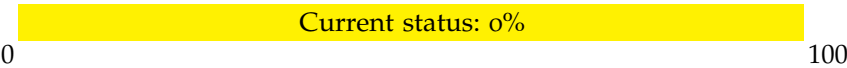
Network Theory Primer

We present the often encountered concepts in the bilateral teleoperation studies in a rather abstract fashion. Our aim is to prepare the basis for the main arguments in the body of this thesis. Hence, the experts of the field can safely skip this appendix. The aim is to run down the basic stability related concepts, hence many circuit theory preliminaries are omitted.

A.1 TERMINOLOGY

When dealing with electrical circuits, often the engineering practice is to neglect any changes to the signal traveling through a wire from location A to B if the distortion from various sources is negligible. This allows us to use the abstraction in block diagrams and calculations that point A and B have the same measurable characteristics through time. This is typically shown with a straight line connecting A and B. The interpretation is that A and B share the same variables of interest on that line. Therefore, A and B are said to be interconnected terminals connected by a wire. Clearly creating terminals are as simple as cutting the connection arbitrarily on a path. Often, we define hypothetical terminals as if there were distinct points on the circuit and we have connected them artificially.

Hence, following Jan C. Willems' formulation for a systematic definition of terminals and ports in [158]; an electrical circuit is a device, a black box, with wires so-called terminals through which the circuit can interact with its surroundings. In electrical circuits, the interaction takes place via the electrical voltage drop across the terminals and the electrical current that flows through the black box. Therefore each terminal admits two real variables attached to it, the potential and the current. Conventionally, the current is denoted with a positive number when it flows into the circuit. Thus, an interconnection is connecting a wire from terminal A of the black box (1) to B of (2) enforcing the following to hold

$$V_A = V_B \quad \text{and} \quad I_A = -I_B$$

Then, we can look at the resulting interconnected system (3) as (1) and (2) combined and exhibiting the same phenomenon at their terminals A and B.

The collection of physically attainable phenomena are abstracted with the notion of the behavior set ([119]): Consider a circuit with N terminals. Let $\mathcal{B} \subseteq$

$(\mathbb{R}^N \times \mathbb{R}^N)^{\mathbb{R}}$ denote the behavior set that is defined as the set of all admissible potential and current trajectories compatible with the network architecture at each terminal. Here $(\mathbb{R}^N \times \mathbb{R}^N)^{\mathbb{R}}$ denotes the set of all maps $f : \mathbb{R} \to \mathbb{R}^N \times \mathbb{R}^N$ e.g. each terminal voltage and current evolution through time and $\mathcal{B}$ is the restriction to the maps that are compatible with the network structure. Roughly speaking, behavior set excludes all the trajectories that are physically impossible to attain by the black box. Thus, when it is said that a particular trajectory is in the behaviour set i.e.,

$$(V_1, \ldots, V_N, I_1, \ldots, I_N) \coloneqq (V, I) \in \mathcal{B}$$

it implies that there exists an initial condition $(V(0), I(0))$ such that (V, I) is a an admissible trajectory through time (with a particular external excitation sequence if present).

Assuming a conservative magnetic field, a circuit obeys the well-known Kirchhoff voltage and current laws compactly described as

$$(V, I) \in \mathcal{B} \implies (V + \alpha \mathbb{1}, I) \in \mathcal{B} \quad \forall \alpha \in \mathbb{R}^{\mathbb{R}} \qquad \text{(KVL)}$$

$$(V, I) \in \mathcal{B} \implies \sum_{k=1}^{N} I_k = \mathbb{1}^T I = 0 \qquad \text{(KCL)}$$

where $\mathbb{1}$ denotes a vector with all entries are equal to 1 whose size is clear from the context.

Let, $P \subseteq \{1, \ldots, N\}$ denote an $m-$tuple selection of indices out of N terminals of a circuit. Then, terminals P_i for all $i \in P$ are said to form a port if

$$(V, I) \in \mathcal{B} \implies p^T I = 0 \qquad \text{(Port KCL)}$$

where p is a vector with $k-$th entry being 1 if $k \in P$ and 0 otherwise. This is nothing but a reformulation of the well-known port condition from circuit theory. Thus, we can also define a port as the set of terminals that satisfy port KCL. Given a port with $n-$terminals with V, I denoting the through and across variables, the instantaneous power is given by

$$P = \sum_{k=1}^{n} V_k(t) I_k(t)$$

and the energy transfered in the time interval is given by the total power delivered to/from that port in the time interval $[t_1, t_2]$:

$$E = \int_{t_1}^{t_2} \sum_{k=1}^{n} V_k(t) I_k(t) dt$$

These formulas hold only if the terminals form a port and a port can have arbitrary number of terminals e.g., op-amps, transistors, $Y - \Delta$ resistance networks are examples for three terminal ports.

Using a mechanical-electrical analogy, the mechanical teleoperation devices are converted to a network of ports. In network theory applications to bilateral teleoperation, the "system" refers to the network model that is hypothetically disconnected (thus admitting virtual terminals) from its "surroundings" such as the "load" and the "source" of a circuit. This system is allowed to interact with its surroundings via "ports". In our context, load refers to the environment that is to be explored and the source is the human exploring the environment from a distance via the teleoperation system.

Remark 17. *We have to note that, in this formulation, a single mass can not be interpreted as a port: The mass does not satisfy the port KCL unless it is thought to be applying an opposite force to a fixed inertial frame at a distance. This is the underlying reason for the electrical analog of a mass (in the force-current context) is required to be a* grounded *capacitor (see [143] for the development of the exact mechanical analogue of a capacitor,* the inerter *which is succesfully implemented by McLaren Mercedes and Renault F1 teams and being used succesfully since 2005[1]). We will not go into the details and and simply refer to [158] for a thorough analysis of the pitfalls and quite nonintuitive power/energy results. Though, the inappropriateness of such view is brought to attention in numerous studies by Jan C. Willems and his colleagues, we are obliged to use the input/output formulation as we have no results regarding the behavioral approach to bilateral teleoperation systems (yet). However, we remind the reader that the potential of a behavioral modeling of teleoperation systems is just unavoidable.*

Since every two-terminal port can be characterized by two variables ("through" and "across" quantities), it is possible to characterize the interconnected $n-$port networks as if one quantity is due to the other. This is done by imposing an artificial causality scheme, two of these time-dependent trajectories can be selected as free variables and the remaining ones become dependent variables ([119]). This is the simplest kind of input/output view of physical systems via treating one port variable as the *cause* and the other one as the *effect* to this cause e.g. the current is due to the voltage drop across the terminals or vice versa.

Depending on the choice of the free variables, the system can be expressed in terms of impedance, admittance and hybrid parameters for two-port networks and their combinations for general n-port network interconnections. In the cases where the two-port is LTI, with a slight abuse of notation, we will use the term "immitance" matrix to refer to any of these representations. Suppose that a two-port

---

[1]According to the official statements.

immitance matrix is partitioned as

$$\begin{pmatrix} q \\ y \end{pmatrix} = \begin{pmatrix} G_1 & G_2 \\ G_3 & G_4 \end{pmatrix} \begin{pmatrix} p \\ u \end{pmatrix}$$

where q, y, p, u represent the flow (current, velocity etc.) and the effort (potential difference, force etc.) signals. Then, obtaining one representation from another is possible by a combination of the following elementary "permutation" and "partial inversion" operations:

$$\begin{pmatrix} q \\ y \end{pmatrix} = \begin{pmatrix} G_2 & G_1 \\ G_4 & G_3 \end{pmatrix} \begin{pmatrix} u \\ p \end{pmatrix}, \qquad\qquad\qquad \text{(Permutation)}$$

$$\begin{pmatrix} p \\ y \end{pmatrix} = \begin{pmatrix} G_1^{-1} & -G_1^{-1}G_2 \\ G_3G_1^{-1} & G_4 - G_3G_1^{-1}G_2 \end{pmatrix} \begin{pmatrix} q \\ u \end{pmatrix}. \qquad \text{(Partial Inversion)}$$

In the latter operation it is assumed that the inverse exists. The existence of inverses are limiting the realizability of networks as impedance or admittance matrices. Moreover, in [2], it has been shown that a hybrid matrix realization is always possible regardless. This is yet another artifact of input/output formulation.

For our purposes, we consider only the immitance matrices that describe G as an input-output mapping (as opposed to transmission or ABCD parameters) as follows:

$$\begin{pmatrix} q \\ y \end{pmatrix} = \begin{pmatrix} G_1 & G_2 \\ G_3 & G_4 \end{pmatrix} \begin{pmatrix} p \\ u \end{pmatrix} , \quad \begin{pmatrix} p \\ u \end{pmatrix} = \begin{pmatrix} \Delta_s & 0 \\ 0 & \Delta_l \end{pmatrix} \begin{pmatrix} q \\ y \end{pmatrix}. \tag{A.1}$$

Therefore, the overall interconnection can be depicted by the block diagram given in Figure 2.2a. In relation to teleoperation, the blocks Δ_s and Δ_l refer to the human and the unknown environment.

A.2   Passivity Theorem

In this section passivity related important concepts are defined in a compact fashion. Nevertheless, the material given here is well-known and can be found in many classical sources such as [28, 56, 132]. We chose to follow closely [28] for the presentation style.

Let V be a linear space equipped with a scalar product, $\mathcal{T}$ be the index set of time and F be a class of functions $x : \mathcal{T} \to V$.

Definition 6. *A linear truncation operator P_T is defined on F as*

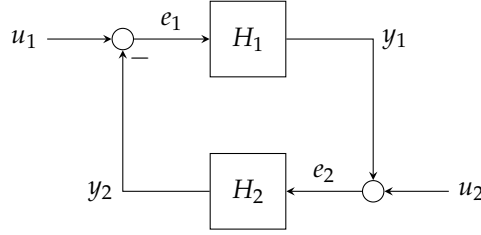$$P_T(x)(t) = \begin{cases} x(t) & \text{for } t \leq T \\ 0 & \text{for } t > T \end{cases} \tag{A.2}$$

Figure A.1: Negative feedback interconnection

In most of the cases, $\mathcal{T}$ is the closed positive real line and $V = \mathbb{R}^n$, hence the scalar product becomes the inner product defined on $\mathbb{R}^n$. The subscript $\cdot_T$ will be used as a shorthand notation for $P_T(\cdot)$. We also define $\mathcal{H}$ and its extension $\mathcal{H}_e$ as

$$\mathcal{H} := \left\{ x \in F \mid \|x\|^2 = \langle x_T, x_T \rangle < \infty \right\}$$

and

$$\mathcal{H}_e := \left\{ x \in F \mid \forall T \in \mathcal{T}, \|x_t\|^2 = \langle x_T, x_T \rangle < \infty \right\}$$

Definition 7. *Let $H : \mathcal{H}_e \to \mathcal{H}_e$. H is said to be passive if and only if there exists a constant β such that*

$$\langle Hx, x \rangle_T \geq \beta \quad \forall x \in \mathcal{H}_e, \forall t \in \mathcal{T}$$

If moreover, there exists positive real number δ such that

$$\langle Hx, x \rangle_T \geq \delta \|x_T\|^2 + \beta \quad \forall x \in \mathcal{H}_e, \forall t \in \mathcal{T}$$

H is said to be strictly passive.

The scalar β is used to model the initial offset for nonlinear systems and will be taken as zero since we would be focusing on linear systems exclusively.

Definition 8. *For an LTI operator H, passivity is equivalent to the corresponding transfer function $H(s)$ being positive real:*

$$\text{Re}\left\{H(i\omega)\right\} \geq 0 \Longleftrightarrow \hat{u}^*(i\omega) \, \text{Re}\left\{H(i\omega)\right\} \hat{u}(i\omega) \geq 0$$
$$\Longleftrightarrow \int_{-\infty}^{\infty} \hat{u}^*(i\omega) \, \text{Re}\left\{H(i\omega)\right\} \hat{u}(i\omega) d\omega \geq 0$$
$$\Longleftrightarrow \int_{-\infty}^{\infty} [H(i\omega)\hat{u}(i\omega)]^* \hat{u}(i\omega) d\omega \geq 0$$

for all $\omega \in \mathbb{R}_e$ and for all $u \in \mathcal{L}_2^n$. Furthermore, if the condition

$$\int_0^{\infty} H(u)(\tau)^T u(\tau) d\tau \geq \delta \|u\|_2^2 + \epsilon \|H(u)\|_2^2$$

is satisfied with $\delta > 0$, $\epsilon = 0$ (or $\delta = 0$, $\epsilon > 0$) then the operator is said to be Strictly Input (Output) Passive with level δ (or level ϵ) respectively.

Suppose we are given with two dynamical systems $H_1, H_2 : \mathcal{H}_e \to \mathcal{H}_e$ for which the system structure is given in time-domain with

$$\dot{x} = f(x, e) \tag{A.3}$$

$$y = h(x, e) \tag{A.4}$$

for both systems where $f : \mathbb{R}^n \times \mathbb{R}^m \mapsto \mathbb{R}^n$ is locally Lipschitz and $h : \mathbb{R}^n \times \mathbb{R}^m \mapsto \mathbb{R}^p$ is a continous function satisfying $f(0, 0) = 0$, $h(0, 0) = 0$.

Definition 9 (Well-posedness)**.** *Consider the system interconnection given in Figure A.1. The interconnection is said to be well-posed if there exist unique solutions e_1, e_2 to the equations*

$$e_1 = u_1 - h_2(x_2, e_2) \tag{A.5}$$

$$e_2 = u_2 + h_1(x_1, e_1) \tag{A.6}$$

for all admissible (x_1, x_2, u_1, u_2). In the LTI case, assume that the respective transfer functions $H_1, H_2 \in \mathcal{RH}_\infty$. Then the interconnection is well posed if $(I - H_1 H_2)^{-1}$ is a proper transfer matrix.

Note that, in our context u_1, u_2 model the voluntary part of the human/environment force input as mentioned in Chapter 2.

Theorem 22. *Consider the well-posed feedback interconnection shown in Figure A.1 and described by Equations (A.5) and (A.6). Assume that there exist constants $\gamma_1, \beta_1, \delta_1, \beta'_1, \epsilon_2, \beta'_2$ such that the following conditions hold*

$$\|H_1 x\|_T \leq \gamma_1 \|x_T\| + \beta_1 \tag{A.7}$$

$$\langle x, H_1 x \rangle_T \geq \delta_1 \|x_T\|^2 + \beta'_1 \tag{A.8}$$

$$\langle H_2 x, x \rangle_T \geq \epsilon_2 \|H_2 x_T\|^2 + \beta'_2 \tag{A.9}$$

for all $x \in \mathcal{H}_e$ and for all $T \in \mathcal{T}$. If

$$\delta_1 + \epsilon_2 > 0 \tag{A.10}$$

then, $u_1, u_2 \in \mathcal{H}$ imply that $e_1, e_2, y_1, y_2 \in \mathcal{H}$

A well-known absolute stability analysis result for the LTI network is due to Llewellyn [91]. An explicit indication of the frequency dependence is omitted for notational convenience.

Theorem 23 (Llewellyn's Criteria). *A two-port network N, described by its transfer matrix*

$$N(i\omega) = \begin{pmatrix} N_{11}(i\omega) & N_{12}(i\omega) \\ N_{21}(i\omega) & N_{22}(i\omega) \end{pmatrix}$$

and interconnected to passive LTI termination immitances as in Figure 2.2a, is stable if and only if

$$R_{11} > 0 \text{ or } R_{22} > 0, \tag{A.11}$$

and

$$4\left(R_{11}R_{22} + X_{12}X_{21}\right)\left(R_{11}R_{22} - R_{12}R_{21}\right) - \left(R_{12}X_{21} - R_{21}X_{12}\right)^2 > 0 \tag{A.12}$$

or

$$2R_{11}R_{22} - |N_{12}N_{21}| - \operatorname{Re}\{N_{12}N_{21}\} > 0 \tag{A.12$'$}$$

for all $\omega \in \mathbb{R}_e$, where R_{ij} and X_{ij} denote the real and imaginary parts of N_{ij} respectively.

Similarly, as is for Llewellyn's stability conditions, it is straightforward to derive unconditional stability tests if the network is represented by scattering parameters. In what follows, we denote transformed passive LTI uncertainties with $\tilde{\Delta}_s, \tilde{\Delta}_l$ which are unity gain bounded. The corresponding interconnection is supposed to be given by the loop equations $q = Sp$, $p = \tilde{\Delta}q$ i.e.

$$\underbrace{\begin{pmatrix} q_1 \\ q_2 \end{pmatrix}}_{q} = \underbrace{\begin{pmatrix} S_{11} & S_{12} \\ S_{21} & S_{22} \end{pmatrix}}_{S} \underbrace{\begin{pmatrix} p_1 \\ p_2 \end{pmatrix}}_{p}, \quad \begin{pmatrix} p_1 \\ p_2 \end{pmatrix} = \underbrace{\begin{pmatrix} \tilde{\Delta}_s & 0 \\ 0 & \tilde{\Delta}_l \end{pmatrix}}_{\tilde{\Delta}} \begin{pmatrix} q_1 \\ q_2 \end{pmatrix}. \tag{A.13}$$

Rollett's conditions ([85, 127, 146]) for stability are then formulated as follows:

Theorem 24. *Consider the same network given in Llewellyn's criteria which is represented in scattering parameters. The interconnection is stable if and only if the inequality*

$$K = \frac{1 + |\nabla|^2 - |S_{11}|^2 - |S_{22}|^2}{2|S_{12}S_{21}|} > 1 \tag{A.14}$$

holds for all frequencies together with an auxiliary condition in terms of $\nabla = S_{11}S_{22} - S_{12}S_{21}$. This extra condition can be stated in at least five different ways, such as

$$1 - |S_{11}|^2 > |S_{12}S_{21}| \quad \text{or} \quad (1 - |S_{22}|^2) > |S_{12}S_{21}|.$$

(See [29] for further details).

In [29], Edwards and Sinsky reduced Rollet's conditions to a single quantity denoted as μ to be checked for being greater than unity for all $\omega \in \mathbb{R}_e$.

Theorem 25. *Verifying Rollet's conditions is equivalent to verifying the single condition*

$$\mu := \frac{1 - |S_{11}|^2}{|S_{22} - S_{11}^*\Delta| + |S_{12}S_{21}|} > 1 \qquad \forall \omega \in \mathbb{R}_e.$$

References

[1]   American Council of the Blind. *A Brief Description of Braille* (cit. on p. 11).
        URL: `http://acb.org/node/67` (visited on [visited on 06/22/2012]).

[2]   B. D. O. Anderson, R. Newcomb, and J. Zuidweg. "On the Existence of *H* Matrices".
        In: *IEEE Transactions on Circuit Theory* 13.1 (1966), pp. 109–110 (cit. on p. 108).
        DOI: `10.1109/TCT.1966.1082537`.

[3]   R. Anderson and M. Spong. "Bilateral control of teleoperators with time delay". In:
        IEEE Transactions on Automatic Control 34.5 (1989), pp. 494–501 (cit. on pp. 20, 30, 36,
        39, 43, 44, 57, 64).
        DOI: `10.1109/9.24201`.

[4]   C. Andriot and R. Fournier. "Bilateral control of teleoperators with flexible joints by
        the H_∞ approach". In: *Telemanipulator Technology*. Ed. by H. Das. Vol. 1833. 1. Boston,
        MA, USA: SPIE, 1993, pp. 80–91 (cit. on p. 31).
        DOI: `10.1117/12.142099`.

[5]   P. Arcara and C. Melchiorri. "Control schemes for teleoperation with time delay:
        A comparative study". In: *Robotics and Autonomous Systems* 38.1 (2002), pp. 49–64
        (cit. on p. 57).
        DOI: `10.1016/S0921-8890(01)00164-6`.

[6]   A. Aziminejad, M. Tavakoli, R. V. Patel, and M. Moallem. "Transparent Time-Delayed
        Bilateral Teleoperation Using Wave Variables". In: *IEEE Transactions on Control
        Systems Technology* 16.3 (2008), pp. 548–555 (cit. on p. 57).
        DOI: `10.1109/TCST.2007.908222`.

[7]   H. Bart, I. Gohberg, M. A. Kaashoek, and A. C. M. Ran. *A State Space Approach to
        Canonical Factorization with Applications*. Vol. 200. Operator Theory: Advances and
        Applications. Springer-Verlag, 2010, p. 432 (cit. on p. 94).
        DOI: `10.1007/978-3-7643-8753-2`.

[8]   L. Basañez and R. Suárez. "Teleoperation". In: *Springer Handbook of Automation*.
        Ed. by S. Y. Nof. Springer Berlin Heidelberg, 2009, pp. 449–468 (cit. on p. 20).
        DOI: `10.1007/978-3-540-78831-7_27`.

[9]   A. Bemporad. "Predictive control of teleoperated constrained systems with un-
        bounded communication delays". In: *Proc. 37th IEEE Conf. Decision and Control*.
        Vol. 2. 1998, pp. 2133–2138 (cit. on p. 46).

[10] S. J. Biggs and M. A. Srinivasan. "Haptic Interfaces". In: ed. by K. M. Stanney. Vol. 39. Handbook of virtual environments: Design, implementation, and applications.Human factors and ergonomics. Lawrence Erlbaum Associates, 2002. Chap. 5, pp. 93–116 (cit. on p. 13).

[11] E. F. Bolinder. "Survey of Some Properties of Linear Networks". In: *IRE Transactions on Circuit Theory* 4.3 (1957), pp. 70–78 (cit. on p. 34).
DOI: 10.1109/TCT.1957.1086385.

[12] S. Boyd, L. E. Ghaoui, E. Feron, and V. Balakrishnan. *Linear Matrix Inequalities in System and Control Theory*. Vol. 15. Studies in Applied Mathematics. Society for Industrial and Applied Mathematics (SIAM), 1994 (cit. on p. 66).

[13] S. P. Buerger and N. Hogan. "Complementary Stability and Loop Shaping for Improved Human–Robot Interaction". In: *IEEE Transactions on Robotics* 23.2 (2007), pp. 232–244 (cit. on pp. 30, 31, 74).
DOI: 10.1109/TRO.2007.892229.

[14] G. Burdea. *Force and touch feedback for Virtual Reality*. New York: Wiley, 1996 (cit. on pp. 10, 20).

[15] P. Buttolo, P. Braathen, and B. Hannaford. "Sliding control of force reflecting teleoperation - Preliminary studies". In: *Presence* 3.2 (1994), pp. 158–172 (cit. on p. 46).

[16] W.-K. Chen. *Active network analysis*. Singapore Teaneck, N.J: World Scientific, 1991 (cit. on pp. 32, 34).

[17] H. C. Cho and J. H. Park. "Impedance Control with Variable Damping for Bilateral Teleoperation under Time Delay". In: *JSME International Journal Series C Mechanical Systems, Machine Elements and Manufacturing* 48.4 (2005), pp. 695–703 (cit. on p. 60).

[18] N. Chopra, P. Berestesky, and M. W. Spong. "Bilateral Teleoperation Over Unreliable Communication Networks". In: *IEEE Transactions on Control Systems Technology* 16.2 (2008), pp. 304–313 (cit. on p. 45).
DOI: 10.1109/TCST.2007.903397.

[19] N. Chopra, M. W. Spong, R. Ortega, and N. E. Barabanov. "On tracking performance in bilateral teleoperation". In: *IEEE Transactions on Robotics* 22.4 (2006), pp. 861–866 (cit. on p. 45).
DOI: 10.1109/TRO.2006.878942.

[20] G. A. V. Christiansson. "Wave Variables and the 4 Channel Architecture for Haptic Teleoperation". In: *Haptics: Perception, Devices and Scenarios*. Vol. 5024. Lecture Notes in Computer Science. Springer Berlin / Heidelberg, 2008, pp. 169–174 (cit. on p. 44).
DOI: 10.1007/978-3-540-69057-3_20.

[21] E. J. Colgate. "The control of dynamically interacting systems". PhD thesis. Massachusetts Institute of Technology, 1988 (cit. on p. 32).
DOI: 1721.1/14380.

[22] E. J. Colgate and N. Hogan. "Robust control of dynamically interacting systems". In: *International Journal of Control* 48.1 (1988), pp. 65–88 (cit. on pp. 24, 29, 32). DOI: 10.1080/00207178808906161.

[23] J. E. Colgate. "Coordinate Transformations and Logical Operations for Minimizing Conservativeness in Coupled Stability Criteria". In: *Journal of Dynamic Systems, Measurement, and Control* 116.4 (1994), pp. 643–649 (cit. on pp. 36, 38, 62, 64). DOI: 10.1115/1.2899263.

[24] J. Colgate. "Robust impedance shaping telemanipulation". In: *IEEE Transactions on Robotics and Automation* 9.4 (1993), pp. 374–384 (cit. on pp. 31, 63). DOI: 10.1109/70.246049.

[25] J. Colgate and G. Schenkel. "Passivity of a class of sampled-data systems: Application to haptic interfaces". In: *Journal of Robotic Systems* 14.1 (1997), pp. 37–47 (cit. on pp. 62–64). DOI: 10.1002/(SICI)1097-4563(199701)14:1<37::AID-ROB4>3.0.CO;2-V.

[26] R. Daniel and P. McAree. "Fundamental Limits of Performance for Force Reflecting Teleoperation". In: *The International Journal of Robotics Research* 17.8 (1998), pp. 811–830 (cit. on p. 69). DOI: 10.1177/027836499801700801.

[27] E. Delgado, M. Diaz-Cacho, D. Bustelo, and A. Barreiro. "Generic Approach to Stability Under Time-Varying Delay in Teleoperation: Application to the Position-Error Control of a Gantry Crane". In: *IEEE/ASME Transactions on Mechatronics* PP.99 (2012), pp. 1–11 (cit. on p. 57). DOI: 10.1109/TMECH.2012.2208758.

[28] C. A. Desoer and M. Vidyasagar. *Feedback Systems: Input-Output Properties*. Electrical Science Series. Academic Press, New York, 1975, p. 280 (cit. on pp. 35, 51, 108).

[29] M. Edwards and J. Sinsky. "A new criterion for linear 2-port stability using a single geometrically derived parameter". In: *IEEE Transactions on Microwave Theory and Techniques* 40.12 (1992), pp. 2303–2311 (cit. on pp. 37, 62, 64, 111). DOI: 10.1109/22.179894.

[30] S. E.Salcudean, M. Zhu, W.-H. Zhu, and K. Hashtrudi-Zaad. "Transparent Bilateral Teleoperation under Position and Rate Control". In: *The International Journal of Robotics Research* 19.12 (2000), pp. 1185–1202 (cit. on p. 41). DOI: 10.1177/02783640022068020.

[31] L. Eusebi and C. Melchiorri. "Force reflecting telemanipulators with time-delay: stability analysis and control design". In: *IEEE Transactions on Robotics and Automation* 14.4 (1998), pp. 635–640 (cit. on p. 57). DOI: 10.1109/70.704237.

[32] J. F. Sturm. "Using SeDuMi 1.02, a Matlab Toolbox for Optimization Over Symmetric Cones," in: *Optimization Methods and Software* 11.12 (1999), pp. 625–653 (cit. on p. 69).

[33]   M. Fan, A. Tits, and J. Doyle. "Robustness in the presence of mixed parametric uncertainty and unmodeled dynamics". In: *IEEE Transactions on Automatic Control* 36.1 (1991), pp. 25–38 (cit. on pp. 54, 66).
DOI: 10.1109/9.62265.

[34]   B. A. Francis. *A Course on $\mathcal{H}_\infty$ Control Theory*. Vol. 88. Lecture Notes in Control and Information Sciences. Springer Berlin / Heidelberg, 1987 (cit. on pp. 67, 94).
DOI: 10.1007/BFb0007371.

[35]   M. Fu, H. Li, and S. Niculescu. "Robust stability and stabilization of time-delay systems via integral quadratic constraint approach". In: *Stability and Control of Time-delay Systems*. Ed. by L. Dugard and E. Verriest. Vol. 228. Lecture Notes in Control and Information Sciences. Springer Berlin / Heidelberg, 1998, pp. 101–116 (cit. on p. 57).
DOI: 10.1007/BFb0027482.

[36]   M. J. Fu and M. C. Çavuşoğlu. "Three-dimensional human arm and hand dynamics and variability model for a stylus-based haptic interface". In: *IEEE International Conference on Robotics and Automation (ICRA)*. 2010, pp. 1339–1346 (cit. on p. 31).
DOI: 10.1109/ROBOT.2010.5509927.

[37]   K. Furuta, K. Kosuge, Y. Shiote, and H. Hatano. "Master-slave manipulator based on virtual internal model following control concept". In: *Proc. IEEE Int. Conf. Robotics and Automation*. Vol. 4. 1987, pp. 567–572 (cit. on p. 20).
DOI: 10.1109/ROBOT.1987.1088064.

[38]   P. Gahinet. "Explicit controller formulas for LMI-based H_∞ synthesis". In: *Automatica* 32.7 (1996), pp. 1007–1014 (cit. on p. 82).
DOI: 10.1016/0005-1098(96)00033-7.

[39]   P. Gahinet and P. Apkarian. "A linear matrix inequality approach to H_∞ control". In: *International Journal of Robust and Nonlinear Control* 4.4 (1994), pp. 421–448 (cit. on pp. 82, 98).
DOI: 10.1002/rnc.4590040403.

[40]   P. J. Gawthrop and G. P. Bevan. "Bond-graph modeling". In: *IEEE Control Systems Magazine* 27.2 (2007), pp. 24–45 (cit. on p. 23).

[41]   M. A. Geeves and K. C. Holmes. "Structural mechanism of muscle contraction." In: *Annual Review of Biochemistry* 68 (1999), pp. 687–728 (cit. on p. 25).
DOI: 10.1146/annurev.biochem.68.1.687.

[42]   R. C. Goertz and W. M. Thompson. "Elecrtonically Controlled Manipulator". In: *Nucleonics* 12.12 (1954), pp. 46–47 (cit. on p. 20).

[43]   K.-C. Goh. "Canonical factorization for generalized positive real transfer functions". In: *Proc. 35th IEEE Conf. Decision and Control (CDC)*. Vol. 3. 1996, pp. 2848–2853 (cit. on pp. 90, 94, 97).
DOI: 10.1109/CDC.1996.573550.

[44]   K.-C. Goh. "Structure and factorization of quadratic constraints for robustness analysis". In: *Proc. 35th IEEE Conf. Decision and Control (CDC)*. Vol. 4. 1996, pp. 4649–4654 (cit. on pp. 90, 92, 93).
       DOI: 10.1109/CDC.1996.577607.

[45]   A. Haddadi and K. Hashtrudi-Zaad. "Bounded-Impedance Absolute Stability of Bilateral Teleoperation Control Systems". In: *IEEE Transactions on Haptics* 3 (2009), pp. 15–27 (cit. on pp. 52, 60, 62).
       DOI: 10.1109/TOH.2009.48.

[46]   B. Hannaford. "A design framework for teleoperators with kinesthetic feedback". In: *IEEE Transactions on Robotics and Automation* 5.4 (1989), pp. 426–434 (cit. on pp. 20, 21, 30).
       DOI: 10.1109/70.88057.

[47]   B. Hannaford and J.-H. Ryu. "Time-domain passivity control of haptic interfaces". In: *IEEE Transactions on Robotics and Automation* 18.1 (2002), pp. 1–10 (cit. on pp. 22, 45).
       DOI: 10.1109/70.988969.

[48]   K. Hashtrudi-Zaad and S. Salcudean. "Transparency in time-delayed systems and the effect of local force feedback for transparent teleoperation". In: *IEEE Transactions on Robotics and Automation* 18.1 (2002), pp. 108–114 (cit. on p. 41).
       DOI: 10.1109/70.988981.

[49]   K. Hashtrudi-Zaad and S. E. Salcudean. "Analysis of Control Architectures for Teleoperation Systems with Impedance/Admittance Master and Slave Manipulators". In: *The International Journal of Robotics Research* 20.6 (2001), pp. 419–445 (cit. on p. 60).
       DOI: 10.1177/02783640122067471.

[50]   K. Hastrudi-Zaad and S. E. Salcudean. "On the use of local force feedback for transparent teleoperation". In: *Proc. IEEE Int Robotics and Automation Conf*. Vol. 3. 1999, pp. 1863–1869 (cit. on pp. 41, 42).
       DOI: 10.1109/ROBOT.1999.770380.

[51]   S. S. Haykin. *Active Network Theory*. Addison-Wesley Series in Electrical Engineering. Addison-Wesley, 1970 (cit. on p. 32).

[52]   M. V. Headrick. "Origin and evolution of the anchor clock escapement". In: *IEEE Control Systems Magazine* 22.2 (2002), pp. 41–52 (cit. on p. 26).
       DOI: 10.1109/37.993314.

[53]   A. Helmersson. "An IQC-based Stability Criterion for Systems with Slowly Varying Parameters". In: *14th World Congress of IFAC*. Vol. F. IFAC. Beijing, China, 1999, pp. 525–530 (cit. on p. 55).

[54]   A. Helmersson. "Employing Kronecker Canonical Form for LMI-Based H_∞ Synthesis Problems". In: *IEEE Transactions on Automatic Control* 57.8 (2012), pp. 2062–2067 (cit. on p. 98).
       DOI: 10.1109/TAC.2011.2179846.

[55]   A. Helmersson. "IQC Synthesis based on Inertia Constraints". In: *14th World Congress of IFAC*. Beijing,China, 1999, pp. 163–168 (cit. on p. 90).

[56]   D. Hill and P. Moylan. "Stability results for nonlinear feedback systems". In: *Automatica* 13.4 (1977), pp. 377–382 (cit. on p. 108).
       DOI: 10.1016/0005-1098(77)90020-6.

[57]   S. Hirche and M. Buss. "Human-Oriented Control for Haptic Teleoperation". In: *Proceedings of the IEEE* 100.3 (2012), pp. 623–647 (cit. on p. 45).
       DOI: 10.1109/JPROC.2011.2175150.

[58]   N. Hogan. "Controlling impedance at the man/machine interface". In: *IEEE International Conference on Robotics and Automation (ICRA)*. Vol. 3. 1989, pp. 1626–1631 (cit. on pp. 24, 25, 30).
       DOI: 10.1109/ROBOT.1989.100210.

[59]   N. Hogan. "Impedance Control: An Approach to Manipulation: Part I — Theory". In: *Journal of Dynamic Systems, Measurement, and Control* 107.1 (1985), pp. 1–7 (cit. on p. 23).
       DOI: 10.1115/1.3140702.

[60]   N. Hogan. "Impedance Control: An Approach to Manipulation: Part II — Implementation". In: *Journal of Dynamic Systems, Measurement, and Control* 107.1 (1985), pp. 8–16 (cit. on p. 23).
       DOI: 10.1115/1.3140713.

[61]   N. Hogan. "Impedance Control: An Approach to Manipulation: Part III — Applications". In: *Journal of Dynamic Systems, Measurement, and Control* 107.1 (1985), pp. 17–24 (cit. on p. 23).
       DOI: 10.1115/1.3140701.

[62]   P. F. Hokayem and M. W. Spong. "Bilateral teleoperation: An historical survey". In: *Automatica* 42.12 (2006), pp. 2035–2057 (cit. on pp. 20, 57).
       DOI: 10.1016/j.automatica.2006.06.027.

[63]   R. Horowits and R. J. Podolsky. "The positional stability of thick filaments in activated skeletal muscle depends on sarcomere length: evidence for the role of titin filaments." In: *The Journal of Cell Biology* 105.5 (1987), pp. 2217–2223 (cit. on p. 25).
       DOI: 10.1083/jcb.105.5.2217.

[64]   J. C. Houk and Z. W. Rymer. "Neural Control of Muscle Length and Tension". In: *Comprehensive Physiology*. Vol. II. John Wiley & Sons, Inc., 2011. Chap. 8, pp. 257–323 (cit. on p. 28).
       DOI: 10.1002/cphy.cp010208.

[65]   Z. Hu, S. Salcudean, and P. Loewen. "Robust controller design for teleoperation systems". In: *IEEE International Conference on Systems, Man and Cybernetics*. Vol. 3. 1995, pp. 2127–2132 (cit. on p. 31).
       DOI: 10.1109/ICSMC.1995.538094.

[66] T. Iwasaki and S. Hara. "Generalized KYP lemma: unified frequency domain in-
      equalities with design applications". In: *IEEE Transactions on Automatic Control* 50.1
      (2005), pp. 41–59 (cit. on p. 51).
      DOI: 10.1109/TAC.2004.840475(410)50.

[67] T. Iwasaki and S. Hara. "Well-posedness of feedback systems: insights into exact ro-
      bustness analysis and approximate computations". In: *IEEE Transactions on Automatic
      Control* 43.5 (1998), pp. 619–630 (cit. on p. 47).
      DOI: 10.1109/9.668829.

[68] A. Jazayeri and M. Tavakoli. "Revisiting Llewellyn's absolute stability criterion
      for bilateral teleoperation systems under non-passive operator or environment".
      In: *IEEE/RSJ International Conference on Intelligent Robots and Systems (IROS)*. 2012,
      pp. 70–75 (cit. on pp. 64, 65).
      DOI: 10.1109/IROS.2012.6385949.

[69] U. Jönsson and A. Rantzer. "Systems with Uncertain Parameters – Time-Variations
      with Bounded Derivatives". In: *International Journal of Robust and Nonlinear Control*
      6.9/10 (1996), pp. 969–982 (cit. on p. 55).

[70] M. Jun and M. Safonov. "Rational multiplier IQCs for uncertain time-delays and
      LMI stability conditions". In: *IEEE Transactions on Automatic Control* 47.11 (2002),
      pp. 1871–1875 (cit. on p. 57).
      DOI: 10.1109/TAC.2002.804477.

[71] E. Kandel, J. Schwartz, T. Jessell, S. Siegelbaum, and A. Hudspeth, eds. *Principles of
      Neural Science*. 5th ed. McGraw-Hill, 2000, p. 1760 (cit. on p. 9).

[72] C.-Y. Kao and A. Rantzer. "Stability analysis of systems with uncertain time-varying
      delays". In: *Automatica* 43.6 (2007), pp. 959–970 (cit. on p. 57).
      DOI: 10.1016/j.automatica.2006.12.006.

[73] H. Kazerooni, T.-I. Tsay, and K. Hollerbach. "A controller design framework for
      telerobotic systems". In: *IEEE Transactions on Control Systems Technology* 1.1 (1993),
      pp. 50–62 (cit. on pp. 29–31).
      DOI: 10.1109/87.221351.

[74] B. Khademian and K. Hashtrudi-Zaad. "Unconditional stability analysis of dual-user
      teleoperation systems". In: *Proceedings of IEEE Haptics Symposium*. 2010, pp. 161–166
      (cit. on pp. 60, 61).
      DOI: 10.1109/HAPTIC.2010.5444660.

[75] H. K. Khalil. *Nonlinear Systems*. 3rd ed. Prentice Hall, 2002 (cit. on p. 32).

[76] J.-P. Kim and J. Ryu. "Robustly Stable Haptic Interaction Control using an Energy-
      bounding Algorithm". In: *The International Journal of Robotics Research* 29.6 (2010),
      pp. 666–679 (cit. on p. 46).
      DOI: 10.1177/0278364909338770.

[77] Y. S. Kim and B. Hannaford. "Some practical issues in time domain passivity control of haptic interfaces". In: *Proc. IEEE/RSJ Int Intelligent Robots and Systems Conference*. Vol. 3. 2001, pp. 1744–1750 (cit. on p. 46).

[78] F. M. Klomp. "Haptic Control for Dummies: An introduction and analysis". MSc Thesis. Technische Universiteit Eindhoven (TU/e), Control Systems Technology Group, 2006 (cit. on p. 46).
URL: `http://alexandria.tue.nl/repository/books/633244.pdf`.

[79] D. A. Kontarinis and R. D. Howe. "Tactile Display of Vibratory Information in Teleoperation and Virtual Environments". In: *Presence* 4.4 (1995), pp. 387–402 (cit. on p. 10).

[80] H. Köroğlu and C. W. Scherer. "Robust Performance Analysis for Structured Linear Time-Varying Perturbations With Bounded Rates-of-Variation". In: *IEEE Transactions on Automatic Control* 52.2 (2007), pp. 197–211 (cit. on p. 55).
DOI: `10.1109/TAC.2006.890482`.

[81] K. Kosuge, Y. Fujisawa, and T. Fukuda. "Control Of Mechanical System With Man-machine Interaction". In: *Proceedings of the lEEE/RSJ International Conference on Intelligent Robots and Systems (IROS)*. Vol. 1. 1992, pp. 87–92 (cit. on p. 31).
DOI: `10.1109/IROS.1992.587304`.

[82] K. Krishnaswamy. "Passive teleoperation of hydraulic systems". PhD thesis. University of Minnesota, 2004 (cit. on p. 23).

[83] V. Kučera. "A review of the matrix Riccati equation". In: *Kybernetika* 9.1 (1973), pp. 42–61 (cit. on p. 93).
URL: `http://dml.cz/dmlcz/124651`.

[84] R.-F. Kuo and T.-H. Chu. "Unconditional Stability Boundaries of a Three-Port Network". In: *IEEE Transactions on Microwave Theory and Techniques* 58.2 (2010), pp. 363–371 (cit. on p. 61).
DOI: `10.1109/TMTT.2009.2038660`.

[85] K. Kurokawa. "Power Waves and Scattering Matrix". In: *IEEE Transactions on Microwave Theory and Techniques* 13.3 (1965), pp. 194–202 (cit. on p. 111).
DOI: `10.1109/TMTT.1965.1125964`.

[86] E. Laroche, L. Barbé and, B. Bayle, and M. de Mathelin. "A methodology for identification of uncertain LFR model of the human operator for telemanipulation with force-feedback". In: *49th IEEE Conference on Decision and Control (CDC)*. 2010, pp. 2005–2010 (cit. on p. 31).
DOI: `10.1109/CDC.2010.5717433`.

[87] D. Lawrence. "Stability and transparency in bilateral teleoperation". In: *IEEE Transactions on Robotics and Automation* 9.5 (1992), pp. 625–637 (cit. on pp. 32, 41).
DOI: `10.1109/70.258054`.

[88]   D. Lee and M. W. Spong. "Passive Bilateral Teleoperation With Constant Time Delay".
       In: *Robotics, IEEE Transactions on* 22.2 (2006), pp. 269–281 (cit. on p. 57).
       DOI: 10.1109/TRO.2005.862037.

[89]   S. Lee and H. S. Lee. "Modeling, design, and evaluation of advanced teleopera-
       tor control systems with short time delay". In: *IEEE Transactions on Robotics and
       Automation* 9.5 (1993), pp. 607–623 (cit. on pp. 30, 32).
       DOI: 10.1109/70.258053.

[90]   G. Leung, B. Francis, and J. Apkarian. "Bilateral controller for teleoperators with
       time delay via μ-synthesis". In: *IEEE Transactions on Robotics and Automation* 11.1
       (1995), pp. 105–116 (cit. on pp. 31, 39, 45, 57).
       DOI: 10.1109/70.345941.

[91]   F. B. Llewellyn. "Some fundamental properties of transmission systems". In: *Proceed-
       ings of the IRE* 40.3 (1952), pp. 271–283 (cit. on pp. 34, 110).
       DOI: 10.1109/JRPROC.1952.273783.

[92]   J. Löfberg. " YALMIP : A Toolbox for Modeling and Optimization in MATLAB". In:
       Proceedings of the CACSD Conference. Taipei, Taiwan, 2004 (cit. on pp. 66, 69).
       URL: http://users.isy.liu.se/johanl/yalmip.

[93]   G. Lombardi and B. Neri. "Criteria for the evaluation of unconditional stability of
       microwave linear two-ports: a critical review and new proof". In: *IEEE Transactions
       on Microwave Theory and Techniques* 47.6 (1999), pp. 746–751 (cit. on p. 62).
       DOI: 10.1109/22.769346.

[94]   R. Lozano, N. Chopra, and M. Spong. "Passivation Of Force Reflecting Bilateral
       Teleoperators With Time Varying Delay". In: *Proceedings of the 8. Mechatronics Forum*.
       2002, pp. 24–26 (cit. on p. 57).

[95]   I. Masubuchi, A. Ohara, and N. Suda. "LMI-based controller synthesis: A unified
       formulation and solution". In: *International Journal of Robust and Nonlinear Control* 8.8
       (1998), pp. 669–686 (cit. on p. 82).
       DOI: 10.1002/(SICI)1099-1239(19980715)8:8<669::AID-RNC337>3.0.CO;2-W.

[96]   D. McNeill, L. Quaeghebeur, and S. Duncan. "IW - The Man Who Lost His Body".
       In: *Handbook of Phenomenology and Cognitive Science*. Ed. by D. Schmicking and S.
       Gallagher. Springer Netherlands, 2010, pp. 519–543 (cit. on p. 13).
       DOI: 10.1007/978-90-481-2646-0_27.

[97]   D. T. Mcruer. *Pilot-Induced Oscillations and Dynamic Human Behavior*. NASA Con-
       tractor Report 4683. National Aeronautics and Space Administration (NASA), 1995
       (cit. on p. 25).

[98]   A. Megretski and A. Rantzer. "System analysis via integral quadratic constraints".
       In: *IEEE Transactions on Automatic Control* 42.6 (1997), pp. 819–830 (cit. on pp. 47–49,
       68).
       DOI: 10.1109/9.587335.

[99]   A. Megretski and S. Treil. "Power Distribution Inequalities in Optimization and Robustness of Uncertain Systems". In: *Journal of Mathematical Systems, Estimation, and Control* 3.3 (1993), pp. 301–317 (cit. on p. 92).

[100] G. Meinsma, Y. Shrivastava, and M. Fu. "A dual formulation of mixed μ and on the losslessness of (D, G) scaling". In: *IEEE Transactions on Automatic Control* 42.7 (1997), pp. 1032–1036 (cit. on p. 54).
       DOI: 10.1109/9.599990.

[101] B. M. Millman. "The Filament Lattice of Striated Muscle". In: *Physiological Reviews* 78.2 (1998), pp. 359–391 (cit. on p. 25).

[102] S. K. Mitra. *Analysis and synthesis of linear active networks*. New York: J. Wiley, 1969 (cit. on p. 32).

[103] F. Miyazaki, S. Matsubayashi, T. Yoshimi, and S. Arimoto. "A new control methodology toward advanced teleoperation of master-slave robot systems". In: *Proc. IEEE International Conference on Robotics and Automation (ICRA)*. Vol. 3. 1986, pp. 997–1002 (cit. on p. 20).
       DOI: 10.1109/ROBOT.1986.1087546.

[104] S. Munir and W. J. Book. "Internet-based teleoperation using wave variables with prediction". In: *IEEE/ASME Transactions on Mechatronics* 7.2 (2002), pp. 124–133 (cit. on p. 45).
       DOI: 10.1109/TMECH.2002.1011249.

[105] F. Mussa-Ivaldi, N. Hogan, and E. Bizzi. "Neural, mechanical, and geometric factors subserving arm posture in humans". In: *The Journal of Neuroscience* 5.10 (1985), pp. 2732–2743 (cit. on pp. 25, 28).
       URL: http://www.jneurosci.org/content/5/10/2732.

[106] G. Niemeyer and J.-J. E. Slotine. "Designing force reflecting teleoperators with large time delays to appear as virtual tools". In: *Proc. IEEE International Conference on Robotics and Automation*. Vol. 3. 1997, pp. 2212–2218 (cit. on p. 45).

[107] G. Niemeyer and J. J. Slotine. "Stable adaptive teleoperation". In: *IEEE Journal of Oceanic Engineering* 16.1 (1991), pp. 152–162 (cit. on pp. 20, 30, 36, 39, 43, 57, 64).
       DOI: 10.1109/48.64895.

[108] G. Niemeyer and J. J. Slotine. "Telemanipulation with Time Delays". In: *The International Journal of Robotics Research* 23.9 (2004), pp. 873–890 (cit. on pp. 43, 57, 64).
       DOI: 10.1177/0278364904045563.

[109] G. Offer and K. Ranatunga. "Crossbridge and filament compliance in muscle: implications for tension generation and lever arm swing". In: *Journal of Muscle Research and Cell Motility* 31 (4 2010), pp. 245–265 (cit. on pp. 25, 26).
       DOI: 10.1007/s10974-010-9232-7.

[110]   A. Packard and J. Doyle. "The complex structured singular value". In: *Automatica*
        29.1 (1993), pp. 71–109 (cit. on pp. 51, 66).
        DOI: `DOI:10.1016/0005-1098(93)90175-S`.

[111]   A. Packard and J. Teng. "Robust Stability with Time Varying Perturbations". In:
        Proceedings of 28th Allerton Conference. 1990 (cit. on p. 55).

[112]   J. H. Park and H. C. Cho. "Sliding-mode controller for bilateral teleoperation with
        varying time delay". In: *IEEE/ASME International Conference on Advanced Intelligent
        Mechatronics*, 1999, pp. 311–316 (cit. on pp. 46, 57).
        DOI: `10.1109/AIM.1999.803184`.

[113]   A. Pinkus. *N-widths in Approximation Theory, , 1980*. Springer Verlag, New York, 1980
        (cit. on p. 67).

[114]   M. Pirola and G. Ghione. "Immittance and *S*-Parameter-Based Criteria for the
        Unconditional Stability of Linear Two-Ports: Relations and Invariance Properties".
        In: *IEEE Transactions on Microwave Theory and Techniques* 57.3 (2009), pp. 519–523
        (cit. on p. 62).
        DOI: `10.1109/TMTT.2009.2013310`.

[115]   İ. Polat. "A Note on Passivity Based Stability Conditions for Bilateral Teleoperation".
        In: *Proceedings of 18th IFAC World Congress, Milano*. 2011 (cit. on p. 47).
        DOI: `10.3182/20110828-6-IT-1002.00665`.

[116]   İ. Polat. "An IQC formulation of stability analysis for bilateral teleoperation systems
        with time delays". In: *Proceedings of IEEE World Haptics Conference, (WHC)*. 2011,
        pp. 505–509 (cit. on p. 47).
        DOI: `10.1109/WHC.2011.5945537`.

[117]   İ. Polat. "Stability analysis of bilateral teleoperation systems with time-varying
        environments". In: *American Control Conference (ACC), 2011*. 2011, pp. 1139–1144
        (cit. on p. 47).

[118]   İ. Polat and C. W. Scherer. "Stability Analysis for Bilateral Teleoperation: An IQC
        Formulation". In: *IEEE Transactions on Robotics* 28.6 (2012), pp. 1294–1308 (cit. on
        pp. 47, 77).
        DOI: `10.1109/TRO.2012.2209230`.

[119]   J. W. Polderman and J. C. Willems. *Introduction to Mathematical Systems Theory: A
        behavioral approach*. Vol. 26. Texts In Applied Mathematics. Springer New York, 1998
        (cit. on pp. 105, 107).

[120]   E. B. V. Poorten, Y. Yokokohji, and T. Yoshikawa. "Stability analysis and robust
        control for fixed-scale teleoperation". In: *Advanced Robotics* 20.6 (2006), pp. 681–706
        (cit. on p. 35).
        DOI: `10.1163/156855306777361640`.

[121]   P. Prekopiou, S. Tzafestas, and W. Harwin. "Towards variable-time-delays-robust telemanipulation through master state prediction". In: *Proceedings of 1999 IEEE/ASME International Conference on Advanced Intelligent Mechatronics*. IEEE. 1999, pp. 305–310 (cit. on p. 32).
DOI: `10.1109/AIM.1999.803183`.

[122]   G. Raisbeck. "A Definition of Passive Linear Networks in Terms of Time and Energy". In: *Journal of Applied Physics* 25.12 (1954), pp. 1510–1514 (cit. on p. 59).
DOI: `10.1063/1.1702374`.

[123]   G. J. Raju. "Operator adjustable impedance in bilateral remote manipulation". PhD thesis. Massachusetts Institute of Technology, 1989 (cit. on p. 30).
DOI: `1721.1/14445`.

[124]   A. Ran. "Necessary and sufficient conditions for existence of J-spectral factorization for para-Hermitian rational matrix functions". In: *Automatica* 39.11 (2003), pp. 1935–1939 (cit. on p. 93).
DOI: `10.1016/S0005-1098(03)00201-2`.

[125]   A. Rantzer. "On the Kalman–Yakubovich–Popov Lemma". In: *Systems & Control Letters* 28.1 (1996), pp. 7–10 (cit. on pp. 51, 67).
DOI: `DOI:10.1016/0167-6911(95)00063-1`.

[126]   J.-P. Richard. "Time-delay systems: An overview of some recent advances and open problems". In: *Automatica* 39.10 (2003), pp. 1667–1694 (cit. on p. 57).
DOI: `DOI:10.1016/S0005-1098(03)00167-5`.

[127]   J. Rollett. "Stability and Power-Gain Invariants of Linear Twoports". In: *IRE Transactions on Circuit Theory* 9.1 (1962), pp. 29–32 (cit. on pp. 34, 58, 111).
DOI: `10.1109/TCT.1962.1086854`.

[128]   J.-H. Ryu, J. Artigas, and C. Preusche. "A passive bilateral control scheme for a teleoperator with time-varying communication delay". In: *Mechatronics* 20.7 (2010). Special Issue on Design and Control Methodologies in Telerobotics, pp. 812–823 (cit. on p. 45).
DOI: `10.1016/j.mechatronics.2010.07.006`.

[129]   J.-H. Ryu, D.-S. Kwon, and B. Hannaford. "Stability guaranteed control: time domain passivity approach". In: *IEEE Transactions on Control Systems Technology* 12.6 (2004), pp. 860–868 (cit. on p. 45).
DOI: `10.1109/TCST.2004.833648`.

[130]   J.-H. Ryu, D.-S. Kwon, and B. Hannaford. "Stable teleoperation with time-domain passivity control". In: *IEEE Transactions on Robotics and Automation* 20.2 (2004), pp. 365–373 (cit. on p. 45).
DOI: `10.1109/TRA.2004.824689`.

[131]   M. G. Safonov. *Stability and Robustness of Multivariable Feedback Systems*. MIT Press, Cambridge, MA, 1980 (cit. on pp. 47, 48).

[132]   A. van der Schaft. *L₂-Gain and Passivity Techniques in Nonlinear Control*. Ed. by M. Thoma. Vol. 218. Lecture Notes in Control and Information Sciences. Springer Berlin / Heidelberg, 1996 (cit. on p. 108).
DOI: 10.1007/3-540-76074-1.

[133]   C. W. Scherer. "LPV Control and Full Block Multipliers". In: *Automatica* 37.3 (2001), pp. 361–375 (cit. on p. 47).
DOI: DOI:10.1016/S0005-1098(00)00176-X.

[134]   C. W. Scherer. "Relaxations for Robust Linear Matrix Inequality Problems with Verifications for Exactness". In: *SIAM Journal on Matrix Analysis and Applications* 27.2 (2005), pp. 365–395 (cit. on p. 66).
DOI: 10.1137/S0895479803430953.

[135]   C. W. Scherer. "Robust Controller Synthesis is Convex for Systems without Control Channel Uncertainties". In: *Model-Based Control : Bridging Rigorous Theory and Advanced Technology*. Springer US, 2009, pp. 13–30 (cit. on pp. 75, 79).
DOI: 10.1007/978-1-4419-0895-7_2.

[136]   C. W. Scherer., P. Gahinet, and M. Chilali. "Multiobjective output-feedback control via LMI optimization". In: *IEEE Transactions on Automatic Control* 42.7 (1997), pp. 896–911 (cit. on pp. 81, 82).
DOI: 10.1109/9.599969.

[137]   C. W. Scherer and S. Weiland. *Linear Matrix Inequalities in Control*. Unpublished Lecture Notes, Online Available, 1999 (cit. on pp. 81, 87, 100).
URL: http://www.dcsc.tudelft.nl/~cscherer/lmi/notes99.pdf.

[138]   G. Scorletti. "Robustness analysis with time-delays". In: *Proceedings of the 36th IEEE Conference on Decision and Control*. Vol. 4. 1997, pp. 3824–3829 (cit. on p. 57).
DOI: 10.1109/CDC.1997.652457.

[139]   C. Seo, J. Kim, J.-P. Kim, J. H. Yoon, and J. Ryu. "Stable bilateral teleoperation using the energy-bounding algorithm: Basic idea and feasibility tests". In: *IEEE/ASME International Conference on Advanced Intelligent Mechatronics (AIM)*. 2008, pp. 335–340 (cit. on p. 46).
DOI: 10.1109/AIM.2008.4601683.

[140]   J. Sheng and M. W. Spong. "Model predictive control for bilateral teleoperation systems with time delays". In: *Proc. Canadian Conf. Electrical and Computer Engineering*. Vol. 4. 2004, pp. 1877–1880 (cit. on p. 46).
DOI: 10.1109/CCECE.2004.1347575.

[141]   T. B. Sheridan and W. R. Ferrell. "Remote Manipulative Control with Transmission Delay". In: *IEEE Transactions on Human Factors in Electronics* HFE-4.1 (1963), pp. 25–29 (cit. on p. 36).
DOI: 10.1109/THFE.1963.231283.

[142]   T. Sheridan. "Telerobotics". In: *Automatica* 25.4 (1989), pp. 487–507 (cit. on p. 20).
DOI: 10.1016/0005-1098(89)90093-9.

[143]   M. C. Smith. "Synthesis of mechanical networks: the inerter". In: *IEEE Transactions on Automatic Control* 47.10 (2002), pp. 1648–1662 (cit. on p. 107).
DOI: 10.1109/TAC.2002.803532.

[144]   J. E. Speich, L. Shao, and M. Goldfarb. "Modeling the human hand as it interacts with a telemanipulation system". In: *Mechatronics* 15.9 (2005), pp. 1127–1142 (cit. on p. 31).
DOI: 10.1016/j.mechatronics.2005.06.001.

[145]   J. A. Spudich. "The myosin swinging cross-bridge model." In: *Nature Reviews. Molecular Cell Biology* 2.5 (2001), pp. 387–392 (cit. on p. 25).
DOI: 10.1038/35073086.

[146]   A. P. Stern. "Stability and Power Gain of Tuned Transistor Amplifiers". In: *Proceedings of the IRE* 45.3 (1957), pp. 335–343 (cit. on p. 111).
DOI: 10.1109/JRPROC.1957.278369.

[147]   S. Stramigioli, A. van der Schaft, B. Maschke, and C. Melchiorri. "Geometric scattering in robotic telemanipulation". In: *IEEE Transactions on Robotics and Automation* 18.4 (2002), pp. 588–596 (cit. on p. 45).
DOI: 10.1109/TRA.2002.802200.

[148]   E. L. Tan. "Simplified graphical analysis of linear three-port stability". In: *IEE Proceedings Microwaves, Antennas and Propagation* 152.4 (2005), pp. 209–213 (cit. on p. 61).
DOI: 10.1049/ip-map:20045035.

[149]   T. Tsuji, K. Goto, M. Moritani, M. Kaneko, and P. Morasso. "Spatial characteristics of human hand impedance in multi-joint arm movements". In: *Proceedings of the IEEE/RSJ/GI International Conference on Intelligent Robots and Systems (IROS)*. Vol. 1. 1994, 423–430 vol.1 (cit. on p. 31).
DOI: 10.1109/IROS.1994.407441.

[150]   T. Tsuji, P. Morasso, K. Goto, and K. Ito. "Human hand impedance characteristics during maintained posture". In: *Biological Cybernetics* 72 (6 1995), pp. 475–485 (cit. on p. 30).
DOI: 10.1007/BF00199890.

[151]   R. H. Tütüncü, K. C. Toh, and M. J. Todd. "Solving semidefinite-quadratic-linear programs using SDPT3". In: *Mathematical Programming* 95.2 (2003), pp. 189–217 (cit. on p. 69).
DOI: 10.1007/s10107-002-0347-5.

[152]   J. Ueda and T. Yoshikawa. "Force-reflecting bilateral teleoperation with time delay by signal filtering". In: *IEEE Transactions on Robotics and Automation* 20.3 (2004), pp. 613–619 (cit. on p. 45).
DOI: 10.1109/TRA.2004.825516.

[153]   J. Veenman and C. W. Scherer. "IQC-Synthesis with General Dynamic Multipliers".
        In: *Proceedings of 18th IFAC World Congress, Milano*. 2011, pp. 4600–4605 (cit. on pp. 75,
        90).
        DOI: 10.3182/20110828-6-IT-1002.00776.

[154]   J. Vertut and P. Coiffet. *Teleoperation and robotics*. London Englewood Cliffs, N.J:
        Prentice-Hall, 1986 (cit. on p. 20).

[155]   A. Villaverde, A. Blas, J. Carrasco, and A. Torrico. "Reset Control for Passive Bilateral
        Teleoperation". In: *IEEE Transactions on Industrial Electronics* 58.7 (2011), pp. 3037–
        3045 (cit. on p. 46).
        DOI: 10.1109/TIE.2010.2077610.

[156]   B. Willaert, B. Corteville, D. Reynaerts, H. Van Brussel, and E. Vander Poorten.
        "Bounded Environment Passivity of the Classical Position-Force Teleoperation Con-
        troller". In: *IEEE/RSJ International Conference on Intelligent Robots and Systems (IROS)*.
        2009, pp. 4622–4628 (cit. on pp. 66, 69, 70).
        DOI: 10.1109/IROS.2009.5354510.

[157]   B. Willaert, B. Corteville, D. Reynaerts, H. Van Brussel, and E. B. Vander Poorten. "A
        Mechatronic Analysis of the Classical Position-Force Controller Based on Bounded
        Environment Passivity". In: *The International Journal of Robotics Research* 30.4 (2010),
        pp. 444–462 (cit. on pp. 60, 66).
        DOI: 10.1177/0278364910378334.

[158]   J. C. Willems. "The Behavioral Approach to Open and Interconnected Systems". In:
        IEEE Control Systems Magazine 27.6 (2007), pp. 46–99 (cit. on pp. 105, 107).
        DOI: 10.1109/MCS.2007.906923.

[159]   D. Woods. "Reappraisal of the unconditional stability criteria for active 2-port
        networks in terms of S parameters". In: *IEEE Transactions on Circuits and Systems* 23.2
        (1976), pp. 73–81 (cit. on p. 62).
        DOI: 10.1109/TCS.1976.1084179.

[160]   A. Yıldız, J. N. Forkey, et al. "Myosin V Walks Hand-Over-Hand: Single Fluorophore
        Imaging with 1.5 nm Localization". In: *Science* 300.5628 (2003), pp. 2061–2065 (cit. on
        p. 25).
        DOI: 10.1126/science.1084398.

[161]   Y. Yokokohji, T. Imaida, and T. Yoshikawa. "Bilateral teleoperation under time-
        varying communication delay". In: *IEEE/RSJ International Conference on Intelligent
        Robots and Systems,(IROS)*. Vol. 3. 1999, pp. 1854–1859 (cit. on pp. 45, 57).
        DOI: 10.1109/IROS.1999.811748.

[162]   Y. Yokokohji and T. Yoshikawa. "Bilateral control of master-slave manipulators for
        ideal kinesthetic coupling-formulation and experiment". In: *IEEE Transactions on
        Robotics and Automation* 10.5 (1994), pp. 605–620 (cit. on pp. 29, 30).
        DOI: 10.1109/70.326566.

[163] D. C. Youla. "On the factorization of rational matrices". In: *IRE Transactions on Information Theory* 7.3 (1961), pp. 172–189 (cit. on p. 94).
DOI: `10.1109/TIT.1961.1057636`.

[164] C. Youngblut, R. Johnston, S. H. Nash, R. A. Wienclaw, and C. A. Will. *Review of Virtual Environment Interface Technology*. Tech. rep. ADA314134. Institute for Defense Analyses, 1996 (cit. on pp. 10, 11).

[165] K. Zhou, J. C. Doyle, and K. Glover. *Robust and Optimal Control*. Prentice-Hall, Upper Saddle River, 1996 (cit. on pp. 77, 94).